THE IMPACT OF PROTECTION SYSTEM FAILURES ON POWER SYSTEM RELIABILITY EVALUATION

A Dissertation

by

KAI JIANG

Submitted to the Office of Graduate Studies of
Texas A&M University
in partial fulfillment of the requirements for the degree of

DOCTOR OF PHILOSOPHY

Approved by:

Chair of Committee,	Chanan Singh
Committee Members,	Mladen Kezunovic
	Alex Sprintson
	Lewis Ntaimo
Head of Department,	Costas N. Georghiades

December 2012

Major Subject: Electrical Engineering

ABSTRACT

The reliability of protection systems has emerged as an important topic because protection failures have critical influence on the reliability of power systems. The goal of this research is to develop novel approaches for modeling and analysis of the impact of protection system failures on power system reliability.

It is shown that repairable and non-repairable assumptions make a remarkable difference in reliability modeling. A typical all-digital protection system architecture is modeled and numerically analyzed. If an all-digital protection system is indeed repairable but is modeled in a non-repairable manner for analysis, the calculated values of reliability indices could be grossly pessimistic.

The smart grid is emerging with the penetration of information-age technologies and the development of the Special Protection System (SPS) will be greatly influenced. A conceptual all-digital SPS architecture is proposed for the future smart grid. Calculation of important reliability indices by the network reduction method and the Markov modeling method is illustrated in detail.

Two different Markov models are proposed for reliability evaluation of the 2-out-of-3 voting gates structure in a generation rejection scheme. If the model with consideration of both detectable and undetectable logic gate failures is used as a benchmark, the simple model which only considers detectable failures will significantly overestimate the reliability of the 2-out-of-3 voting gates structure.

The two types of protection failures, undesired-tripping mode and fail-to-operate mode are discussed. A complete Markov model for current-carrying components is established and its simplified form is then derived. The simplified model can appropriately describe the overall reliability situation of individual components under the circumstances of complex interactions between components due to protection failures.

New concepts of the self-down state and the induced-down state are introduced and utilized to build up the composite unit model. Finally, a two-layer Markov model for power systems with protection failures is proposed. It can quantify the impact of protection failures on power system reliability. Using the developed methodology, we can see that the assumption of perfectly reliable protection can introduce errors in reliability evaluation of power systems.

DEDICATION

To my parents and my family for their love and support

ACKNOWLEDGEMENTS

I would like to express my special thanks to my committee chair, Dr. Singh, for his guidance and support throughout the course of this research.

I would also like to thank my committee members, Dr. Kezunovic, Dr. Sprintson, and Dr. Ntaimo, for their time, comments and support.

Thanks also go to my friends and colleagues and the department faculty and staff for making my time at Texas A&M University a great experience.

I also want to extend my gratitude to the Power Systems Engineering Research Center (PSERC), which provided the financial support for part of this research.

Finally, thanks to my friends and colleagues in Consolidated Edison Company of New York for helping me learn a lot during my intern period.

TABLE OF CONTENTS

Page

Page

Page

LIST OF FIGURES

Page

Page

Page

LIST OF TABLES

Page

1. INTRODUCTION

1.1. Research Objectives

Reliability evaluation is one of the most important tasks of power system analysis. During the past few decades, quantitative analysis based on probability theory has been applied to power systems and considerable progress has been made in power system reliability modeling and computation [1]-[67].

In addition, reliability of protection systems has emerged as an important topic because protection failures have critical impact on the reliability of power systems [68]. There are two aspects of protection system reliability, i.e. dependability and security. Dependability indicates the ability of the protection system to perform correctly when required. Unsatisfactory dependability corresponds to the fact that the protection system may fail to operate when required due to hidden or undetected faults in it. On the other hand, security is the ability of the protection system to avoid unnecessary operation during the absence of fault or faults outside the protection zone. Unsatisfactory security will result in undesired tripping of the associated circuit breaker(s).

The goal of this research is to develop novel approaches for modeling and analysis of the impact of protection system failures on power system reliability. It includes the following specific objectives.

(1) Analysis of the repair factor that may influence the reliability modeling of protection systems;

(2) Developing new perspectives for analyzing the impact mechanism of protection system failures;

(3) Developing applicable methodology for power system reliability evaluation including protection system failures.

1.2. Nature of the Problem

Protection systems are indispensable to power systems. If assumed perfectly reliable, they will provide isolation of faulted current-carrying components in the power system to minimize the impact to the rest of the power system. However, the protection system itself is also complex and it usually consists of various types and sets of protective relays. Actually, it may fail to operate or cause undesired tripping action associated with dependability and security issues, respectively. Consequently, more components of the power system than necessary will be out of service and the reliability situation of the power system will be worse than that with perfect protections. Thus, assuming the protection system to be perfectly reliable may give optimistic estimation of the reliability of the power system. The nature of the problem can be illustrated by Figure 1-1 as following.

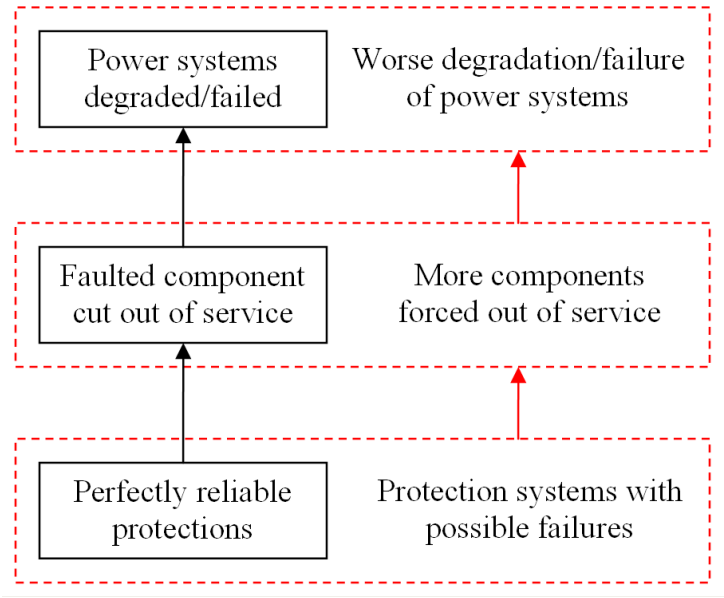

Figure 1-1. The nature of the problem.

According to Figure 1-1, there are hierarchical layers of three levels for this problem. These layers are listed as follows.

(1) Layer 1 (the lower level): This is the protection system level. The main issue of this level would be how to model and evaluate the protection system reliability, considering interactions among the elements of a protection system. The possible research topics could be but not limited to traditional protection systems and the new all-digital protection systems.

(2) Layer 2 (the intermediate level): This is the current-carrying component level. The main issue of this level would be how to model and evaluate the reliability situation of current-carrying components, considering interactions between protection systems and the protected components. The possible research topics could be but not limited to

the impact of fail-to-operate protection failures and the impact of undesired-tripping protection failures.

(3) Layer 3 (the upper level): This is the power system level. The main issue of this level would be how the power system reliability is affected by protection system failures, considering interactions among current-carrying components due to protection failures. The possible research topics could be but not limited to the influence on system states and reliability indices.

1.3. Present Status of the Problem

In the past few decades, considerable research has been done on reliability modeling of conventional protection systems. For Layer 1 and Layer 2, researchers have drawn attention to hidden or undetected failures of protection systems and a unique concept for the analysis of protection system reliability was introduced by the idea of "unreadiness probability" [69]. Based on this concept of "unreadiness probability", some other reliability indices such as "abnormal unavailability" and "protective system unavailability" [70]-[72] have been developed in order to provide appropriate reliability analysis of protection system failures. Much of these works and reliability indices are based on the macro-level analysis of conventional protection systems in which the interaction is between the protection systems and the current-carrying components protected.

However, a new concept called all-digital protection system is now developing which is different from conventional ones in many ways. In such a system, not only relays are digital (computer relays), but also the output signals of instrument transformers which are now non-conventional are digital. These digital signals are conveyed to the digital relays through a digital process bus [73], [74]. Reliability analysis of the all-digital protection can play an important role in evaluating its merits and guiding its development in a cost-effective and reliable manner.

A typical all-digital protection system is mainly composed of merging units, Ethernet switches, time synchronization sources, digital protective relays, and Ethernet communication media. An all-digital protection has more components and of different type than the conventional one, which should have some influence on its reliability indices. Thus it is also important to evaluate reliability based on the micro-level analysis in which the interaction among components of the all-digital protection system is considered. In recent years, some architectures of all-digital protection systems have been proposed and some reliability indices including MTTF have been analyzed [75]. However, this analysis has not considered the effect of component repair.

For Layer 2 and Layer 3, researchers have been continuously trying to identify the effects of protection failures on power systems, to incorporate protection failures into power system analysis, and to enhance power system reliability evaluation considering protection failures [76]-[89]. Nevertheless, in spite of the mentioned efforts, the methodology of analyzing power system reliability including protection failures has not gone yet far enough. In typical composite power system reliability analysis, the

protection systems are still assumed to be perfectly reliable, which means that the failure of a current-carrying component results in the removal of that component, and that if the power can be redispatched to satisfy all loads, the system state is assumed to have no load loss. It is worth pointing out that even if the protection systems worked perfectly, the removal of a transmission line can lead to cascading failures as a result of the post-fault overloading or transient stability problems but such events are not considered in a typical composite power system reliability analysis, although they can be included.

However, when the protection failure modes and their probabilities are included, complicated interactions among current-carrying components do exist such that both component and system states experience intricate changes. There is a finite probability of more components than the faulted one being isolated. Thus, we need to reconsider the reliability situation of current-carrying components including the impact of protection failures, as protection system failures can change their operation behavior drastically. Analysis at power system level may be inadequate and even misleading if we do not incorporate protection system failures into the component modeling.

When a fault occurs on a current-carrying component in the power system, the status of adjacent components may also be affected depending on the operation of the protection system. If the protection system is healthy and acts as intended, the faulted component alone is isolated. However, a protection system may be faulted but its unhealthy condition may not be known unless it is called upon to do its job. In such a situation, adjacent components other than the faulted one may also be isolated due to the operation of back up protection. To consider such a possibility, a three-stage multistate

Markov model for a single current-carrying component was proposed, which identified the most complex undetected faults in the protection system [80].

Based on this three-stage multistate model, reliability analysis of the composite generation and transmission systems can be more practically achieved [90]. Nevertheless, the number of states for even a single component is still so large that direct application of this model in power system reliability is indeed limited. Thus, new models and concepts are necessary for reliability analysis including protection system failures at both the current-carrying component level and the power system level.

1.4. Organization of Dissertation

The dissertation will be organized as follows. Section 2 explores the impact of including component repair on the reliability modeling of all-digital protection systems. Section 3 proposes a conceptual all-digital SPS architecture for the future smart grid and shows how to apply the reliability analysis approaches. Section 4 focuses on reliability modeling of the 2-out-of-3 voting gates structure in a generation rejection scheme. Section 5 reconsiders the reliability modeling of current-carrying components with protection system failures from a new perspective. Section 6 develops new models and concepts for incorporating the effect of protection system failures into power system reliability evaluation. Section 7 gives the conclusions of the dissertation. The References and the Appendix are attached at the end.

2. RELIABILITY MODELING OF ALL-DIGITAL PROTECTION SYSTEMS INCLUDING IMPACT OF REPAIR *

2.1. Introduction

The Mean Time To Failure (MTTF) and the Mean Time To First Failure (MTTFF) are important indices in the area of reliability analysis. Although their exact definitions may differ in various applications, we can give their descriptive meanings as following.

In general, MTTF represents the average time between system breakdowns or loss of service. For reasons of avoiding confusion, the same concept is sometimes expressed as the Mean Up Time (MUT) or the Mean Time Between Failures (MTBF).

In contrast, MTTFF represents the mean value of time from the moment system starts operating until it fails for the first time. It is, in fact, the concept of the first passage time applied to the reliability engineering field [2].

---

* Part of this section is reprinted from copyrighted material with permission from IEEE. ©2010 IEEE. Reprinted, with permission, from Kai Jiang and Chanan Singh, "Reliability modeling of all-digital protection systems including impact of repair", *IEEE Trans. Power Delivery*, vol. 25, no. 2, pp. 579-587, Apr. 2010.
For more information go to
http://thesis.tamu.edu/forms/IEEE%20permission%20note.pdf/view.

It is important to differentiate between the concepts of MTTF and MTTFF. We can illustrate this difference graphically by a system realization as shown in Figure 2-1. Here we use a sequence of U_i to represent each time period that the system is in success states, and a sequence of D_i to represent time periods of system failures. Then MTTF is the mean value of all the U_i, while MTTFF is the expected value of U_1, the first one of the U_i sequence.

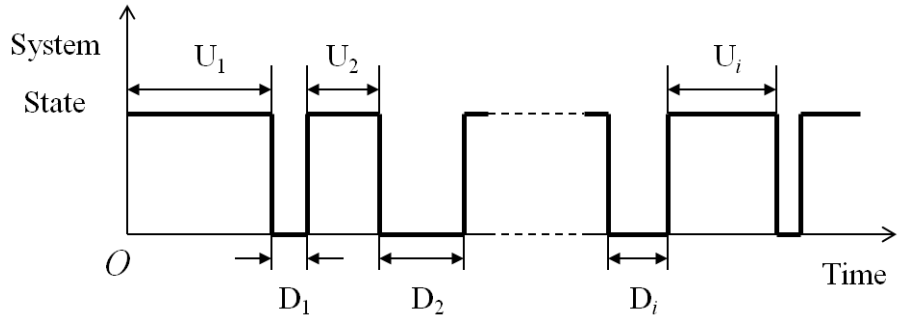

Figure 2-1. Illustration of MTTF and MTTFF.

This section mainly discusses the relationships between repairable and non-repairable MTTF and MTTFF for all-digital protection system modeling. The remainder of the section is organized as follows. Section 2.2 first describes the analysis and insights of basic structures. Section 2.3 then analyzes an all-digital protection system including some numerical results. Section 2.4 is the summary of this section.

2.2. Theoretical Analysis of Basic System Structures Consisting of Two Components

Because the overall all-digital protection system can be considered as a complex of series and parallel structures, it is important to examine the theoretical analysis of basic system structures consisting of two components. This could help us not only gain an intuitive appreciation, but also understand better the analysis of the more complex structure of an all-digital protection system.

2.2.1. *Repairable Systems*

2.2.1.1. Parallel systems

The system structure and the Markov model for a repairable parallel system are shown in Figure 2-2. The letters ‘U’ and ‘D’ in the figure represent the up and down states of the component.

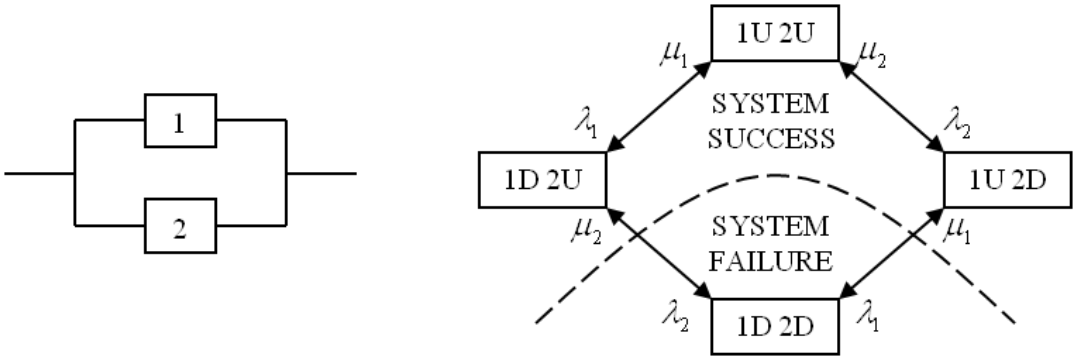

(a) System structure (b) Markov model

Figure 2-2. Repairable parallel system consisting of two components.

2.2.1.1.1. *MTTF of the system*

For steady state, the probabilities of system failure and system success are shown below.

$$p_f = p_{1f}\, p_{2f} = \frac{\lambda_1}{\lambda_1+\mu_1} \times \frac{\lambda_2}{\lambda_2+\mu_2} = \frac{\lambda_1\lambda_2}{(\lambda_1+\mu_1)(\lambda_2+\mu_2)}$$

$$p_s = 1 - p_f = 1 - \frac{\lambda_1\lambda_2}{(\lambda_1+\mu_1)(\lambda_2+\mu_2)} = \frac{\lambda_1\mu_2+\mu_1\lambda_2+\mu_1\mu_2}{(\lambda_1+\mu_1)(\lambda_2+\mu_2)}$$

The system repair rate and failure rate are obtained using the concept of equivalent transition rate [91] as follows.

$$\mu_{sys} = \frac{Fr_s}{p_f} = \frac{p_f\mu_1 + p_f\mu_2}{p_f} = \mu_1+\mu_2$$

$$\lambda_{sys} = \frac{Fr_f}{p_s} = \frac{Fr_s}{p_s} = \frac{p_f\mu_{sys}}{p_s} = \frac{\lambda_1\lambda_2(\mu_1+\mu_2)}{\lambda_1\mu_2+\mu_1\lambda_2+\mu_1\mu_2}$$

The MTTF is the reciprocal of the system failure rate, i.e.

$$MTTF = \frac{1}{\lambda_{sys}} = \frac{\lambda_1\mu_2 + \mu_1\lambda_2 + \mu_1\mu_2}{\lambda_1\lambda_2(\mu_1 + \mu_2)}. \quad (2.1)$$

2.2.1.1.2. *MTTFF of the system*

The calculation of MTTFF is more complex than that of MTTF and it can be obtained from the transition rate matrix of the system [2] as follows.

$$MTTFF = p_+(0)(-R_{11})^{-1}U_k$$

Here, R_{11} is the sub-matrix of the full system transition rate matrix $R = \begin{bmatrix} R_{11} & R_{12} \\ R_{21} & R_{22} \end{bmatrix}$ and represents the set of transition rates from system success to system success. And $p_+(0)$ is the probability vector of system success states for the initial state (all components up), while U_k is the unit vector of dimension k which is equal to the number of states of system success.

For a repairable parallel system, the full system transition rate matrix is

$$R = \begin{bmatrix} -(\lambda_1 + \lambda_2) & \lambda_1 & \lambda_2 & \vdots & 0 \\ \mu_1 & -(\mu_1 + \lambda_2) & 0 & \vdots & \lambda_2 \\ \mu_2 & 0 & -(\lambda_1 + \mu_2) & \vdots & \lambda_1 \\ \cdots & \cdots & \cdots & \cdots & \cdots \\ 0 & \mu_2 & \mu_1 & \vdots & -(\mu_1 + \mu_2) \end{bmatrix}.$$

Therefore,

$$R_{11} = \begin{bmatrix} -(\lambda_1 + \lambda_2) & \lambda_1 & \lambda_2 \\ \mu_1 & -(\mu_1 + \lambda_2) & 0 \\ \mu_2 & 0 & -(\lambda_1 + \mu_2) \end{bmatrix},$$

$$p_+(0) = [1 \quad 0 \quad 0],$$

$$U_k = \begin{bmatrix} 1 \\ 1 \\ 1 \end{bmatrix}.$$

Thus, the MTTFF of the system is obtained as below.

$$MTTFF = p_+(0)(-R_{11})^{-1}U_k = [1 \quad 0 \quad 0](-R_{11})^{-1}\begin{bmatrix} 1 \\ 1 \\ 1 \end{bmatrix}$$

$$= \frac{\lambda_1\mu_1 + \lambda_1\lambda_2 + \mu_1\mu_2 + \lambda_2\mu_2 + \lambda_1^2 + \lambda_1\mu_2 + \mu_1\lambda_2 + \lambda_2^2}{\lambda_1\lambda_2(\lambda_1 + \mu_1 + \lambda_2 + \mu_2)} \tag{2.2}$$

2.2.1.2. Series systems

The system structure and the Markov model for a repairable series system are shown in Figure 2-3.

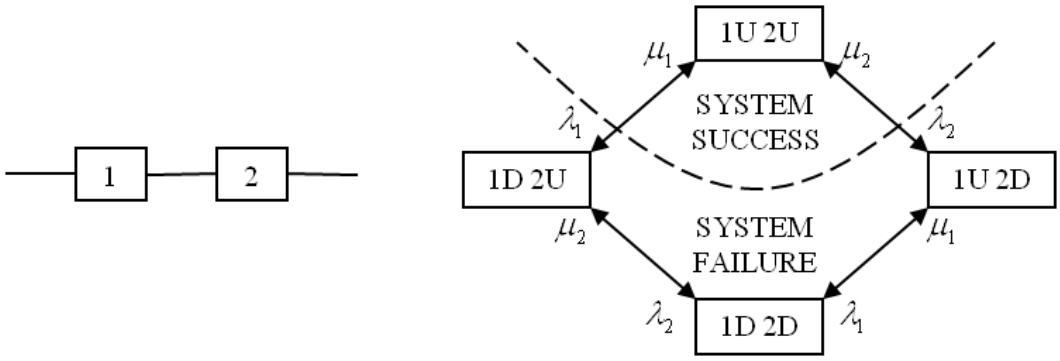

(a) System structure (b) Markov model

Figure 2-3. Repairable series system consisting of two components.

2.2.1.2.1. *MTTF of the system*

The system failure rate and the MTTF are given below.

$$\lambda_{sys} = \frac{Fr_f}{p_s} = \frac{p_s\lambda_1 + p_s\lambda_2}{p_s} = \lambda_1 + \lambda_2$$

$$MTTF = \frac{1}{\lambda_{sys}} = \frac{1}{\lambda_1 + \lambda_2} \tag{2.3}$$

2.2.1.2.2. *MTTFF of the system*

For a repairable series system, the full system transition rate matrix is

$$R = \begin{bmatrix} -(\lambda_1+\lambda_2) & \vdots & \lambda_1 & \lambda_2 & 0 \\ \cdots & \cdots & \cdots & \cdots & \cdots \\ \mu_1 & \vdots & -(\mu_1+\lambda_2) & 0 & \lambda_2 \\ \mu_2 & \vdots & 0 & -(\lambda_1+\mu_2) & \lambda_1 \\ 0 & \vdots & \mu_2 & \mu_1 & -(\mu_1+\mu_2) \end{bmatrix}.$$

Therefore,

$$R_{11} = -(\lambda_1 + \lambda_2)\,,$$

$$p_+(0) = 1,$$

$$U_k = 1,$$

$$MTTFF = p_+(0)(-R_{11})^{-1}U_k = [1]\cdot\left[\frac{1}{\lambda_1+\lambda_2}\right]\cdot[1] = \frac{1}{\lambda_1+\lambda_2} \tag{2.4}$$

2.2.2. *Non-repairable Systems*

For a non-repairable system, the MTTF is actually the same as MTTFF. This is because when the system enters its failed states for the first time, it can never return to a success state.

2.2.2.1. Parallel systems

The reliability of a non-repairable parallel system is

$$R_{sys}(t) = p_s = 1 - p_f = 1 - p_{1f}\,p_{2f} = 1 - (1 - p_{1s})(1 - p_{2s}) = 1 - (1 - e^{-\lambda_1 t})(1 - e^{-\lambda_2 t})$$

$$= e^{-\lambda_1 t} + e^{-\lambda_2 t} - e^{-(\lambda_1 + \lambda_2)t}.$$

By definition [92], [93],

$$MTTF = \int_0^\infty R_{sys}(t)dt.$$

Thus,

$$MTTF = \int_0^\infty (e^{-\lambda_1 t} + e^{-\lambda_2 t} - e^{-(\lambda_1 + \lambda_2)t})dt = \frac{1}{\lambda_1} + \frac{1}{\lambda_2} - \frac{1}{\lambda_1 + \lambda_2},$$

$$MTTFF = MTTF = \frac{1}{\lambda_1} + \frac{1}{\lambda_2} - \frac{1}{\lambda_1 + \lambda_2}. \qquad (2.5)$$

2.2.2.2. Series systems

The reliability of a non-repairable series system is

$$R_{sys}(t) = p_s = p_{1s} p_{2s} = e^{-\lambda_1 t} e^{-\lambda_2 t} = e^{-(\lambda_1+\lambda_2)t}.$$

Hence,

$$MTTF = \int_0^\infty R_{sys}(t)dt = \int_0^\infty e^{-(\lambda_1+\lambda_2)t} dt = \frac{1}{\lambda_1+\lambda_2},$$

$$MTTFF = MTTF = \frac{1}{\lambda_1+\lambda_2}. \tag{2.6}$$

2.2.3. *Differences of Repairable and Non-repairable MTTF and MTTFF*

It is easy to see that for a repairable system, MTTF is different from MTTFF. The reason is that when a system returns to success status after repair, it does not always return to the same state given that the number of success states is more than one. In special situations when the system has only one success state or it always returns to the same state after repair, the MTTF and MTTFF become identical and actually series system represents one example of such systems.

2.2.3.1. Comparisons of parallel systems

2.2.3.1.1. *MTTFF and MTTF of repairable systems*

From (2.1) and (2.2), we can see that

$$MTTFF_R - MTTF_R = \frac{\lambda_1\mu_1^2 + \lambda_1^2\mu_1 + \lambda_2\mu_2^2 + \lambda_2^2\mu_2}{\lambda_1\lambda_2(\lambda_1 + \mu_1 + \lambda_2 + \mu_2)(\mu_1 + \mu_2)}. \quad (2.7)$$

Since $\lambda_1, \lambda_2, \mu_1, \mu_2$ are all positive values, we know that the result of (2.7) must be greater than zero. Thus, for a repairable parallel system, the value of MTTFF is greater than that of MTTF.

2.2.3.1.2. *MTTFF of repairable and non-repairable systems*

From (2.2) and (2.5), we have

$$MTTFF_R - MTTFF_N = \frac{\lambda_1\mu_1\lambda_2 + \lambda_1\mu_1\mu_2 + \lambda_1\lambda_2\mu_2 + \mu_1\lambda_2\mu_2}{\lambda_1\lambda_2(\lambda_1 + \mu_1 + \lambda_2 + \mu_2)(\lambda_1 + \lambda_2)}. \quad (2.8)$$

Again, we know that the result of (2.8) must be greater than zero because $\lambda_1, \lambda_2, \mu_1, \mu_2$ are all positive. Thus, the value of MTTFF of a repairable parallel system is greater than that of a non-repairable one.

2.2.3.1.3. *MTTF of repairable and non-repairable systems*

From (2.1) and (2.5), we get

$$MTTF_R - MTTF_N = \frac{\lambda_1\mu_1(\mu_2 - \lambda_1) + \lambda_2\mu_2(\mu_1 - \lambda_2)}{\lambda_1\lambda_2(\lambda_1 + \lambda_2)(\mu_1 + \mu_2)}. \quad (2.9)$$

It is easy to see that for $\mu_2 > \lambda_1$ and $\mu_1 > \lambda_2$, expression (2.9) has a positive value. It means the MTTF of a repairable parallel system would be greater than that of a non-repairable one if these conditions are satisfied.

The physical meaning of this result is obvious. If one component of the repairable parallel system is failed, as long as it can be repaired before the other component fails, the system can still be in state of success. Given this condition, the repairable parallel system is sure to survive better than the non-repairable one.

However, we find it interesting to note that the **MTTF of a repairable parallel system could be smaller than that of a non-repairable one**, depending on the sign of the numerator in expression (2.9). This phenomenon can easily be observed especially in case $\mu_2 < \lambda_1$ and $\mu_1 < \lambda_2$ simultaneously.

2.2.3.2. Comparisons of series systems

2.2.3.2.1. *MTTFF and MTTF of repairable systems*

From (2.3) and (2.4) we can see that

$$MTTFF_R - MTTF_R = 0.$$

2.2.3.2.2. *MTTFF of repairable and non-repairable systems*

From (2.4) and (2.6) we also have

$$MTTFF_R - MTTFF_N = 0.$$

2.2.3.2.3. *MTTF of repairable and non-repairable systems*

Similarly, from (2.3) and (2.6) we get

$$MTTF_R - MTTF_N = 0.$$

We can easily conclude from the above comparisons that for a series system, the values of MTTFF and MTTF are all the same, no matter the system is repairable or not. It sounds reasonable because any component failure of a series system will cause the system to fail.

2.3. Analysis of All-digital Protection Systems

Compared to the basic systems with only two components, all-digital protection systems have a variety of more complex structures and thus the reliability results are not easy to obtain directly. However, the methodology that we used previously to analyze the basic systems can still be applied to all-digital protection systems.

Since the overall protection system will not work properly without correct signal, we assume the digital instrument transducers to be extremely reliable. Hence, they are not considered in the following analysis. For simplicity, we also assume that one merging unit can perform the full function needed for one set of protection, instead of several units in reality processing different signals, respectively. In addition, the Ethernet interface is assumed to be a part of the corresponding IED device (i.e. computer relay,

merging unit, Ethernet switcher) and its reliability is already included in these devices [75].

The main functional parts of a protection system are usually designed to be located in isolated places where the physical distances between them are far enough to avoid mutual interference. Hence, we can assume that all the components of the all-digital protection system are independent of each other in most cases. In addition, the component state durations are assumed to be exponentially distributed.

The major threats that can cause the common mode failures are intentional destruction (e.g. war, terrorism), fire, and more commonly power failures. However, the role of the protection system is so important that every set of protection is designed to be supplied by multiple power sources simultaneously, including AC, batteries, and UPS, etc. So, we can assume its power supplies to be extremely reliable. Now that almost every monitoring and control cabinet is designed with effective measures against fire spread by cables, we also assume the common mode failures by fire to be neglected for simplicity. As for intentional destruction, it is naturally not considered.

Based on the previous assumptions, we will analyze a typical all-digital protection system architecture as shown in Figure 2-4 [75] but similar analysis can be conducted for other configurations. In this architecture, the protection system consists of two redundant full functional units and each unit comprises a set of digital protective relay (PR), Ethernet switch (SW), merging unit (MU), time synchronization source (TS), and Ethernet communication media (EM). In order to reduce the probability of system

failure due to time synchronization, the time synchronization sources of the two units are shared with each other and thus act as mutual backup of each other.

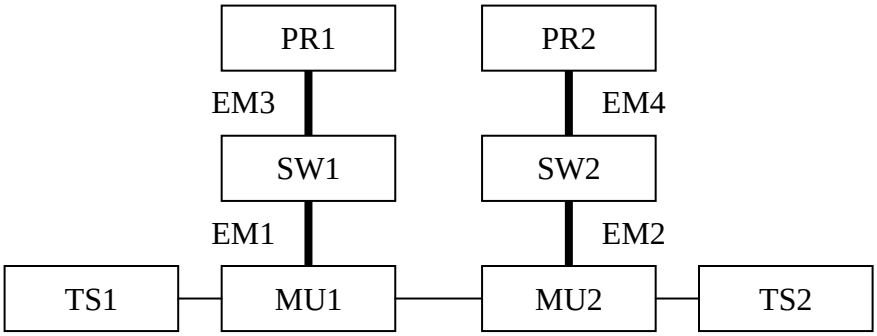

Figure 2-4. An example all-digital protection system architecture.

2.3.1. *Non-repairable System Model*

Reference [75] assumes this system to be non-repairable and its MTTF is obtained as

$$MTTF = \int_0^\infty R_{sys}(t)dt$$

wherein the system reliability is given by

$$\begin{aligned} R_{sys}(t) = &-2p_{ts}p_{mu}^2p_{pr}^2p_{sw}^2p_{em}^4 + p_{ts}^2p_{mu}^2p_{pr}^2p_{sw}^2p_{em}^4 \\ &-2p_{ts}^2p_{mu}p_{pr}p_{sw}p_{em}^2 + 4p_{ts}p_{mu}p_{pr}p_{sw}p_{em}^2 \end{aligned}$$

and in which the probability of a component *i* in its success state with a constant failure rate λ_i is

$$p_i = e^{-\lambda_i t}.$$

Given that the Ethernet communication media have a failure rate of $\lambda_{em} = 0.003 year^{-1}$, and all other components as $\lambda_{ts} = \lambda_{mu} = \lambda_{sw} = \lambda_{pr} = 0.01 year^{-1}$, the MTTF of the system is calculated to be 37.3 years [75].

2.3.2. *Repairable System Model*

As we know, if there is any recognized problem with the protection, utilities would either fix or replace the problematic components so as to keep the whole protection system up. Thus, we need to analyze the protection system reliability with a repairable model. Since the estimated repair time for any failed equipment is usually prescribed in power industry and the maintenance staff always conforms to this guideline, we can assume constant repair rates for our repairable model.

2.3.2.1. MTTF of the repairable protection system

Using the concept of equivalent transition rates [91], we simplify the original reliability block diagram shown in Figure 2-5(a) [75] to the one in Figure 2-5 (b). The simplified system will have the same value of the MTTF as that of the original one.

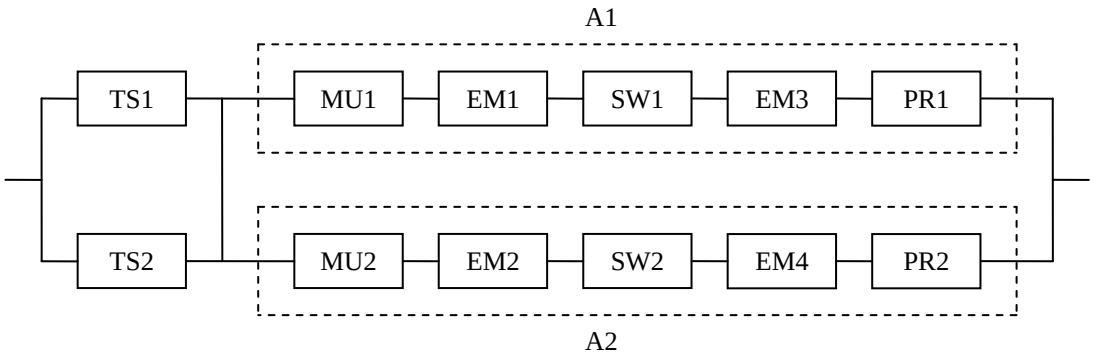

(a) Original reliability block diagram

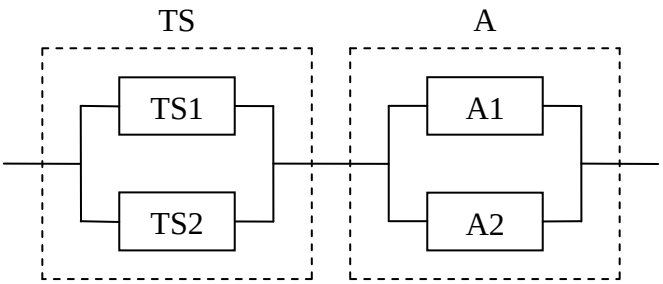

(b) Simplified reliability block diagram

Figure 2-5. Simplification of the reliability block diagram.

For the series chain A1 in Figure 2-5(a), the steady state probabilities and the transition rates are

$$p_{A1,s} = p_{MU1,s}\, p_{EM1,s}\, p_{SW1,s}\, p_{EM3,s}\, p_{PR1,s} = \frac{\mu_{mu}\mu_{em}^2\mu_{sw}\mu_{pr}}{(\lambda_{mu}+\mu_{mu})(\lambda_{em}+\mu_{em})^2(\lambda_{sw}+\mu_{sw})(\lambda_{pr}+\mu_{pr})},$$

$$p_{A1,f} = 1 - p_{A1,s} = 1 - \frac{\mu_{mu}\mu_{em}^2\mu_{sw}\mu_{pr}}{(\lambda_{mu}+\mu_{mu})(\lambda_{em}+\mu_{em})^2(\lambda_{sw}+\mu_{sw})(\lambda_{pr}+\mu_{pr})},$$

$$\lambda_{A1} = \lambda_{MU1} + \lambda_{EM1} + \lambda_{SW1} + \lambda_{EM3} + \lambda_{PR1} = \lambda_{mu} + 2\lambda_{em} + \lambda_{sw} + \lambda_{pr},$$

$$\mu_{A1} = \frac{Fr_{A1,s}}{p_{A1,f}} = \frac{Fr_{A1,f}}{p_{A1,f}} = \frac{p_{A1,s}\lambda_{A1}}{p_{A1,f}} = \frac{\mu_{mu}\mu_{em}^2\mu_{sw}\mu_{pr}(\lambda_{mu}+2\lambda_{em}+\lambda_{sw}+\lambda_{pr})}{(\lambda_{mu}+\mu_{mu})(\lambda_{em}+\mu_{em})^2(\lambda_{sw}+\mu_{sw})(\lambda_{pr}+\mu_{pr}) - \mu_{mu}\mu_{em}^2\mu_{sw}\mu_{pr}}.$$

Similarly, for the series chain A2 in Figure 2-5(a), the steady state probabilities and the transition rates are

$$p_{A2,s} = p_{MU2,s}\, p_{EM2,s}\, p_{SW2,s}\, p_{EM4,s}\, p_{PR2,s} = \frac{\mu_{mu}\mu_{em}^2\mu_{sw}\mu_{pr}}{(\lambda_{mu}+\mu_{mu})(\lambda_{em}+\mu_{em})^2(\lambda_{sw}+\mu_{sw})(\lambda_{pr}+\mu_{pr})},$$

$$p_{A2,f} = 1 - p_{A2,s} = 1 - \frac{\mu_{mu}\mu_{em}^2\mu_{sw}\mu_{pr}}{(\lambda_{mu}+\mu_{mu})(\lambda_{em}+\mu_{em})^2(\lambda_{sw}+\mu_{sw})(\lambda_{pr}+\mu_{pr})},$$

$$\lambda_{A2} = \lambda_{MU2} + \lambda_{EM2} + \lambda_{SW2} + \lambda_{EM4} + \lambda_{PR2} = \lambda_{mu} + 2\lambda_{em} + \lambda_{sw} + \lambda_{pr},$$

$$\mu_{A2} = \frac{Fr_{A2,s}}{p_{A2,f}} = \frac{Fr_{A2,f}}{p_{A2,f}} = \frac{p_{A2,s}\lambda_{A2}}{p_{A2,f}} = \frac{\mu_{mu}\mu_{em}^2\mu_{sw}\mu_{pr}(\lambda_{mu}+2\lambda_{em}+\lambda_{sw}+\lambda_{pr})}{(\lambda_{mu}+\mu_{mu})(\lambda_{em}+\mu_{em})^2(\lambda_{sw}+\mu_{sw})(\lambda_{pr}+\mu_{pr}) - \mu_{mu}\mu_{em}^2\mu_{sw}\mu_{pr}}.$$

Since the series chains A1 and A2 have the same probabilities and the transition rates, we can get the probabilistic results of the parallel structure A in Figure 2-5(b) as following.

$$p_{A,f} = p_{A1,f}\, p_{A2,f} = \left(\frac{\lambda_{A1}}{\lambda_{A1}+\mu_{A1}}\right)^2$$

$$p_{A,s} = 1 - p_{A,f} = 1 - \left(\frac{\lambda_{A1}}{\lambda_{A1}+\mu_{A1}}\right)^2$$

$$\mu_A = \mu_{A1} + \mu_{A2} = 2\mu_{A1}$$

$$\lambda_A = \frac{Fr_{A,f}}{p_{A,s}} = \frac{Fr_{A,s}}{p_{A,s}} = \frac{p_{A,f}\mu_A}{p_{A,s}} = \frac{2\lambda_{A1}^2}{2\lambda_{A1}+\mu_{A1}}$$

For the parallel structure TS in Figure 2-5(b), we have

$$p_{TS,f} = p_{TS1,f}\, p_{TS2,f} = \left(\frac{\lambda_{ts}}{\lambda_{ts}+\mu_{ts}}\right)^2,$$

$$p_{TS,s} = 1 - p_{TS,f} = 1 - \left(\frac{\lambda_{ts}}{\lambda_{ts} + \mu_{ts}} \right)^2 ,$$

$$\mu_{TS} = \mu_{TS1} + \mu_{TS2} = 2\mu_{ts},$$

$$\lambda_{TS} = \frac{Fr_{TS,f}}{p_{TS,s}} = \frac{Fr_{TS,s}}{p_{TS,s}} = \frac{p_{TS,f}\,\mu_{TS}}{p_{TS,s}} = \frac{2\lambda_{ts}^2}{2\lambda_{ts} + \mu_{ts}} .$$

Thus, we could get the system failure rate as

$$\lambda_{sys} = \lambda_{TS} + \lambda_A .$$

Therefore, the MTTF of the all-digital protection system is

$$MTTF = \frac{1}{\lambda_{sys}} = \frac{1}{\lambda_{TS} + \lambda_A}.$$

In order to get a comparable result with the non-repairable system, we use the same component failure rates as in [75], i.e. the Ethernet communication media $\lambda_{em} = 0.003 year^{-1}$ and all other components $\lambda_{ts} = \lambda_{mu} = \lambda_{sw} = \lambda_{pr} = 0.01 year^{-1}$. In addition, we assume that the Ethernet communication media could be fixed or replaced in 2 days and all other components in 7 days, i.e.

$$\mu_{em} = 1/(2days) = 182.5 year^{-1},$$

$$\mu_{ts} = \mu_{mu} = \mu_{sw} = \mu_{pr} = 1/(7days) = 52.14 year^{-1}.$$

These are perhaps conservative values for the repair rates of the components. And we calculate the MTTF of the repairable protection system as 21016 years which is much larger than 37.3 years as in [75].

2.3.2.2. MTTFF of the repairable protection system

For the MTTFF of an all-digital protection system, the formula that we used previously to analyze the basic systems is still valid. We rewrite this formula below for convenience.

$$MTTFF = p_+(0)(-R_{11})^{-1}U_k \tag{2.10}$$

However, it is really not simple to utilize this formula for practical calculations. Unlike the analysis of the basic structures, we do not know just at a glance how many success states this system would have. We only know its total number of states as $2^{12} = 4096$ since the system consists of 12 components. In addition, it seems that we also cannot give the details of vectors $p_+(0)$ and U_k unless we know the number of states of system success, or the dimension of the matrix R_{11}. But the details of R_{11} are even more difficult to know. So, we must use a systematic strategy to obtain the MTTFF value of the all-digital protection system. The key issue is that we can get R_{11} after we obtain the full system transition rate matrix R which is $2^{12} \times 2^{12}$ in its size. The strategy to obtain this is illustrated in the following steps.

2.3.2.2.1. *Step I: Initializing the state matrix*

We initially form a state matrix which can represent the status of the system and all of its components. In this state matrix, each row represents a distinct state of the

system and each column represents a component state. For a system consisting of n components, the size of this state matrix would be $2^n \times n$. For our all-digital protection system to be analyzed, this state matrix size is $2^{12} \times 12$. Now every element of this matrix represents the status of a component in a specific system state. If we use the values 0 and 1 indicating the success and failure states of a component, respectively, the complete system states can be represented by this state matrix consisting of exhaustive combinations of 0's and 1's as shown in Table 2-1.

Table 2-1 Initial state matrix

Components	TS1	MU1	EM1	SW1	EM3	PR1	TS2	MU2	EM2	SW2	EM4	PR2
State 0001	0	0	0	0	0	0	0	0	0	0	0	0
State 0002	0	0	0	0	0	0	0	0	0	0	0	1
State 0003	0	0	0	0	0	0	0	0	0	0	1	0
State 0004	0	0	0	0	0	0	0	0	0	0	1	1
State 0005	0	0	0	0	0	0	0	0	0	1	0	0
⋮	⋮	⋮	⋮	⋮	⋮	⋮	⋮	⋮	⋮	⋮	⋮	⋮
State 4092	1	1	1	1	1	1	1	1	1	0	1	1
State 4093	1	1	1	1	1	1	1	1	1	1	0	0
State 4094	1	1	1	1	1	1	1	1	1	1	0	1
State 4095	1	1	1	1	1	1	1	1	1	1	1	0
State 4096	1	1	1	1	1	1	1	1	1	1	1	1

2.3.2.2.2. *Step II: Identifying system states of success and failure*

It is natural to think that we can use the minimal cut set method to distinguish system states of success and failure. The procedure could be carried out in three steps: Firstly, we find all the minimal cut sets of the system; Secondly, we use minimal cut sets to find all the system states of failure; Finally, the rest of the states are the system states of success. However, this method is not smart and convenient for our all-digital architecture to be analyzed. One reason is that it is not easy to find out all the minimal cut sets if the number of components of the system is relatively large. Another reason is that there will be some overlapping system states of failure based on different minimal cut sets. Unless we can identify all the overlapping states, this method is prone to yield a wrong number of system states of failure.

Here we propose a better way to distinguish system states of success and failure for our all-digital architecture. Although this method is also based on the concept of cut set, the distinguishing difference is that we do not need to search all the minimal cut sets of the system. Since the reliability block diagram of this all-digital protection system can be decomposed into combinations of simple series and parallel structures, we can get the logical chain of the system as shown in Figure 2-6.

$$\text{System fails} \Leftrightarrow \begin{cases} \text{(TS) fails} \Leftrightarrow \begin{cases} \text{(TS1) fails} \\ \textit{AND} \\ \text{(TS2) fails} \end{cases} \\ \textit{OR} \\ \text{(A) fails} \Leftrightarrow \begin{cases} \text{(A1) fails} \Leftrightarrow \text{(MU1) } \textit{OR} \text{ (EM1) } \textit{OR} \text{ (SW1) } \textit{OR} \text{ (EM3) } \textit{OR} \text{ (PR1) fails} \\ \textit{AND} \\ \text{(A2) fails} \Leftrightarrow \text{(MU2) } \textit{OR} \text{ (EM2) } \textit{OR} \text{ (SW2) } \textit{OR} \text{ (EM4) } \textit{OR} \text{ (PR2) fails} \end{cases} \end{cases}$$

Figure 2-6. Logical chain of the system.

In the previous Step I of initializing the state matrix, we have already used the values 0 and 1 indicating the success and failure states of a component, respectively. Now in the logical chain in Figure 2-6, let us replace each component by its state value (0 or 1) and treat the conditions "AND" and "OR" as the corresponding logical operation symbols. Thus, the logical chain in Figure 2-6 is translated into a Boolean calculation. And the final result of the Boolean calculation is just the indication of the system state, i.e., the value 0 of "System fails" indicates the system success and the value 1 as system failure. If we scan each row of the initial state matrix already set up in Step I and do the Boolean calculation, all the system states can be distinguished as success or failure without omission or overlapping.

For our all-digital architecture to be analyzed, the number of states of system success and failure are counted to be 189 and 3907, respectively. After all the system states are identified, we can reorder for better use the initial state matrix as shown in Table 2-2, i.e., all the system states of success are moved to the first 189 rows of the state matrix and all the system states of failure are gathered in the latter part of 3907 rows in our case.

Table 2-2 Rearranged state matrix

Components		TS1	MU1	EM1	SW1	EM3	PR1	TS2	MU2	EM2	SW2	EM4	PR2
Success	State 0001	0	0	0	0	0	0	0	0	0	0	0	0
	⋮	⋮	⋮	⋮	⋮	⋮	⋮	⋮	⋮	⋮	⋮	⋮	⋮
	State 0189	1	1	1	1	1	1	0	0	0	0	0	0
Failure	State 0190	0	0	0	0	0	1	0	0	0	0	0	1
	⋮	⋮	⋮	⋮	⋮	⋮	⋮	⋮	⋮	⋮	⋮	⋮	⋮
	State 4096	1	1	1	1	1	1	1	1	1	1	1	1

2.3.2.2.3. *Step III: Forming the full system transition rate matrix R*

Since we have identified all the system states of success and failure and rearranged the state matrix, it is now possible for us to obtain the full system transition rate matrix *R*. However, the diagonal and off-diagonal elements of the transition rate matrix *R* are very different. They represent the single-step transition rates from a given state to itself and to another state, respectively. As a strategy, we need to know the off-diagonal elements of the transition rate matrix *R* first and then obtain the diagonal elements from the non-diagonal elements.

There are two types of relationships between any two system states [94]. Suppose we choose two arbitrary system states *i* and *j*. If we need at least two components to change their status for a transition between system states *i* and *j*, the interstate relationship is not a single-step transition and thus the corresponding transition rates do

not exist, i.e., the elements (i, j) and (j, i) of the matrix R are both zeroes. If, however, there is only one component, say component k, that changes its status between system states i and j, then the interstate relationship is indeed a single-step transition and the corresponding transition rates do exist. Further in this case, if the component k is working in system state i and fails in system state j, then the transition rate from state i to j is the failure rate of the component k, i.e., the element (i, j) of the matrix R is λ_k. Similarly, the transition rate from state j to i is the repair rate of the component k, i.e., the element (j, i) of the matrix R is μ_k. After we scrutinize all the interstate relationships of any two distinct system states, we can get all the off-diagonal elements of the transition rate matrix R. Figure 2-7 is a brief flow chart of this algorithm.

Now it is easy to calculate the diagonal elements of the full transition rate matrix R because they have a definite relationship with the off-diagonal ones of the same row [2], i.e.

$$r_{ii} + \sum_{j \neq i} r_{ij} = 0$$

wherein r_{ii} and r_{ij} represent diagonal and off-diagonal elements, respectively. The subscripts i and j here represent the indices of row and column of the matrix R, respectively. Then the diagonal elements can be obtained by the formula as below.

$$r_{ii} = -\sum_{j \neq i} r_{ij}$$

Thus, the full system transition rate matrix R can be obtained after we know all of its elements.

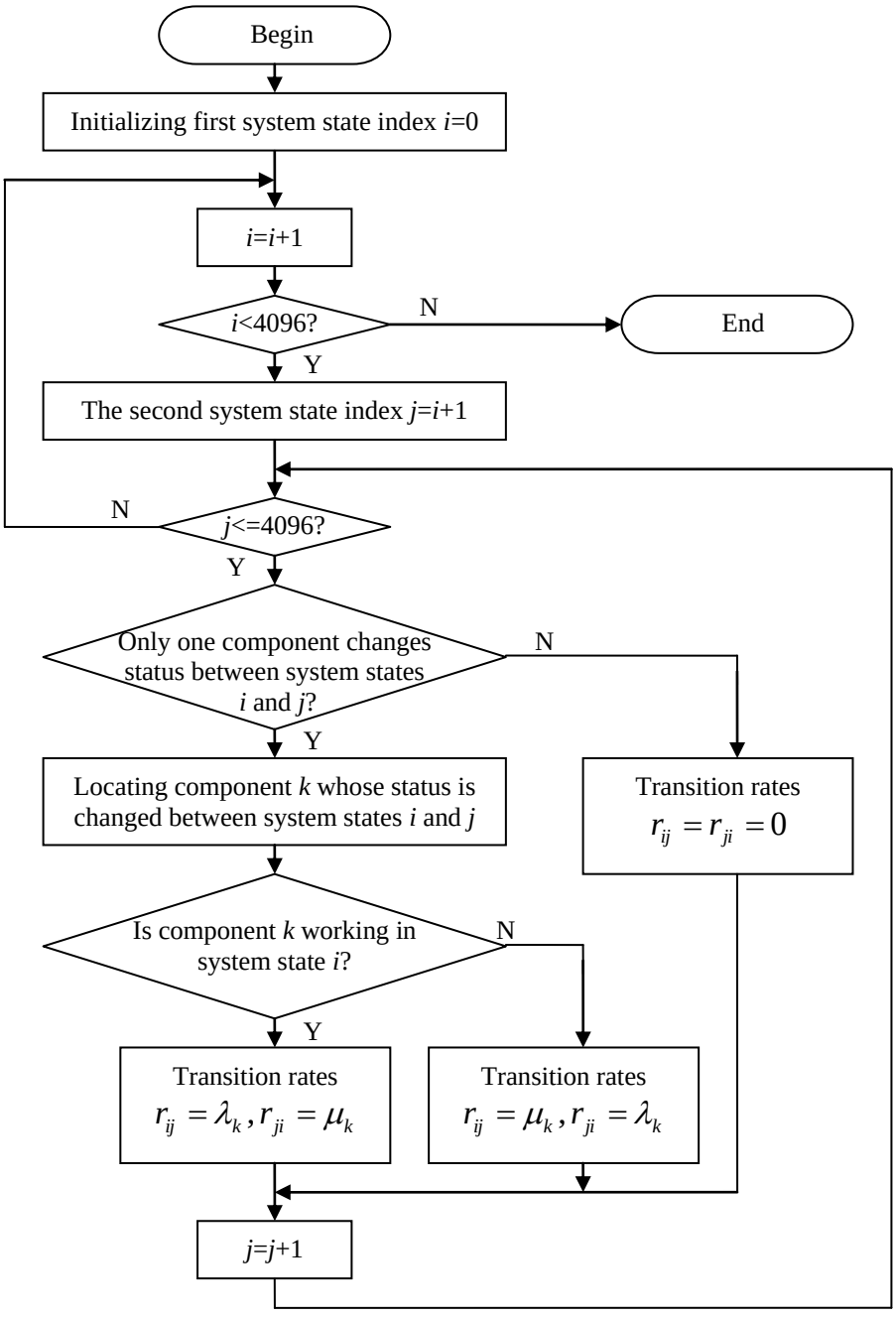

Figure 2-7. Algorithm to obtain off-diagonal elements of the matrix R.

2.3.2.2.4. *Step IV: Extracting the submatrix R_{11} from the full system transition rate matrix R*

If we form the full system transition rate matrix *R* based on the rearranged state matrix as shown in Table 2-2 of Step II, we can see that it is quite easy to obtain R_{11}, the set of transition rates between states of system success. Because all the system states of success are located in the first 189 rows of the rearranged state matrix, R_{11} is just the upper left square submatrix (size 189×189) of the matrix *R* (size 4096×4096) obtained in Step III. In a word, we can extract the submatrix R_{11} directly from the matrix *R* as shown in Figure 2-8.

$$
\begin{array}{c}
\leftarrow \ \textit{state } j \ \rightarrow \\
\uparrow \\
\textit{state } i \\
\downarrow
\end{array}
\underbrace{\left[\begin{array}{c:c}
R_{11} & R_{12} \\
(189 \times 189) & (189 \times 3907) \\
\cdots\ \cdots\ \cdots\ \cdots & \cdots\ \cdots\ \cdots\ \cdots \\
\hdashline
R_{12} & R_{22} \\
(3907 \times 189) & (3907 \times 3907)
\end{array}\right]}_{R(4096 \times 4096)}
$$

Figure 2-8. Extraction of submatrix R_{11} from matrix R.

2.3.2.2.5. *Step V: Computing the MTTFF of the system*

As the final step of the strategy, we are now able to compute the MTTFF of the all-digital protection system by using (2.10). Since we have obtained the submatrix R_{11}, we can give the details of vectors $p_+(0)$ and U_k as following.

The probability vector of system success states for the initial state (all components up) is

$$p_+(0) = [1 \quad \underbrace{0 \quad 0 \quad \cdots \quad 0}_{188\ 0\text{'s}}].$$

The unit vector of dimension *k* which is equal to the number of states of system success is

$$U_k = [\underbrace{1 \quad 1 \quad \cdots \quad 1}_{189\ 1\text{'s}}]^T.$$

Using the same failure and repair rates of the components as we did in calculating the repairable MTTF, we figure out that the MTTFF of this repairable all-digital protection system is 21029 years.

2.3.3. *The Influence of Repair in Protection System Modeling*

2.3.3.1. Difference of repairable and non-repairable system MTTF and MTTFF

The calculated results of our all-digital protection system model are summarized in Table 2-3. We can see that for the repairable model, the value of MTTFF is larger

than that of MTTF though the difference is rather small. In addition, the values of repairable MTTFF and MTTF are both remarkably larger than those of corresponding non-repairable indices.

Table 2-3 Calculation of repairable and non-repairable system models

Indices	Repairable system model	Non-repairable system model
MTTFF	21029 years	37.3 years
MTTF	21016 years	37.3 years

The relative behavior of MTTFF and MTFF of repairable and non-reparable all-digital system can be explained and proven as follows. Our all-digital protection system can, in fact, be regarded as a combination of basic parallel and series structures. Since the basic series structures have no influence on the differences of repairable and non-repairable MTTF and MTTFF, we can intuitively sense that their differences of the overall protection system are the accumulated contributions of its basic parallel structures. The proof is briefly given below.

Let us first look at the series chain A1 in Figure 2-5. If it is non-repairable, its reliability would be

$$\begin{aligned} R_{sys}(t) &= p_{A1,s} = p_{MU1,s}\, p_{EM1,s}\, p_{SW1,s}\, p_{EM3,s}\, p_{PR1,s} \\ &= e^{-\lambda_{mu}t} e^{-\lambda_{em}t} e^{-\lambda_{sw}t} e^{-\lambda_{em}t} e^{-\lambda_{pr}t} \\ &= e^{-(\lambda_{mu}+2\lambda_{em}+\lambda_{sw}+\lambda_{pr})t} \end{aligned} \quad .$$

Hence,

$$MTTFF_N = MTTF_N = \int_0^\infty R_{sys}(t)dt = \frac{1}{\lambda_{mu} + 2\lambda_{em} + \lambda_{sw} + \lambda_{pr}}.$$

However, if A1 is repairable, we already have previously

$$\lambda_{A1} = \lambda_{mu} + 2\lambda_{em} + \lambda_{sw} + \lambda_{pr}.$$

Thus,

$$MTTF_R = \frac{1}{\lambda_{A1}} = \frac{1}{\lambda_{mu} + 2\lambda_{em} + \lambda_{sw} + \lambda_{pr}}.$$

Alternatively, it is not difficult to get

$$R_{11} = -(\lambda_{mu} + 2\lambda_{em} + \lambda_{sw} + \lambda_{pr}),$$

$$p_+(0) = 1,$$

$$U_k = 1,$$

$$MTTFF_R = p_+(0)(-R_{11})^{-1}U_k = \frac{1}{\lambda_{mu} + 2\lambda_{em} + \lambda_{sw} + \lambda_{pr}}.$$

Therefore,

$$MTTFF_R = MTTF_R = MTTFF_N = MTTF_N.$$

Similarly, the series chain A2 will also have the same result.

Next, let us regard the series chains A1 and A2 as two composite components with their derived transition rates. They definitely form a basic parallel structure, i.e. A in Figure 2-5, which has been discussed in Section 2.2. Once we have derived the equivalent transition rates for A1 and A2, the expressions (2.7), (2.8), and (2.9) can be used. The only difference is that we need to substitute the subscripts A1 for 1 and also A2 for 2.

Similarly, components TS1 and TS2 form a basic parallel structure, i.e. TS in Figure 2-5. We can also obtain the results using (2.7), (2.8), and (2.9), just substituting the subscripts TS1 for 1 and TS2 for 2.

Finally, TS and A compose the overall protection system which is just a simple series structure with only two composite components. As discussed in Section 2.2, we can easily obtain

$$MTTFF_R = MTTF_R = \frac{1}{\lambda_{TS,R} + \lambda_{A,R}},$$

$$MTTFF_N = MTTF_N = \frac{1}{\lambda_{TS,N} + \lambda_{A,N}}.$$

Here $\lambda_{TS,R}$, $\lambda_{A,R}$ refer to the repairable systems and $\lambda_{TS,N}$, $\lambda_{A,N}$ are for non-repairable systems.

It can be seen from the above derivation that, the parallel structure provides the actual contribution to the differences of the MTTFF and MTTF of our all-digital protection system.

Since all the transition rates are positive values, using (2.7), (2.8), and (2.9) we can conclude the following for our protection system discussed:

(1) The repairable system MTTFF is undoubtedly larger than its repairable MTTF;

(2) The repairable MTTFF is unconditionally larger than its non-repairable MTTFF;

(3) The repairable MTTF is generally greater than but under certain conditions can be smaller than its non-repairable MTTF. In other words, the repairable MTTF cannot be guaranteed to be greater than the non-repairable MTTF.

Further for the third point, if we choose parameters in (2.9) such that $\mu_{A2} < \lambda_{A1}$ and $\mu_{A1} < \lambda_{A2}$, and at the same time that $\mu_{TS2} < \lambda_{TS1}$ and $\mu_{TS1} < \lambda_{TS2}$, then the repairable MTTF will be smaller than the non-repairable one. A simple way to guarantee this is just choose failure rates of all the components sufficiently larger than the corresponding repair rates, as we will see later. Our previous numerical data shows that the repairable MTTF is greater than the non-repairable one. This is because all the component repair rates are chosen much bigger than the corresponding failure rates, which is normal in industrial reality.

By the way, there is also a practical meaning to keep the repairable MTTF and MTTFF larger than the non-repairable ones. In power industry, if no in-time remedy is done for an out-of-work component of a still working protection system, the system will tend towards a critical situation and eventually go down much more quickly as more and more components go out of work.

2.3.3.2. The influence of repair on system modeling concerning MTTF and MTTFF

In order to observe the varying trend of the system MTTF and MTTFF with repair, we fix all the component failure rates as in previous data and change simultaneously the entire component repair rates in multiples of the previous ones. The

result is shown in Table 2-4 below. The value of non-repairable MTTF(F) is also included in Table 2-4 for comparison.

Table 2-4 Influence of repair on system MTTF and MTTFF

Multiples of the original μ's	MTTFF (years)	MTTF (years)
10	209996	209983
5	105015	105002
2	42026	42013
1	21029	21016
2^{-1}	10531	10518
5^{-1}	4232	4219
10^{-1}	2133	2120
10^{-2}	243	230
10^{-3}	55.9	41.1
10^{-4}	39.3	23.0
10^{-5}	37.9	21.9
10^{-6}	37.7	21.8
Non-repairable system	37.3	

From the data in Table 2-4, we can see that as component repair rates increase, the system MTTF and MTTFF increase simultaneously. When component repair rates decrease, the system MTTF and MTTFF also decrease simultaneously. In other words, the system MTTF and MTTFF are monotonically influenced by the component repair

rates. This sounds reasonable since higher repair rates actually mean that faster remedies could be made to the failed components. Thus the mean time to failure (MTTF) and the mean time to first failure (MTTFF) of the system are likely to be prolonged.

Table 2-4 justifies our previous findings. First, we find in Table III that for any given set of component transition rates, the value of repairable MTTFF is always larger than that of repairable MTTF. Secondly, the value of repairable MTTFF is surely greater than that of non-repairable MTTFF.

In addition, as all the component repair rates decrease towards zero, the value of repairable MTTFF approaches just the value of the non-repairable system MTTFF. We can naturally see that the non-repairable system MTTFF is just the lower limit of the repairable system MTTFF. This can be proved as follows.

As the conclusion of previous discussion, the parallel structure is the actual contributor to the differences of the MTTFF and MTTF of our all-digital protection system. Since we can obtain the result for our protection system in the same manner as for basic parallel structure just by the substitution of subscripts, let us look at the parameters in (2.8). If the failure rates are fixed and the repair rates tends to zero, we have

$$\lim_{\substack{\mu_1 \to 0 \\ \mu_2 \to 0}} (MTTFF_R - MTTFF_N) = \lim_{\substack{\mu_1 \to 0 \\ \mu_2 \to 0}} \left(\frac{\lambda_1 \lambda_2 (\mu_1 + \mu_2) + (\lambda_1 + \lambda_2) \mu_1 \mu_2}{\lambda_1 \lambda_2 (\lambda_1 + \lambda_2)^2} \right).$$

It is obvious that the numerator of this limit tends to zero while its denominator tends to a finite non-zero value. Therefore,

$$\lim_{\substack{\mu_1 \to 0 \\ \mu_2 \to 0}} (MTTFF_R - MTTFF_N) = 0$$

which means that a repairable system will eventually turn out to be a non-repairable one as all the repair rates become zero.

However, the value of repairable MTTF is NOT guaranteed to be greater than that of non-repairable one. In fact, as the repair rates decrease to a certain value (e.g. 10^{-4} smaller in magnitude of the original μ's as in Table 2-4), the value of repairable MTTF would become smaller than that of non-repairable one. We further observe that the important condition that the repair rate of each component being greater than the corresponding failure rate is no longer satisfied at this time. The repairable MTTF also approaches a value but smaller than that of non-repairable MTTF, as all the component repair rates go down towards zero. It should, however, be noted that the equations used for computing the repairable MTTF assume a finite repair rate and cannot be used when the repair rate is actually zero.

In summary, as all the component repair rates decrease, the value of repairable system MTTFF approaches that of non-repairable one, while the value of repairable MTTF approaches a value smaller than that of non-repairable one. Since a non-repairable system has the same value for MTTFF and MTTF, it just reflects the fact that the MTTF of a non-repairable system has indeed the same meaning as its MTTFF. The interesting relationship between repairable and non-repairable system MTTF and MTTFF can be clearly seen in Figure 2-9 which is drawn from data in Table 2-4.

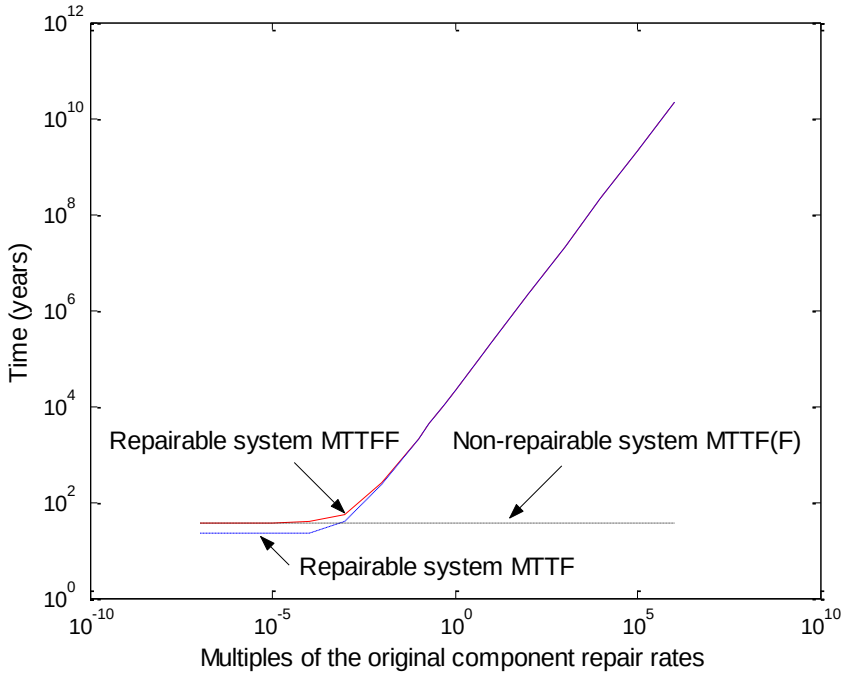

Figure 2-9. The relationship between repairable and non-repairable system MTTFF and MTTF.

We also find in Table 2-3 and Table 2-4 that many repairable MTTF and MTTFF data seems too large to be acceptable in reality. This is because the pre-chosen component failure rates are very small in magnitude compared to the repair rates that we chose. If we fix our component repair rates and change simultaneously the entire failure rates in multiples of the original ones, we can find the computed results become more conservative as shown in Table 2-5 below.

Table 2-5 Influence of failure rate on system MTTF and MTTFF

Multiples of the original λ's	MTTFF (years)	MTTF (years)
1	21029	21016
2	5266	5259
5	846	844
10	213	212
20	54.2	53.5
50	9.06	8.80
100	2.43	2.30

2.4. Summary

It is shown that repair plays an important role in all-digital protection system modeling concerning MTTF and MTTFF. For the all-digital protection system that we have analyzed, we can draw the following conclusions.

(1) For the given component failure rates, the system MTTF and MTTFF are monotonically influenced by the component repair rates. As the component repair rates increase, the system MTTF and MTTFF increase simultaneously. When the component repair rates decrease, the system MTTF and MTTFF also decrease simultaneously.

(2) For the given component transition rates, the value of repairable system MTTFF is always larger than that of repairable system MTTF irrespective of how small the difference is, i.e.

$$MTTFF_R > MTTF_R .$$

(3) For the given component transition rates, the value of repairable system MTTFF is greater than that of non-repairable system MTTFF, i.e.

$$MTTFF_R > MTTFF_N .$$

In addition, as the component repair rates decrease towards zero while the component failure rates stay fixed, the value of repairable system MTTFF approaches that of non-repairable system MTTFF. A repairable system will eventually turn out to be a non-repairable system as all of its component repair rates become zero.

(4) The value of repairable system MTTF is NOT guaranteed to be greater than that of non-repairable system MTTF. In fact, as the component repair rates decrease below a certain level with the component failure rates unchanged, the value of repairable system MTTF would become smaller than that of non-repairable system MTTF. This case is always accompanied by the violation of generally assumed condition that the repair rate of each component is greater than the failure rates of all other components. As component repair rates decrease towards zero, the value of repairable system MTTF approaches a value smaller than that of non-repairable system MTTF.

Perhaps the most important point for practical purposes is that if an all-digital protection system is indeed repairable but is modeled in a non-repairable manner for analysis, the calculated values for the mean time to failure (MTTF) and the mean time to first failure (MTTFF) could be grossly pessimistic [95].

3. RELIABILITY EVALUATION OF A CONCEPTUAL ALL-DIGITAL SPECIAL PROTECTION SYSTEM ARCHITECTURE FOR THE FUTURE SMART GRID *

3.1. Introduction

The Special Protection System (SPS), also called Remedial Action Schemes (RAS) or special protection schemes, is an automatic protection system which is designed to detect abnormal or predetermined system conditions, and take corrective actions to maintain system reliability [96]. It is well accepted that the SPS has critical influence on the power system reliability [97], [98]. Therefore, the reliability of SPS has always been an important issue in the research area of SPS [99]-[102].

---

* Part of this section is reprinted from copyrighted material with permission from IEEE.

The smart grid is emerging with the penetration of information-age technologies bringing potentially significant changes in the development of instrumentation, monitoring, control, and protection systems in power industry, including SPS. As microprocessors become more powerful with even lower cost, they could prevail in the future for the choice of SPS logic solvers. It is notable that digital communication will play an important role in the future power industry. A new concept of digital process bus has been presented in IEC 61850 [73], [74]. With the realization of the electronic hardware sensor, a "one unique" secondary platform, called merging unit (MU), has been developed to interface all other substation equipments such as protection, metering and control devices, also called Intelligent Electronic Devices (IED) [103]. Using the IEC 61850 process bus, a merging unit is capable of executing the trip and control commands as well as communicating to IED its input signals including AC sampled values, contact status information, and a variety of transducer inputs [104]-[106]. Although sensors and actuators of the SPS are different in functions, their data flow can now be integrated in the same platform of the merging unit.

In addition, non-conventional instrument transformers have already been available which can directly output digital signals of current and voltage measurements [103], [107]. These digital signals are all conveyed to the IED through the IEC 61850 process bus. With the help of the Global Positioning System (GPS), a device capable of synchronization called Phasor Measurement Unit (PMU) has been developed rapidly. PMU can provide synchronous measurements of phasors for the same time stamp and

become the foundation of various kinds of wide-area protection and control schemes [108]-[111]. If PMU is utilized as the SPS measurement device, the voltage and current synchrophasors over a large area can be easily obtained and the SPS actually becomes a powerful scheme with capability of wide-area protection and control [112].

It seems that the power industry is getting ready for more aggressive steps by replacing switchyard copper wires with plug-and-play fiber-based schemes [113]. We can envision that a possible SPS scheme in the future can be typically composed of digital logic solvers, Ethernet switches, digital communication media, merging units, time synchronization sources, and phasor measurement units. All the signals in them are digitally conveyed through a virtual IEC 61850 process bus. Since the all-digital SPS scheme has obviously more electronic components than a conventional hardwired one, it should have some influence on its reliability. Thus, reliability analysis of the all-digital SPS can play an important role in evaluating its merits and guiding its development in a cost-effective and reliable manner.

The remainder of this section is organized as follows. Section 3.2 firstly proposes a conceptual all-digital SPS architecture. Section 3.3 then illustrates the reliability evaluation of the proposed SPS architecture by using the network reduction method and the Markov modeling method to compute the specific reliability indices. Section 3.4 gives the numerical case study of the proposed SPS architecture. Section 3.5 is the summary of this section.

3.2. Conceptual All-digital SPS Architecture

There could be various configurations and realizations for an all-digital SPS in the future. In the area of all-digital protection systems, researchers have already presented some possible architectures [75]. Based on the idea of these configurations, here we propose a conceptual all-digital SPS architecture as consideration for future SPS development as shown in Figure 3-1.

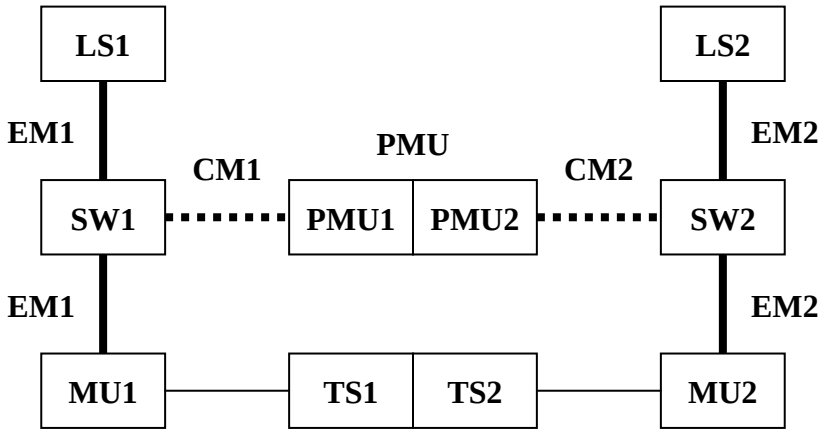

Figure 3-1. A conceptual all-digital SPS architecture.

Because SPS has critical influence on the reliability of the power system, two redundant functional sets are considered in order to achieve a high level of SPS reliability. In the architecture of Figure 3-1, each set can perform the full SPS function independently and consists of a digital logic solver (LS), an Ethernet switch (SW), the Ethernet communication media (EM), the merging unit devices (MU), a time synchronization source (TS), the phasor measurement unit equipments (PMU), and the

digital communication media channels (CM) for PMU. In more detail, components TS1, MU1, EM1, SW1, LS1, PMU1, and CM1 constitute one set of SPS while components TS2, MU2, EM2, SW2, LS2, PMU2, and CM2 make up the other set.

Time synchronization is so important to an all-digital system that the signal processing is meaningless without a proper time stamp. In order to reduce the probability of system failures because of time synchronization problems, the time synchronization sources of the two sets are shared with each other. No matter which source fails (TS1 or TS2), the other is assumed available immediately for the set of SPS missing its original time synchronization source.

A merging unit device can have several functional modules processing different signals simultaneously. If the SPS is complex and needs to control several equipments, a group of merging unit devices may also be necessary to meet the requirements. But for simplicity, we do not distinguish either the modules or differences of the merging units. Here we just assume that one merging unit (MU1 or MU2) alone can perform the full function needed for one set of SPS.

Phasor measurement units are preferred for future SPS applications especially in case the information of a large area is needed to determine the logic of SPS alarm and/or actuation. PMU Redundancy is also necessary due to its unique significance in data collection. Thus, two PMU equipments are considered for each location as shown in Figure 3-2, where $PMU1_i$ and $PMU2_i$ are mutual backup to each other for location i. Therefore, PMU1 and PMU2 in Figure 3-1 are not two individual units but two groups

of PMU sets. Specifically, PMU1 is the group of apparatus $PMU1_i$ $(i = 1,2,\cdots,n)$ and PMU2 is the group of apparatus $PMU2_i$ $(i = 1,2,\cdots,n)$.

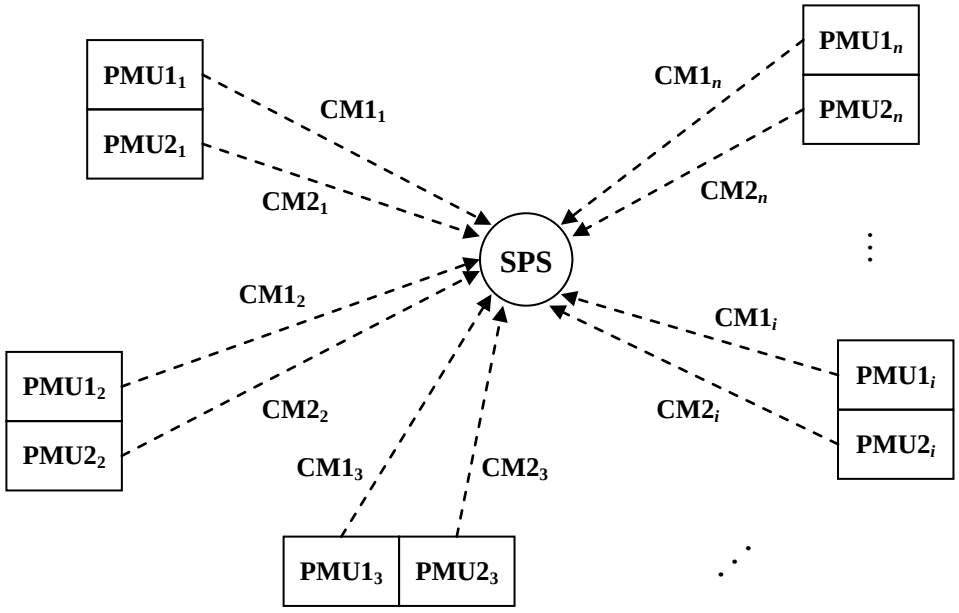

Figure 3-2. Illustration of PMU configuration for SPS implementation.

Similarly, CM1 and CM2 in Figure 3-1 are also two groups of digital communication media channels $CM1_i$ $(i = 1,2,\cdots,n)$ and $CM2_i$ $(i = 1,2,\cdots,n)$, respectively as shown in Figure 3-2. Here we suppose $CM1_i$ and $CM2_i$ are dedicated to the two SPS functional sets, respectively. However, the information of location *i*, i.e. data of $PMU1_i$ and $PMU2_i$ can be transmitted to SPS through either of the two channels $CM1_i$ and $CM2_i$ for best usage and availability of PMU resources.

We will analyze the proposed all-digital SPS scheme using a repairable model because in practice, if there is any fault in the component recognized by either self-test

routine or manual test procedure, utilities would either fix or replace the problematic component so as to keep the whole protection and control system up and ready to perform. In addition, we also make some other assumptions for feasible reliability analysis such as: (1) The components of the all-digital SPS are independent of each other; (2) The component state durations are exponentially distributed; (3) The power supplies to SPS are extremely reliable; (4) The communication interface is a part of the host device (i.e. MU, SW, LS, PMU, etc.) and its reliability is included in the host device.

Although the SPS scheme in Figure 3-1 is only one of the possible architectures, here we focus on how to apply reliability analysis approaches to the conceptual all-digital SPS in the future. Evaluation of important reliability indices such as probability of system failures, frequency and duration of system failures, the mean time to failure (MTTF), and the mean time to first failure (MTTFF) will be illustrated in detail. For other possible SPS configurations, their reliability analysis can be conducted in a similar way.

3.3. Reliability Evaluation of the SPS Architecture

In the proposed SPS architecture, some components are exclusively used for one set of SPS such as the digital logic solver, the Ethernet switch with its corresponding Ethernet media, the merging unit, and the digital communication media channel for PMU. If any of these components fails, this set of SPS can no longer perform its

function properly. Thus, these components are actually functioning in a series relationship from reliability standpoint. As for the time synchronization source and the PMU, they are not designed as dedicated to only one specific set of SPS. Instead, their redundancies are for the reliability of the whole SPS application. Therefore, we can draw the reliability block diagram of the proposed SPS architecture according to the functional relationships of the components as shown in Figure 3-3.

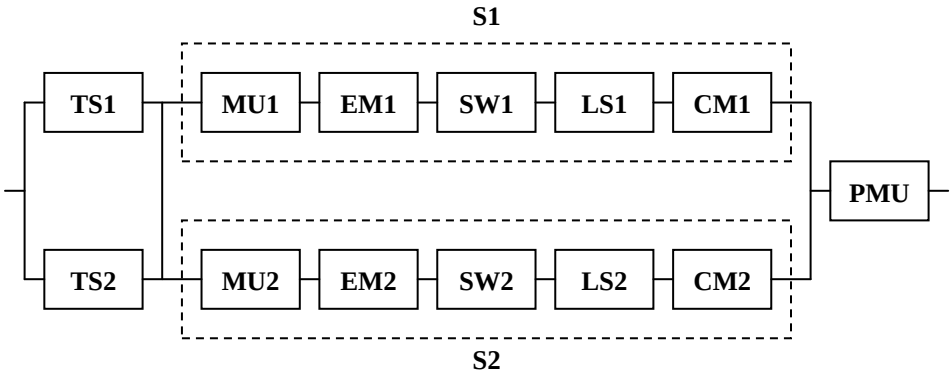

Figure 3-3. SPS reliability block diagram.

In fact, PMU, CM1, and CM2 in Figure 3-3 are conceptually aggregate components including all necessary PMU locations for SPS implementation. According to previous configuration assumptions, their reliability block diagram can be detailed as in Figure 3-4.

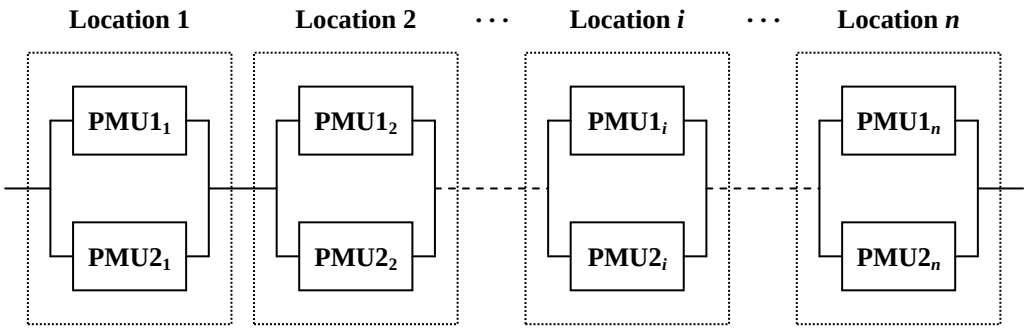

(a) Aggregate component PMU

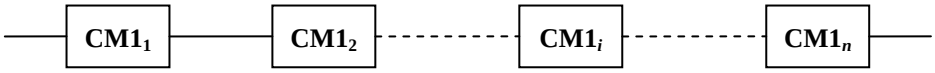

(b) Aggregate component CM1

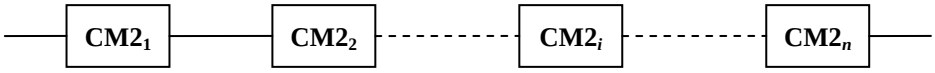

(c) Aggregate component CM2

Figure 3-4. Reliability block diagram of aggregate components.

In general, it is not easy to obtain the reliability indices directly for such a complex system. However, we can use the network reduction method to analyze the SPS reliability. Here we suppose the failure and repair rates of a general component *i* by λ_i and μ_i, respectively. In addition, we use $p_{i,s}, p_{i,f}$ and $f_{i,s}, f_{i,f}$ for component *i* to represent the probabilities of its success and failure states, and the steady state frequencies encountering its state of success and failure, respectively.

3.3.1. *Treatment of Aggregate Components*

In order to reduce the dimension of the problem, we need to merge the models of the aggregate components first before analyzing the system reliability. It also helps us understand the problem from a hierarchical point of view. We can achieve this by using the concept of equivalent transition rate [91]. Then the aggregate component will have the same values of transition rates, state probabilities, and corresponding frequencies as those of its representing group of individual elements taken as an integral part.

3.3.1.1. Aggregate component PMU

For each location *i*, PMU1$_i$ and PMU2$_i$ are in parallel as we can see in Figure 3-4(a). Hence, the equivalent repair rate is

$$\mu_{PMUi} = \sum_{j=1}^{2} \mu_{PMUji} \ . \tag{3.1}$$

The state probabilities are

$$p_{PMUif} = \prod_{j=1}^{2} p_{PMUjif} = \prod_{j=1}^{2} \frac{\lambda_{PMUji}}{\lambda_{PMUji} + \mu_{PMUji}}, \tag{3.2}$$

$$p_{PMUis} = 1 - p_{PMUif} = 1 - \prod_{j=1}^{2} \frac{\lambda_{PMUji}}{\lambda_{PMUji} + \mu_{PMUji}} \ . \tag{3.3}$$

The steady state frequencies are

$$f_{PMUi,f} = f_{PMUi,s} = \left(\prod_{j=1}^{2} \frac{\lambda_{PMUji}}{\lambda_{PMUji} + \mu_{PMUji}} \right) \left(\sum_{j=1}^{2} \mu_{PMUji} \right). \tag{3.4}$$

The equivalent failure rate is

$$\lambda_{PMUi} = \frac{f_{PMUi,f}}{p_{PMUi,s}} = \frac{\left(\prod_{j=1}^{2} \frac{\lambda_{PMUji}}{\lambda_{PMUji} + \mu_{PMUji}}\right)\left(\sum_{j=1}^{2} \mu_{PMUji}\right)}{1 - \prod_{j=1}^{2} \frac{\lambda_{PMUji}}{\lambda_{PMUji} + \mu_{PMUji}}}. \tag{3.5}$$

For the aggregate component PMU, it is all locations connected in series as shown in Figure 3-4(a). Thus, the equivalent failure rate is

$$\lambda_{PMU} = \sum_{i=1}^{n} \lambda_{PMUi} \ . \tag{3.6}$$

The state probabilities are

$$p_{PMU,s} = \prod_{i=1}^{n} p_{PMUi,s} = \prod_{i=1}^{n} \frac{\mu_{PMUi}}{\lambda_{PMUi} + \mu_{PMUi}}, \tag{3.7}$$

$$p_{PMU,f} = 1 - p_{PMU,s} = 1 - \prod_{i=1}^{n} \frac{\mu_{PMUi}}{\lambda_{PMUi} + \mu_{PMUi}}. \tag{3.8}$$

The steady state frequencies are

$$f_{PMU,s} = f_{PMU,f} = \left(\prod_{i=1}^{n} \frac{\mu_{PMUi}}{\lambda_{PMUi} + \mu_{PMUi}}\right)\left(\sum_{i=1}^{n} \lambda_{PMUi}\right). \tag{3.9}$$

The equivalent repair rate is

$$\mu_{PMU} = \frac{f_{PMU,s}}{p_{PMU,f}} = \frac{\left(\prod_{i=1}^{n} \frac{\mu_{PMUi}}{\lambda_{PMUi} + \mu_{PMUi}}\right)\left(\sum_{i=1}^{n} \lambda_{PMUi}\right)}{1 - \prod_{i=1}^{n} \frac{\mu_{PMUi}}{\lambda_{PMUi} + \mu_{PMUi}}}. \tag{3.10}$$

3.3.1.2. Aggregate components CM1 and CM2

The aggregate components CM1 and CM2 are both simple series chains as we can see in Figure 3-4(b) and Figure 3-4(c), respectively. Similar to handling the aggregate component PMU, we can obtain the equivalent transition rates for CM1 and CM2 as below, where $j \in \{1,\ 2\}$.

$$\lambda_{CMj} = \sum_{i=1}^{n} \lambda_{CMji} \tag{3.11}$$

$$\mu_{CMj} = \frac{\left(\prod_{i=1}^{n} \frac{\mu_{CMji}}{\lambda_{CMji} + \mu_{CMji}} \right) \left(\sum_{i=1}^{n} \lambda_{CMji} \right)}{1 - \prod_{i=1}^{n} \frac{\mu_{CMji}}{\lambda_{CMji} + \mu_{CMji}}} \tag{3.12}$$

After we have obtained the equivalent transition rates of the aggregate components, we can from now on regard PMU, CM1, and CM2 as if they were single components in the SPS reliability block diagram of Figure 3-3.

3.3.2. *Reliability Analysis of SPS*

3.3.2.1. Reliability analysis by using the network reduction method

As we observe in Figure 3-3, components MU1, EM1, SW1, LS1, and CM1 comprise the subsystem S1 of a series structure. If we regard S1 as a new composite component using the concept of equivalent transition rate again, this composite

component will have the same values of failure and repair rates, probabilities of success and failure states, and frequencies of encountering success and failure states as the original subsystem. Similarly, we can use another composite component to represent the series subsystem S2 formed by components MU2, EM2, SW2, LS2, and CM2. Then the reliability block diagram can be reduced to a simpler one as shown in Figure 3-5. The equivalent transition rates of subsystems S1 and S2 can be calculated as following, where we suppose $Sj = \{MUj,\ EMj,\ SWj,\ LSj,\ CMj\},\ j \in \{1,\ 2\}$.

$$\lambda_{Sj} = \sum_{i \in Sj} \lambda_i \tag{3.13}$$

$$\mu_{Sj} = \left(\prod_{i \in Sj} \frac{\mu_i}{\lambda_i + \mu_i} \right) \left(\sum_{i \in Sj} \lambda_i \right) \Bigg/ \left(1 - \prod_{i \in Sj} \frac{\mu_i}{\lambda_i + \mu_i} \right) \tag{3.14}$$

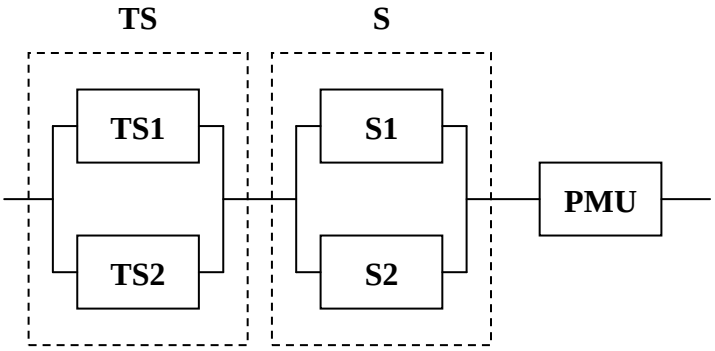

Figure 3-5. Reduction of SPS reliability block diagram.

Now let us see the reduced SPS reliability block diagram of Figure 3-5. There are two parallel structures in this diagram, i.e. components TS1 and TS2 comprise the parallel subsystem TS, while the composite components S1 and S2 form the parallel subsystem S. Again, if we regard these subsystems as two composite components in a

higher level, we can further simplify the SPS reliability block diagram to a much concise one as shown in Figure 3-6. By the concept of equivalent transition rate, the new higher-level composite components will have the same values of transition rates, state probabilities, and corresponding frequencies as the original subsystems TS and S, respectively. The equivalent transition rates of the higher-level subsystems TS and S can be calculated as follows, where we suppose $i \in \{TS,\ S\}$.

$$\mu_i = \sum_{j=1}^{2} \mu_{ij} \tag{3.15}$$

$$\lambda_i = \left(\prod_{j=1}^{2} \frac{\lambda_{ij}}{\lambda_{ij} + \mu_{ij}} \right) \left(\sum_{j=1}^{2} \mu_{ij} \right) \Bigg/ \left(1 - \prod_{j=1}^{2} \frac{\lambda_{ij}}{\lambda_{ij} + \mu_{ij}} \right) \tag{3.16}$$

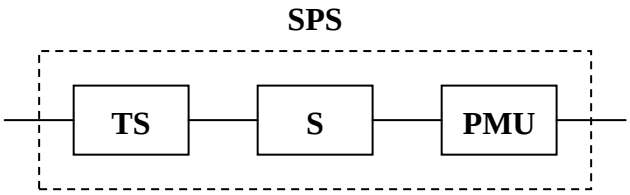

Figure 3-6. Simplified SPS reliability block diagram.

The simplified SPS reliability block diagram of Figure 3-6 consists of only three composite components in series. Thus, it is now easy to get the reliability indices of the whole system of SPS using the parameters of composite components derived previously.

The system reliability of SPS (i.e. probability of SPS success) is

$$p_{SPS,s} = \frac{\mu_{TS}\mu_S\mu_{PMU}}{(\lambda_{TS} + \mu_{TS})(\lambda_S + \mu_S)(\lambda_{PMU} + \mu_{PMU})}. \tag{3.17}$$

The system failure rate of SPS is

$$\lambda_{SPS} = \lambda_{TS} + \lambda_S + \lambda_{PMU}. \tag{3.18}$$

The frequency of SPS system failure is

$$f_{SPS,f} = \frac{\mu_{TS}\mu_S\mu_{PMU}(\lambda_{TS} + \lambda_S + \lambda_{PMU})}{(\lambda_{TS} + \mu_{TS})(\lambda_S + \mu_S)(\lambda_{PMU} + \mu_{PMU})}. \tag{3.19}$$

The mean cycle time of SPS is

$$MCT = \frac{1}{f_{SPS,f}} = \frac{(\lambda_{TS} + \mu_{TS})(\lambda_S + \mu_S)(\lambda_{PMU} + \mu_{PMU})}{\mu_{TS}\mu_S\mu_{PMU}(\lambda_{TS} + \lambda_S + \lambda_{PMU})}. \tag{3.20}$$

The Mean Down Time (MDT) of SPS is

$$MDT = \frac{(\lambda_{TS} + \mu_{TS})(\lambda_S + \mu_S)(\lambda_{PMU} + \mu_{PMU}) - \mu_{TS}\mu_S\mu_{PMU}}{\mu_{TS}\mu_S\mu_{PMU}(\lambda_{TS} + \lambda_S + \lambda_{PMU})}. \tag{3.21}$$

The Mean Time To Failure (MTTF) represents the average time between system breakdowns or loss of service. For reasons of avoiding confusion, the same concept is sometimes expressed as the Mean Up Time (MUT) in the system modeling with repair. Here for our SPS architecture

$$MTTF = MUT = MCT - MDT = \frac{1}{\lambda_{SPS}} = \frac{1}{\lambda_{TS} + \lambda_S + \lambda_{PMU}}. \tag{3.22}$$

3.3.2.2. Reliability analysis by using the Markov modeling method

We already know from Section 2 that the value of Mean Time To First Failure (MTTFF) cannot be obtained from the previous network reduction method. In fact, the calculation of MTTFF is more complex than that of MTTF. Based on the model of

continuous parameter Markov process, we can derive the ultimate formula for calculating MTTFF using the transition rate matrix of the system as follows [2].

$$MTTFF = p_+(0)(-R_{11})^{-1}U_k \tag{3.23}$$

Here, R_{11} is the sub-matrix of the full system transition rate matrix $R = \begin{bmatrix} R_{11} & R_{12} \\ R_{21} & R_{22} \end{bmatrix}$ and represents the set of transition rates from system success to system success. $p_+(0)$ is the probability row vector of system success states for the initial state (i.e. all components up), while U_k is the unit column vector of dimension k which is equal to the number of states of system success.

In practice it is not simple to utilize this formula for computing the MTTFF of the SPS. So, we must use a systematic strategy to obtain the MTTFF value of our SPS. The key issue is that we can get R_{11} after we obtain the full system transition rate matrix R which is $2^{13} \times 2^{13}$ or 8192×8192 in its size. The implementation of this strategy is already illustrated in detail in Section 2.3.2.2. As a result, the structural expressions of the parameters needed in (3.23) are illustrated as follows.

$$\begin{array}{c} \\ \uparrow \\ state\ i \\ \downarrow \end{array} \overbrace{\begin{array}{c} \leftarrow\ state\ j\ \rightarrow \\ \left[\begin{array}{c:c} R_{11} & R_{12} \\ (189 \times 189) & (189 \times 8003) \\ \cdots\ \cdots\ \cdots\ \cdots & \cdots\ \cdots\ \cdots\ \cdots \\ R_{12} & R_{22} \\ (8003 \times 189) & (8003 \times 8003) \end{array}\right] \end{array}}^{R(8192 \times 8192)}$$

$$p_+(0) = (1 \underbrace{\ 0\ \ 0\ \ \cdots\ \ 0}_{188\ \ 0\text{'s}})$$

$$U_k = (\underbrace{1 \quad 1 \quad \cdots \quad 1}_{189\ 1\text{'s}})^T$$

3.4. Numerical Case Study

For better understanding reliability analysis of the proposed all-digital SPS architecture, we give a numerical study as follows. We assume the same parameters for the same type of components, which are shown in Table 3-1. In addition, parameters of aggregate components PMU, CM1, and CM2 are given directly. The computation results of some SPS reliability indices are listed in Table 3-2.

Table 3-1 Reliability parameters of components

Components	Failure rate (1/year)	Repair rate (1/year)
TS1 / TS2	0.01	876
MU1 / MU2	0.01	876
EM1 / EM2	0.01	876
SW1 / SW2	0.01	876
LS1 / LS2	0.01	876
CM1 / CM2	0.03	876
PMU	0.006	786

Table 3-2 SPS reliability indices

Reliability indices	Calculated values
Probability of SPS failure	0.0000076
Frequency of SPS failure (1/year)	0.00601
Mean time to first failure (MTTFF) (years)	166.4

The component failure rates do have an influence on the reliability of SPS. Table 3-3 shows different results of SPS reliability indices by increasing all component failure rates to two, three, and five times of their original values while keeping their repair rates the same as before. From the data in Table 3-3, we observe that as component failure rates increase, the SPS reliability indices get worse accordingly. It simply quantifies the fact that the reliability of SPS will become degraded if its components are less reliable.

Table 3-3 SPS reliability indices for different component failure rates

Reliability indices	Original	Two times	Three times	Five times
Probability of SPS failure	0.0000076	0.000015	0.000023	0.000038
Frequency of SPS failure (1/year)	0.00601	0.0120	0.0181	0.0303
MTTFF (years)	166.4	83.02	55.24	33.02

The factor of repair also plays an important role when considering the reliability of SPS. Figure 3-7 and Figure 3-8 illustrate the trend of probability of SPS failure and

MTTFF of the SPS, respectively, by changing all component repair rates in multiples of the original data simultaneously while fixing their failure rates the same as in Table 3-1. From the figures we can see that increasing the component repair rates is helpful to enhance the system reliability of SPS. It sounds reasonable since higher repair rates actually imply that faster remedies could be made to the failed components. Hence, the probability of SPS failure could be reduced and the mean time to first failure (MTTFF) of the SPS is likely to be prolonged.

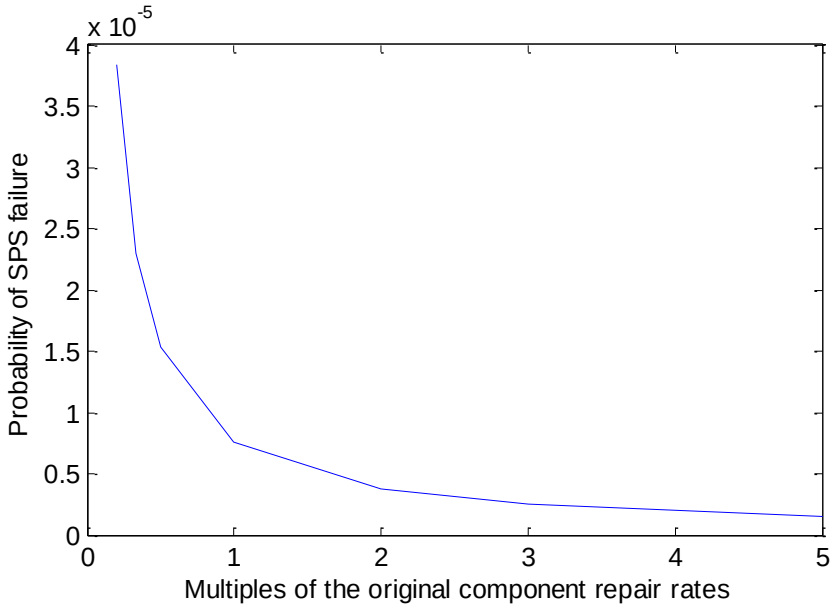

Figure 3-7. Probability of SPS failure for different component repair rates.

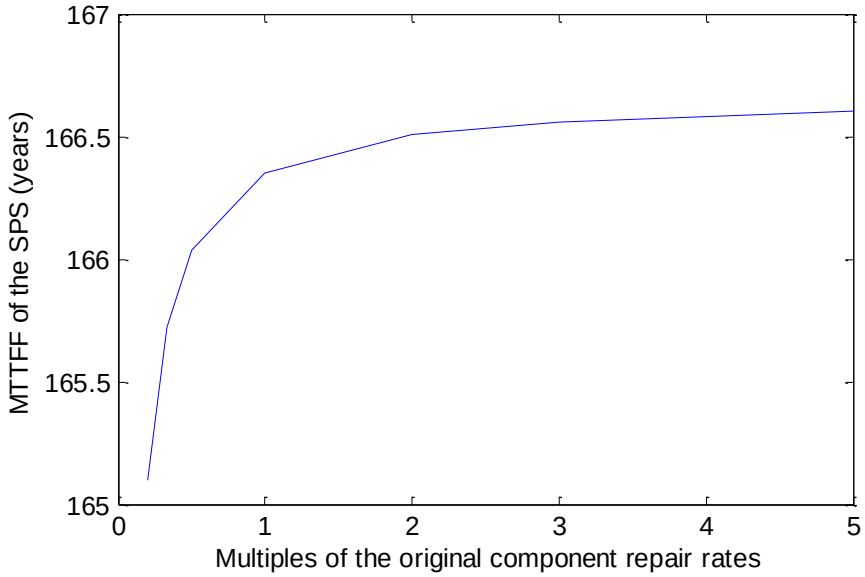

Figure 3-8. MTTFF of the SPS for different component repair rates.

3.5. Summary

In the era of smart grid, the penetration of information-age technologies can bring significant changes to the area of instrumentation, monitoring, control, and protection in power systems. The development of the special protection system (SPS) is also likely to be influenced.

This section proposes a conceptual all-digital SPS architecture for the future smart grid. Since the reliability of SPS is critical to the power system reliability, the focus of this section is how to apply reliability analysis approaches to the new all-digital SPS schemes. Evaluation of important reliability indices by using the network reduction method and the Markov modeling method is illustrated in detail.

The reliability of SPS is closely related to the reliability of its components. If components tend to be less reliable, the SPS reliability will be degraded. However, increasing component repair rates will be helpful to enhance the reliability of SPS. From the numerical case study, we find that the approaches applied in this section can quantify these effects and help in cost-benefit trade-off and selection of components as well as configurations [114], [115].

4. RELIABILITY EVALUATION OF THE 2-OUT-OF-3 VOTING GATES STRUCTURE IN A GENERATION REJECTION SCHEME USING MARKOV MODELS *

4.1. Introduction

Generation Rejection Scheme (GRS) is one of the widely used Special Protection Systems (SPS), accounting for about 21.6% of all SPS used by utilities according to an industry survey. It is designed to improve the transient stability performance of a power system. Figure 4-1 shows a portion of the IEEE Reliability Test System (RTS) together with an illustration of the GRS logic. In this power system line 12~13 and line 13~23 are critical lines. The function of the GRS is that when it detects a line outage on either of these two lines, it promptly trips only one generator to keep the other two generators in service [116].

---

* Part of this section is reprinted from copyrighted material with permission from PMAPS 2012 Organizing Committee.

The working logic of the GRS is explained as follows. When there is a fault on a critical line, the breakers on this line will open. Thus an open signal (high level signal) from any of these breakers energizes the output of the OR logic gate. Then the high level signal from the OR gate output, together with the high level arming signal, will set all AND logic gates outputs in high level, which are inputs to the 2-out-of-3 voting scheme. When two or more of the voting scheme input signals are high, the voting scheme output signal is high; otherwise, it is low. The high level signal from the voting scheme will trip the selected generator [117].

We know from the GRS working logic that the three AND logic gates in the 2-out-of-3 voting scheme play an important role. The design of this voting scheme can tolerate loss of one AND gate without problem regarding its output signal. However, if two or more AND gates fail, the voting scheme can no longer function correctly. Thus the reliability evaluation of these gates is one of the key factors to determine the overall reliability of the generation rejection scheme. In this section we will focus on these 2-out-of-3 voting gates and regard them as a system for reliability analysis using the Markov model approach.

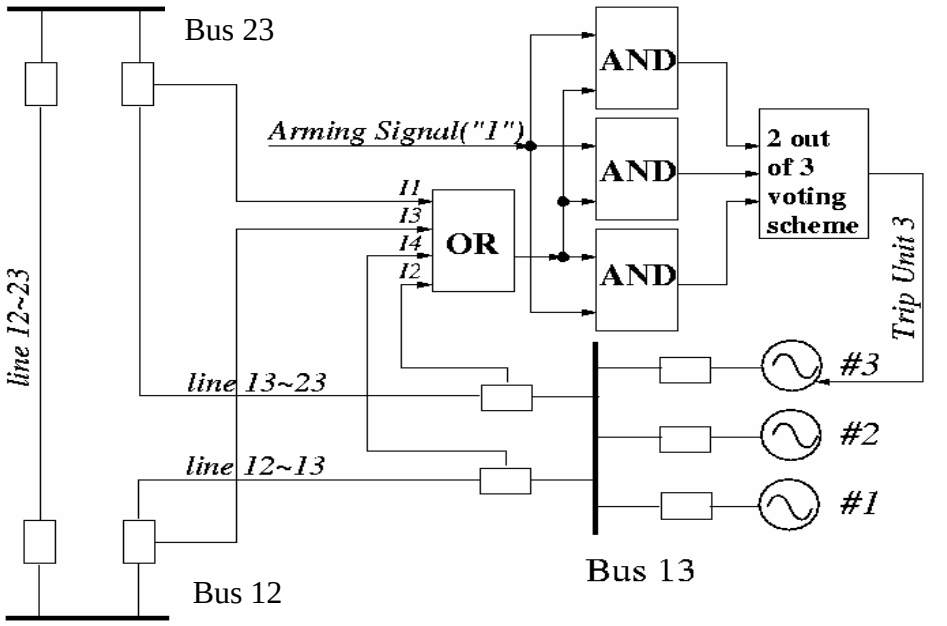

Figure 4-1. The 2-out-of-3 voting gates in a generation rejection scheme.

The remainder of this section is organized as follows. Section 4.2 shows a simple Markov model for analyzing the system reliability of the 2-out-of-3 voting gates structure. Section 4.3 illustrates an advanced Markov model for reliability evaluation in details with consideration of two different types of logic gate failures. Section 4.4 gives the numerical case study of both models proposed. Section 4.5 is the summary of this section.

4.2. Model I - Simple Markov Model

In practice, each AND logic gate represented in such a generation rejection scheme could be an individual electronic circuit module. In addition, all these three

working gates in a specific scheme application are often using the same type of module from the same manufacturer for reasons of interchangeable and economical solution of spare module backups.

From this point of view, we can model the AND logic gates of the 2-out-of-3 voting scheme as three independent and identical components. Thus, the state durations of these components will have the same distribution. Suppose their durations are exponentially distributed and their failure and repair rates are represented by λ and μ, respectively. Then the system Markov Model for the 2-out-of-3 voting gates structure can be drawn as shown in Figure 4-2.

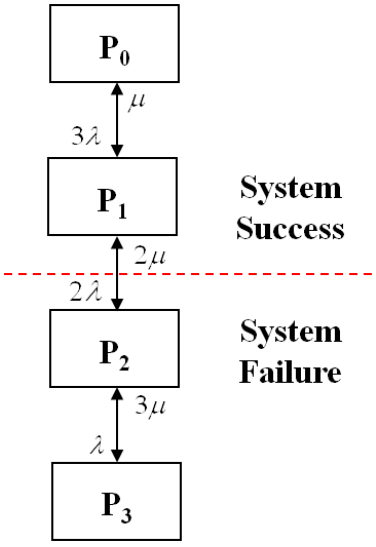

Figure 4-2. Model I - Simple Markov model.

In Figure 4-2, P_0 represents the system state with all gates in good condition, while P_1, P_2, and P_3 refer to groups of system states with one, two, and three gates

failed. Also, we use the symbols for states to indicate their corresponding probabilities. The following equations for each system state can be simply obtained using the frequency balance approach.

$$-P_0 \cdot 3\lambda + P_1 \cdot \mu = 0 \tag{4.1}$$

$$-P_1 \cdot (2\lambda + \mu) + P_0 \cdot 3\lambda + P_2 \cdot 2\mu = 0 \tag{4.2}$$

$$-P_2 \cdot (\lambda + 2\mu) + P_1 \cdot 2\lambda + P_3 \cdot 3\mu = 0 \tag{4.3}$$

$$-P_3 \cdot 3\mu + P_2 \cdot \lambda = 0 \tag{4.4}$$

Since all state probabilities should add up to unity, we have

$$\sum_{i=0}^{3} P_i = 1. \tag{4.5}$$

Using any three of the four equations (4.1)-(4.4) together with (4.5), we can solve and obtain the state probabilities. Here we replace (4.3) with (4.5) and obtain the matrix form of the equations as follows.

$$\mathbf{R_I P_I} = \mathbf{V_I} \tag{4.6}$$

wherein

$$\mathbf{R_I} = \begin{bmatrix} -3\lambda & \mu & 0 & 0 \\ 3\lambda & -(2\lambda + \mu) & 2\mu & 0 \\ 1 & 1 & 1 & 1 \\ 0 & 0 & \lambda & -3\mu \end{bmatrix}, \tag{4.7}$$

$$\mathbf{P_I} = \begin{bmatrix} P_0 \\ P_1 \\ P_2 \\ P_3 \end{bmatrix}, \quad \mathbf{V_I} = \begin{bmatrix} 0 \\ 0 \\ 1 \\ 0 \end{bmatrix}. \tag{4.8}$$

According to the 2-out-of-3 voting scheme designed, we can then compute the state probabilities of system success and failures by the following equations.

$$P_{sys}^{s} = P_0 + P_1, \qquad P_{sys}^{f} = P_2 + P_3 \tag{4.9}$$

The frequency of entering the states of system failure is

$$F_{sys} = P_1 \cdot 2\lambda \tag{4.10}$$

The Mean Up Time (MUT) and Mean Down Time (MDT) of the system can be obtained as follows.

$$MUT = P_{sys}^{s} \big/ F_{sys} \tag{4.11}$$

$$MDT = P_{sys}^{f} \big/ F_{sys} \tag{4.12}$$

4.3. Model II - Advanced Markov Model

Although the Markov model shown in Figure 4-2 (Model I) is simple, it might be inappropriate to evaluate the reliability of a practical 2-out-of-3 voting gates structure used in this section. The reason is that Model I is based on an important assumption that all failures of a gate are detected and known immediately after their occurrences. Here we refer to this kind of failures as detectable. However, the assumption may not be true in reality.

A protection scheme including SPS can be realized by different types of components, including electromechanical, analog electronic, or digital electronic (microprocessor-based) devices. Each scheme could have a self-monitoring function.

Generally, the electromechanical one has the lowest capability to monitor itself. In contrast, the one using digital electronics can have the most powerful mechanism of self-monitoring and may be even capable of self-diagnosis. No matter what type of the scheme is used, a warning signal will be sent to the control center through the alert message system once a failure is detected. Thus either operators or the maintenance staff can know the failure immediately and start the repair procedure.

Therefore, detectability of failures heavily depends on the self-monitoring mechanism of the protection design. In practice no type of self-monitoring mechanism can cover 100% parts of the whole protection scheme, including but not limited to hardware, software and firmware issues. In addition, the self-monitoring mechanism itself may suffer a failure. Thus some of the device failures may happen but cannot be known automatically. Fortunately, almost all these failures can be identified by an appropriate maintenance test.

Unlike some other active components in a power system such as rotating generators, most protection devices including generation rejection schemes are "dormant" during the majority of their life cycles. Although they can be armed for a long time in the working environment, they will not act until the predetermined action conditions are met. This special characteristic just reveals the fact that some protection failures are hidden and cannot be detected immediately until the protection is called upon to action or inspected for maintenance. In this section, we define this kind of hidden failures as undetectable.

Thus we have to take account of undetectable failures along with detectable ones in order to model our 2-out-of-3 voting gates structure more accurately. Suppose we still use λ and μ to represent failure and repair rates of detectable gate failures and use λ' and μ' to represent those of undetectable ones. This important consideration will result in a more complicated system model because each gate now has three states and there will be $3^3 = 27$ system states in total. Here we still assume all three gates to be independent and identical and all transitions between system states are one-step transitions.

4.3.1. *System State with All AND Logic Gates Working*

We continue to use P_0 to represent the system state with all gates in good condition and also its probability. Although the system state itself is the same as in the previous Model I, the transitions related to this state is slightly different than before.

In this section we use a bar overhead and at the bottom of the gate number to represent its detectable and undetectable failures, respectively. So the system state with all gates working well is detailed by $(1,2,3)$ as circled in Figure 4-3. We can see that the system state P_0 can make transitions in six different ways because each gate can fail due to detectable or undetectable failures.

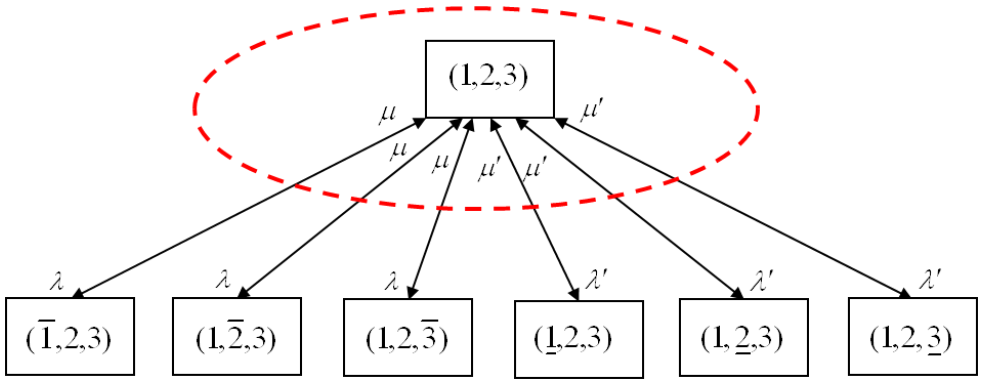

Figure 4-3. System state with all AND logic gates working.

4.3.2. *System State with One AND Logic Gate Failed*

In this case, the 2-out-of-3 voting scheme is still working, though one of the gate has failed. We continue to use P_1 to represent the system state and its probability with one gate failed. Since there are two types of gate failures, the system state P_1 can be further divided in two different groups, i.e., the system state P_{1-1} with one gate failed and detectable, and the system state P_{1-2} with one gate failed but undetectable. For illustration, we assume gate 1 to be the failed one in both scenarios.

4.3.2.1. One AND logic gate failed and detectable

In this case the system state can be detailed by $(\bar{1},2,3)$ as circled in Figure 4-4.

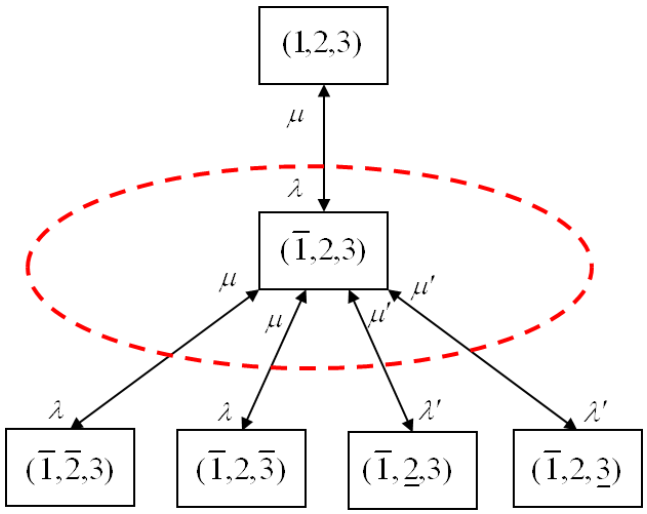

Figure 4-4. System state with one AND logic gate failed and detectable.

We see in Figure 4-4 that if gate 1 is repaired, the system will transit back to state $(1,2,3)$. However, if another gate, say gate 2, fails before gate 1 being repaired, the system will transit either to state $(\bar{1},\bar{2},3)$ or to state $(\bar{1},\underline{2},3)$ as shown in Figure 4-4, depending on which type of failures occurs on gate 2. As we can see in Figure 4-4, there are four possible transitions for state $(\bar{1},2,3)$ toward system states with two gates failed.

4.3.2.2. One AND logic gate failed but undetectable

In this case the system state can be detailed by $(\underline{1},2,3)$ as circled in Figure 4-5. Similarly, the system can transit back to state $(1,2,3)$ if gate 1 is repaired. The system can also transit to four possible system states with two gates failed.

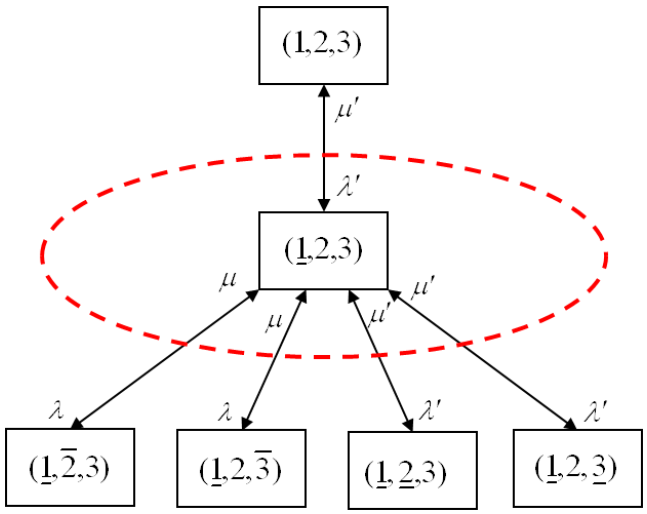

Figure 4-5. System state with one AND logic gate failed but undetectable.

4.3.3. *System State with Two AND Logic Gates Failed*

If two gates have failures on them, the 2-out-of-3 voting scheme will no longer function correctly. In other words, the system has failed. Due to different types of gate failures, it will be difficult for analysis if we use only one system state such as P_2 in Model I of Figure 4-2 to model this case. In fact, we need three categories to classify all these system states.

4.3.3.1. System failed and detectable

We use P_{2-1} to represent the system states of this category. In this scenario, the failures of two failed gates are both detectable. Thus the system failure can be identified

right after it occurs. Suppose gates 1 and 2 are the two failed gates. The system state can now be detailed by state $(\bar{1},\bar{2},3)$ as circled in Figure 4-6.

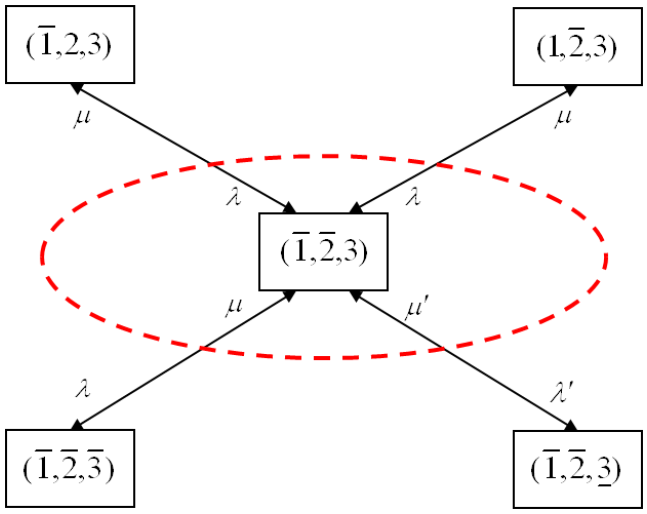

Figure 4-6. Detectable System failure with two AND logic gates failed.

Since each failed gate can be repaired, there will be two transitions for state $(\bar{1},\bar{2},3)$ toward system states with only one gate failed, i.e. state $(\bar{1},2,3)$ and state $(1,\bar{2},3)$ as in Figure 4-6. Because gate 3 may also fail before either gate 1 or 2 gets repaired, there are two other transitions for state $(\bar{1},\bar{2},3)$ toward system states with all gates failed as shown in Figure 4-6.

4.3.3.2. System failed but undetectable

We use P_{2-2} to represent the system states of this category. In this scenario, the failures of two failed gates are both undetectable. Thus the system failure cannot be identified after it occurs. Suppose gates 1 and 2 are the two failed gates. The system state can be detailed by state $(\underline{1},\underline{2},3)$ as circled in Figure 4-7.

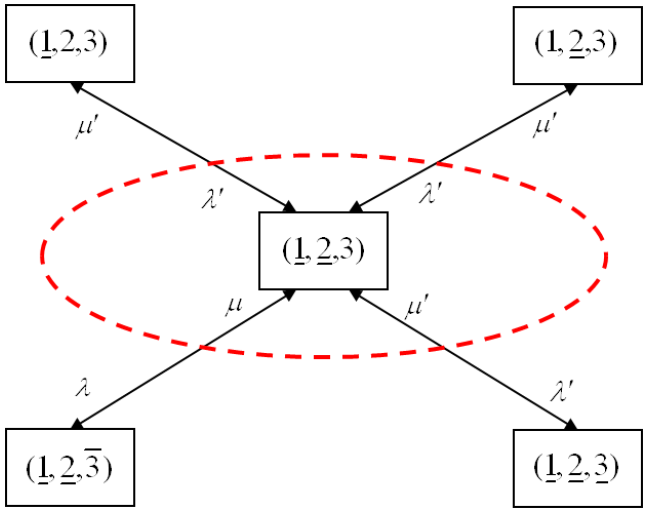

Figure 4-7. Undetectable System failure with two AND logic gates failed.

We can see in Figure 4-7 that the mode of possible transitions for this undetectable system failure is similar to that of previous detectable system failures in Figure 4-6. However, the transitions are totally different due to different system states and different transition rates.

4.3.3.3. System failure neither detectable nor undetectable

We use P_{2-3} to represent the system states of this category. In this scenario, there are two failed gates but one is detectable while the other undetectable. This category of system states is the most confusing one because the system failure can neither be determined as detectable nor be defined as undetectable. It just depends on the system state where it comes from. For illustration, we assume gate 1 failed and detectable while gate 2 failed but undetectable. Then the system state P_{2-3} can be detailed by state $(\bar{1},\underline{2},3)$ as circled in Figure 4-8.

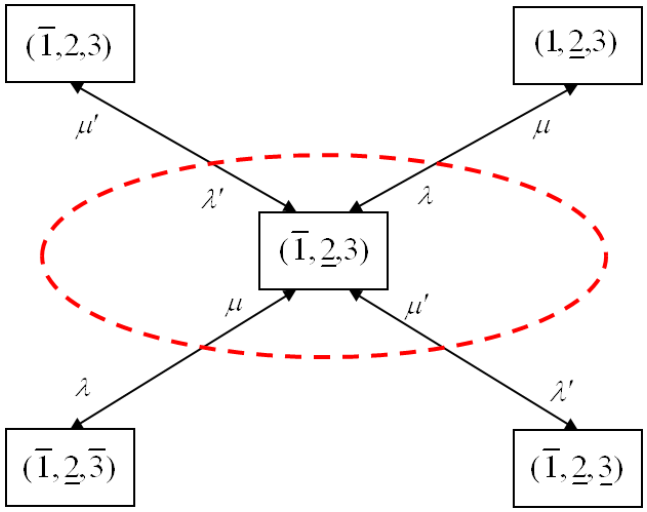

Figure 4-8. System failure with two AND logic gates failed, one detectable and the other undetectable.

There are two possible transitions to state $(\bar{1},\underline{2},3)$ from system states with only one gate failed. In Figure 4-8, if the transition originates from state $(\bar{1},2,3)$, then the

system failure can be treated as undetectable. Although the failure of gate 1 is detectable, it was before the system fails. When the system fails, it is triggered by the undetectable failure of gate 2. Thus the system failure remains unknown until next action or maintenance test.

On the other hand, if the transition originates from state $(1,\underline{2},3)$, the system failure can be paid attention to because the triggering event of gate 1 failure is detectable. Thus the system failure can be regarded as detectable since other gates may be examined for their status.

No matter the system failure is detectable or undetectable, the ambiguous system states of this kind can be handled appropriately as long as we group them as a separate category P_{2-3} different from previous system states P_{2-1} or P_{2-2}. As we can see in Figure 4-8, because gate 3 can fail either detectably or undetectably before any repair to gate 1 or 2, there exist two possible transitions for state $(\overline{1},\underline{2},3)$ toward system states with all gates failed.

4.3.4. *System State with All AND Logic Gates Failed*

It seems unnecessary to analyze the details of the 2-out-of-3 voting gates structure with all gates failed, given the system has already failed since the failures of a second gate. However, we realize that even the system states with all gates failed can distinguish themselves from each other and have different modes that may impact both analytical modeling and maintenance scheduling. Of course this is again caused by

detectable and undetectable gate failures. We need to avoid using only one system state such as P_3 in Model I of Figure 4-2 to model this situation. Instead, we have four groups of these system states.

4.3.4.1. All gates failed and detectable

We use P_{3-1} to represent the system state of this group. In this scenario, because the failures of all failed gates are detectable, the system failure can be identified definitely. There is only one state of this kind and it can be detailed by state $(\overline{1},\overline{2},\overline{3})$ as circled in Figure 4-9.

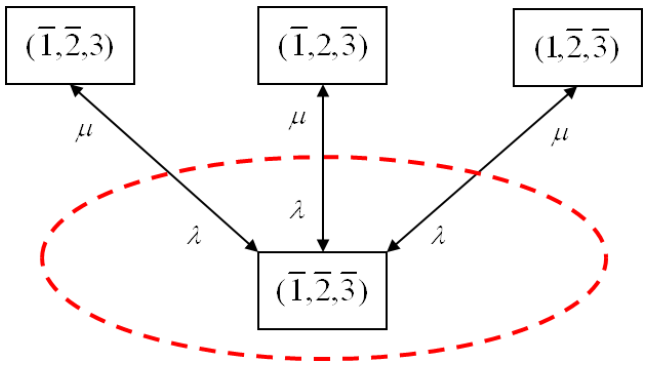

Figure 4-9. System failure with all AND logic gates failed and detectable.

It is easy to see that there are three system states that state $(\overline{1},\overline{2},\overline{3})$ can transit to or from, i.e., state $(\overline{1},\overline{2},3)$, state $(\overline{1},2,\overline{3})$, and state $(1,\overline{2},\overline{3})$. In addition, these three system states belong to the same group P_{2-1}.

4.3.4.2. All gates failed but undetectable

We use P_{3-2} to represent the system state of this group. In this scenario, because all gates have failed but none of them is detectable, the system failure surely cannot be known right after it occurs. There is only one state of this kind and it can be detailed by state $(\underline{1},\underline{2},\underline{3})$ as circled in Figure 4-10. There are three system states of the same group P_{2-2} that state $(\underline{1},\underline{2},\underline{3})$ can transit to or from, i.e., states $(\underline{1},\underline{2},3)$, $(\underline{1},2,\underline{3})$, and $(1,\underline{2},\underline{3})$.

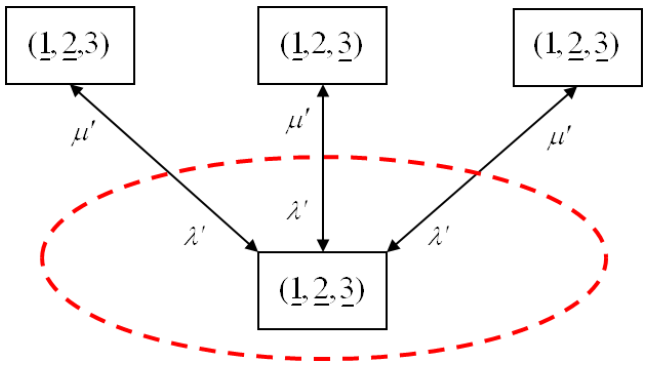

Figure 4-10. System failure with all AND logic gates failed but undetectable.

4.3.4.3. All gates failed, two detectable and one undetectable

We use P_{3-3} to represent the system states of this group. In this scenario, because two of the three failed gates are detectable, the system failure can be identified, too.

We notice that the two types of gate failures in the system state will impact the transitions. For better understanding, we suppose gates 1 and 2 failed and detectable while gate 3 failed but undetectable. The system state group P_{3-3} can now be detailed by state $(\bar{1},\bar{2},\underline{3})$ as circled in Figure 4-11. We can see that among the three system states that state $(\bar{1},\bar{2},\underline{3})$ can transit to or from, state $(\bar{1},\bar{2},3)$ belongs to group P_{2-1} while states $(\bar{1},2,\underline{3})$ and $(1,\bar{2},\underline{3})$ belong to group P_{2-3}.

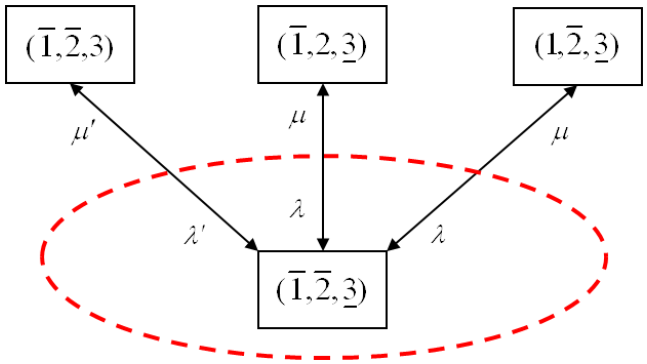

Figure 4-11. System failure with all AND logic gates failed, two detectable and the other undetectable.

4.3.4.4. All gates failed, one detectable and two undetectable

We use P_{3-4} to represent the system states of this group. In this last scenario, we just cannot tell whether the system failure can be identified or not because two of the three failed gates are undetectable. It depends on the system state where it comes from, which is similar to the explanation of previous system state group P_{2-3}.

Nevertheless, we can still know the impact of gate failures on the system state transitions. For illustration, we suppose gate 1 failed and detectable while gates 2 and 3 failed but undetectable. The system state group P_{3-4} can now be detailed by state $(\bar{1},\underline{2},\underline{3})$ as circled in Figure 4-12. We can see that among the three system states that state $(\bar{1},\underline{2},\underline{3})$ can transit to or from, states $(\bar{1},\underline{2},3)$ and $(\bar{1},2,\underline{3})$ belong to group P_{2-3} while state $(1,\underline{2},\underline{3})$ belongs to group P_{2-2}.

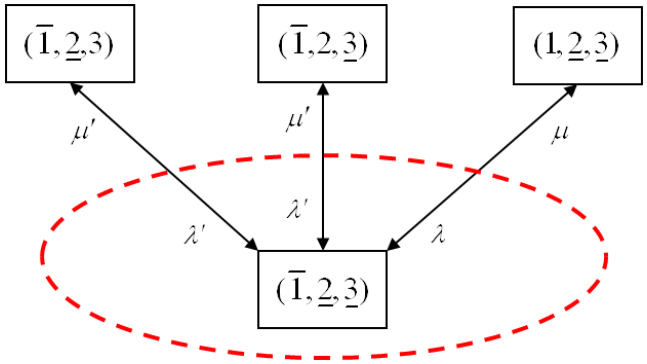

Figure 4-12. System failure with all AND logic gates failed, one detectable and the other two undetectable.

4.3.5. *The Advance Markov Model*

In brief, we have ten groups of system states to model the 2-out-of-3 voting gates structure when the failures of AND logic gates are considered either detectable or undetectable. Table 4-1 is the summary of all these groups of system states.

Using the concept of equivalent transition rate [91], we can give an advanced Markov model for reliability evaluation of the 2-out-of-3 voting gates structure as in Figure 4-13.

Table 4-1 Summary of system state groups

System state group	# of gates failed	System failed?	System failure detectable?	Detail of system states
P_0	0	No	-	$(1,2,3)$
P_{1-1}	1	No	-	$(\bar{1},2,3)$ $(1,\bar{2},3)$ $(1,2,\bar{3})$
P_{1-2}	1	No	-	$(\underline{1},2,3)$ $(1,\underline{2},3)$ $(1,2,\underline{3})$
P_{2-1}	2	Yes	Yes	$(\bar{1},\bar{2},3)$ $(\bar{1},2,\bar{3})$ $(1,\bar{2},\bar{3})$
P_{2-2}	2	Yes	No	$(\underline{1},\underline{2},3)$ $(\underline{1},2,\underline{3})$ $(1,\underline{2},\underline{3})$
P_{2-3}	2	Yes	Depending	$(\bar{1},\underline{2},3)$ $(\bar{1},2,\underline{3})$ $(\underline{1},\bar{2},3)$ $(\underline{1},\bar{2},\underline{3})$ $(\underline{1},2,\bar{3})$ $(1,\underline{2},\bar{3})$
P_{3-1}	3	Yes	Yes	$(\bar{1},\bar{2},\bar{3})$
P_{3-2}	3	Yes	No	$(\underline{1},\underline{2},\underline{3})$
P_{3-3}	3	Yes	Yes	$(\bar{1},\bar{2},\underline{3})$ $(\bar{1},\underline{2},\bar{3})$ $(\underline{1},\bar{2},\bar{3})$
P_{3-4}	3	Yes	Depending	$(\bar{1},\underline{2},\underline{3})$ $(\underline{1},\bar{2},\underline{3})$ $(\underline{1},\underline{2},\bar{3})$

Using the frequency balance approach, we can obtain a set of equations and solve for state probabilities of the advanced Markov model (Model II). This set of equations is expressed in the matrix form as in (4.13). The detail of (4.13) is shown in (4.14).

$$\mathbf{R_{II}P_{II}} = \mathbf{V_{II}} \tag{4.13}$$

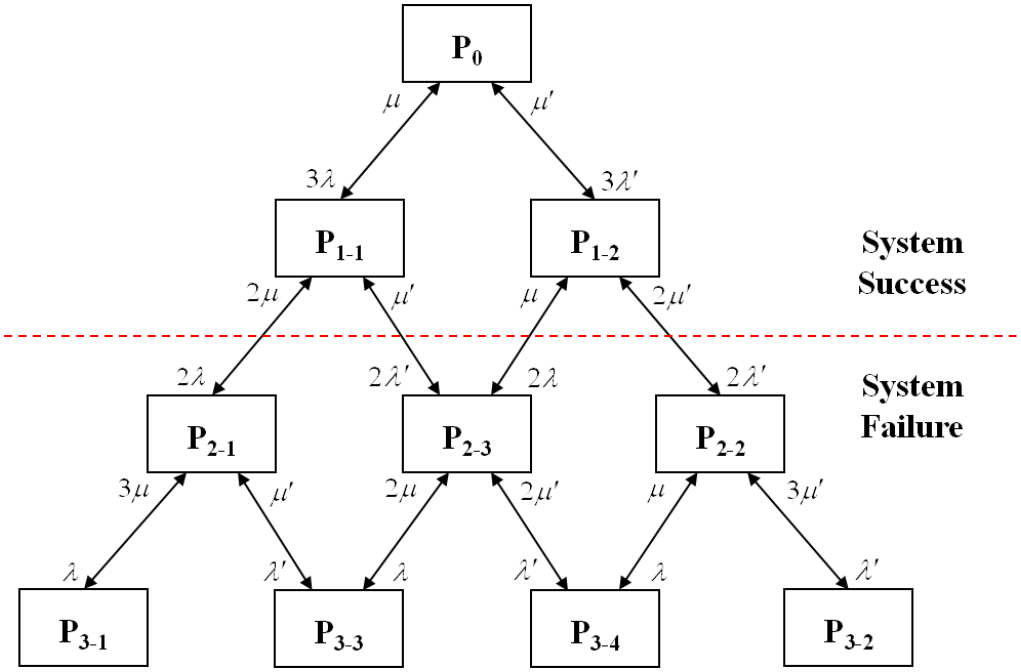

Figure 4-13. Model II - Advanced Markov model.

$$\begin{bmatrix} -(3\lambda+3\lambda') & \mu & \mu' & 0 & 0 & 0 & 0 & 0 & 0 & 0 \\ 3\lambda & -(2\lambda+2\lambda'+\mu) & 0 & 2\mu & 0 & \mu' & 0 & 0 & 0 & 0 \\ 3\lambda' & 0 & -(2\lambda+2\lambda'+\mu') & 0 & 2\mu' & \mu & 0 & 0 & 0 & 0 \\ 0 & 2\lambda & 0 & -(\lambda+\lambda'+2\mu) & 0 & 0 & 3\mu & 0 & \mu' & 0 \\ 0 & 0 & 2\lambda' & 0 & -(\lambda+\lambda'+2\mu') & 0 & 0 & 3\mu' & 0 & \mu \\ 1 & 1 & 1 & 1 & 1 & 1 & 1 & 1 & 1 & 1 \\ 0 & 0 & 0 & \lambda & 0 & 0 & -3\mu & 0 & 0 & 0 \\ 0 & 0 & 0 & 0 & \lambda' & 0 & 0 & -3\mu' & 0 & 0 \\ 0 & 0 & 0 & \lambda' & 0 & \lambda & 0 & 0 & -(2\mu+\mu') & 0 \\ 0 & 0 & 0 & 0 & \lambda & \lambda' & 0 & 0 & 0 & -(\mu+2\mu') \end{bmatrix} \cdot \begin{bmatrix} P_0 \\ P_{1-1} \\ P_{1-2} \\ P_{2-1} \\ P_{2-2} \\ P_{2-3} \\ P_{3-1} \\ P_{3-2} \\ P_{3-3} \\ P_{3-4} \end{bmatrix} = \begin{bmatrix} 0 \\ 0 \\ 0 \\ 0 \\ 0 \\ 1 \\ 0 \\ 0 \\ 0 \\ 0 \end{bmatrix} \quad (4.14)$$

The state probabilities of system success and failures are

$$P_{sys}^{s} = P_0 + \sum_{i=1}^{2} P_{1-i} \,, \tag{4.15}$$

$$P_{sys}^{f} = \sum_{i=1}^{3} P_{2-i} + \sum_{i=1}^{4} P_{3-i} \,. \tag{4.16}$$

The frequency of entering the states of system failure is

$$F_{sys} = 2(\lambda + \lambda') \sum_{i=1}^{2} P_{1-i} \,. \tag{4.17}$$

The formulae to calculate the Mean Up Time (MUT) and Mean Down Time (MDT) of the system are the same as (4.11) and (4.12), respectively.

4.4. Numerical Case Study

In order to compare the two different Markov Models for reliability evaluation of the 2-out-of-3 voting gates structure, we use a numerical case study as follows.

Table 4-2 gives the reliability parameters of the AND logic gate that we used for calculation. For simplicity, we assume that for the total number of gate failures in Model II, two thirds of them are detectable and one third undetectable. In addition, we consider the mean repair time to be 6 hours and the maintenance test interval as 6 months [116].

Table 4-2 Transition rates of the AND logic gate

Transition rates	Model I	Model II
λ (1/year)	0.03	0.02
λ' (1/year)	-	0.01
μ (1/year)	1460	1460
μ' (1/year)	-	2

The computed results for both models proposed in this section are shown in Table 4-3 and Table 4-4. Table 4-3 lists the group probabilities of each model. For comparable states between models, the state probabilities of Model II with the same number of failed gates are added up. Table 4-4 gives the reliability indices of the two models. From these tables we can see that the differences between the results of the two models are significant. Compared with the advanced Markov model (Model II), the simple one (Model I) overestimates the reliability of the 2-out-of-3 voting gates structure significantly.

Table 4-3 Group probabilities of system states

State probabilities	Model I	Model II
P_0 (All gates good)	0.999938	0.985108
P_1 (One gate failed)	6.164×10^{-5}	1.482×10^{-2}
P_2 (Two gates failed)	1.267×10^{-9}	7.429×10^{-5}
P_3 (All gates failed)	9×10^{-15}	1.242×10^{-7}

Table 4-4 Reliability indices of the voting gates structure

Reliability indices	Model I	Model II
Probability of system failure	1.267×10^{-9}	7.441×10^{-5}
Frequency of system failure (1/year)	3.698×10^{-6}	8.890×10^{-4}
Mean up time (hours)	2.369×10^{9}	9.853×10^{6}
Mean down time (hours)	3.000	733.2

4.5. Summary

The special protection systems are critical to power system reliability. As one of the most widely used SPS, the generation rejection scheme plays an important role in improving the transient stability performance of power systems.

This section focuses on reliability modeling of the 2-out-of-3 voting gates structure in a generation rejection scheme. Due to different assumptions, two Markov models are proposed for reliability evaluation. The major difference between these two models is whether the failures of a logic gate are distinguished as detectable or undetectable.

From the numerical case study, we found that the reliability indices obtained from these two models could be very different. While using the advanced Markov model with consideration of both detectable and undetectable logic gate failures as a benchmark, the simple Markov model which only considers detectable failures will overestimate the reliability of the 2-out-of-3 voting gates structure significantly [118].

5. NEW RELIABILITY MODELS FOR CURRENT-CARRYING COMPONENTS INCLUDING PROTECTION SYSTEM FAILURES *

5.1. Introduction

The three-stage multistate Markov model for a single current-carrying component [80] mentioned in Section 1 is the basis for new concepts and models developed in the following research. Thus, we need to review the details of this model as shown in Figure 5-1 before we go further.

---

* Part of this section is reprinted from copyrighted material with permission from IEEE.

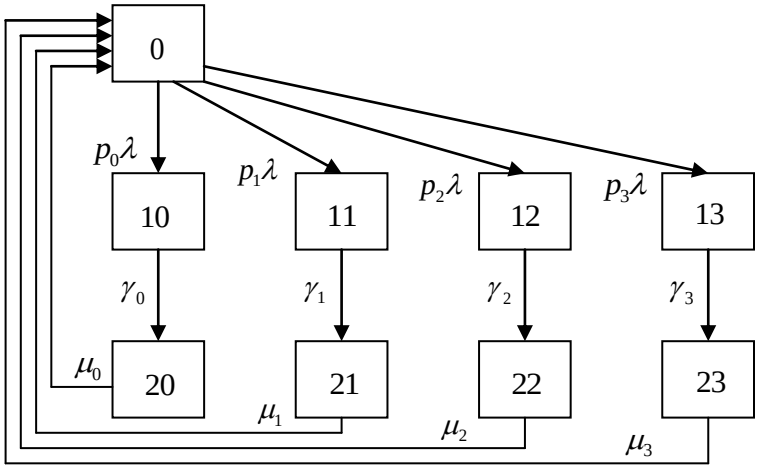

Figure 5-1. Three-stage multistate model of a current-carrying component.

In this model, the faulted current-carrying component is supposed to be isolated by a set of two circuit breakers, denoted by set I, and this set of breakers bounds the protection zone of the component. In practice, a component may associate with more than two breakers, and the configurations of breakers do have influence on substation and system reliability [119]. However, it would be clearer and preferable to describe the modeling concepts assuming only two equivalent breakers for a component, each one of which represents the behavior of the practical breaker(s) associated with the relay and communication schemes. Thus, as the result of protection failures, a combination of breakers can fail to respond to a fault in the protection zone. The various possible combinations are indicated by subsets $I_k \subset I$, i.e. $I_0 = \phi$ (null), $I_1 = \{\text{breaker 1}\}$, $I_2 = \{\text{breaker 2}\}$, $I_3 = \{\text{breaker1, breaker2}\} = I$.

As shown in Figure 5-1, stage 0 is the up state (unfaulted state) of the current-carrying component. Stages 1 and 2 contain down states (faulted states) of the component before and after switching (the unfaulted components isolated by backup protection systems being restored to service), respectively. These down states are indicated by two numbers, the first showing the stage and the second the state number in that stage. State k in stage 1 or 2 means that breakers in subset I_k fail to trip simultaneously. For example, state 13 means that the two breakers of the faulted component fail to trip, causing all its adjacent healthy components on both sides tripped by backup protections. State 23 means that after the checking process, both breakers of the faulted component are manually opened and then the adjacent components previously tripped are restored to service.

The sequence following a fault on a component is as follows. Depending on the operation of the protection, one or more components may be isolated. Then after the correct identification of the faulted component, unfaulted components may be restored to service. Therefore, the transitions from the up state to the down states in stage 1, transitions from the states in stage 1 to corresponding states in stage 2, and eventually transitions from states in stage 2 to the up state are unidirectional. The failing, switching and repair processes are not independent and thus should be integrated into the same model with the probabilities of these states adding to unity. The parameters in Figure 5-1 are defined as:

λ failure rate of the current-carrying component

p_k unreadiness probability of breakers in $I_k \subset I$

γ_k switching rate from state $1k$ to state $2k$

μ_k repair rate of the current-carrying component from state $2k$

The Markov model described in Figure 5-1 assumes the switching (from state $1k$) and repair (from state $2k$) times to be exponentially distributed. It should be noted that there is a single transition into and a single transition out of the state $1k$ or $2k$. It is shown in the Appendix that to compute the steady state probabilities for this special situation, the state residence times can always be assumed exponentially distributed with the equivalent constant transition rates (γ_k and μ_k) equal to the reciprocals of the mean value of the state duration times, irrespective of the actual distribution.

The objective of this section is to contribute to developing new concepts and models for including protection system failures in reliability analysis at current-carrying component level. The remainder of this section is organized as follows. Section 5.2 describes the example power system to be analyzed to illustrate the basic concepts. The necessary assumptions on which the analysis is based are also given. Section 5.3 sets up the initial models for component failures caused by the two types of protection system failures. Section 5.4 discusses decoupling the complicated interactions between components caused by protection failures. Section 5.5 then establishes a complete Markov model for the component. Section 5.6 further simplifies this model into a more applicable and concise one and illustrates the overall reliability situation of individual current-carrying components. Section 5.7 gives the numerical case study of the proposed models. Section 5.8 is the summary of this section.

5.2. The Example Power System and Assumptions

For a clear illustration of concepts and methodology, a simple example power system shown in Figure 5-2 is used. Suppose two current-carrying components (e.g. transmission lines) A and B are connected in series and each is bounded by two circuit breakers, i.e. A_1, A_2, and B_1, B_2, respectively. In Figure 5-2, S_1 and S_2 are two source systems supplying power while L is the load fed by components A and B together.

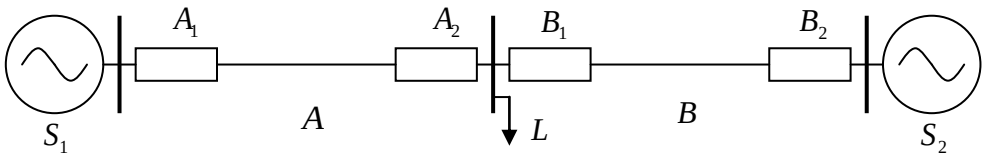

Figure 5-2. Example power system.

Generally, the protection systems are designed in the following way. If there is a fault on component B and the protective relay installed at location B_1 fails to trip, the relay installed at location A_1 will provide remote backup protection while the relay at A_2 will provide local backup protection. Thus, component A will be tripped. For simplicity, we do not distinguish the local backup and remote backup any more since they actually have the same result that A is tripped. We just assume that the protection system of component A (protection A) acts as the backup to the protection system of component B (protection B). Similarly, protection B is also assumed to be the backup to protection A in case breaker A_2 fails to trip when there is a fault on component A.

In addition, we assume that source system S_1 provides backup protection to component A in case breaker A_1 fails to trip when there is a fault on component A, while source system S_2 provides backup protection to component B in case breaker B_2 fails to trip when there is a fault on component B. These backup protections will detach the source system from the corresponding component (A or B) when called upon to act.

Some other important assumptions are listed as following. These assumptions are generally made in power system reliability analysis.

(1) The component state durations are exponentially distributed, which implies that all transition rates are constant.

(2) The failures of protection systems happen independently of the faults of current-carrying components.

(3) The repair of protection systems is always faster than that of the corresponding protected components, which is normal in power industry.

(4) All the protection systems are well coordinated and all the backup functions are perfectly reliable.

(5) All the source systems and the buses connecting components and feeding loads are perfectly reliable.

(6) All the source systems and the components have sufficient power capacity to satisfy the load.

5.3. Initial Modeling of Protection System Failures

There are two significant failure modes of the protection system [80]. One is the fail-to-operate mode, which refers to undetected or hidden faults of the protection system and is associated with the concept of unreadiness probability. The other is the undesired-tripping mode, in which the unfaulted component is tripped by its faulted protection system.

For the fail-to-operate protection failures of components A and B, they can be modeled by the three-stage multistate models as shown in Figure 5-3(a) and Figure 5-3(b), respectively. In fact, these models are directly obtained from that in Figure 5-1, with the only difference being of component symbols A and B added.

As to undesired-tripping protection failures, they can increase the component down-state probability. However, we notice that this failure mode of a protection system has influence only on its own component without interaction with other components. In other words, protection A will only trip component A and protection B will only trip component B. Thus, we can use a two-state process to model the effect of this failure mode, as state A' in Figure 5-4(a) and state B' in Figure 5-4(b).

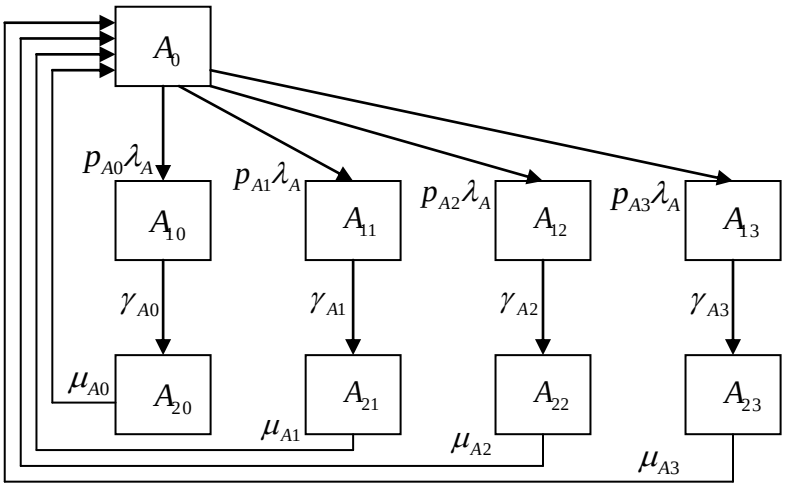

(a) Component A

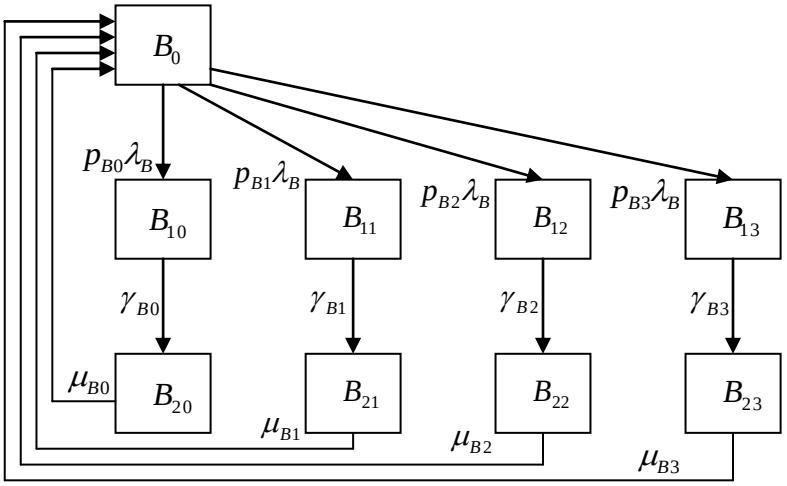

(b) Component B

Figure 5-3. Modeling a component with its fail-to-operate protection failures.

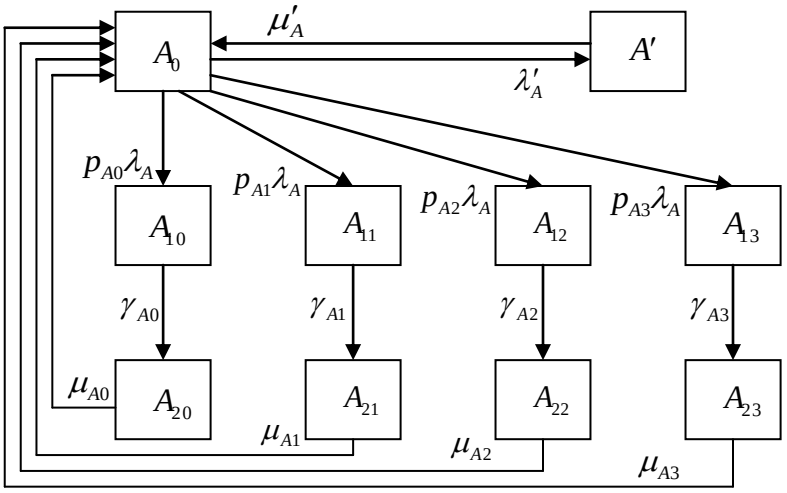

(a) Component A

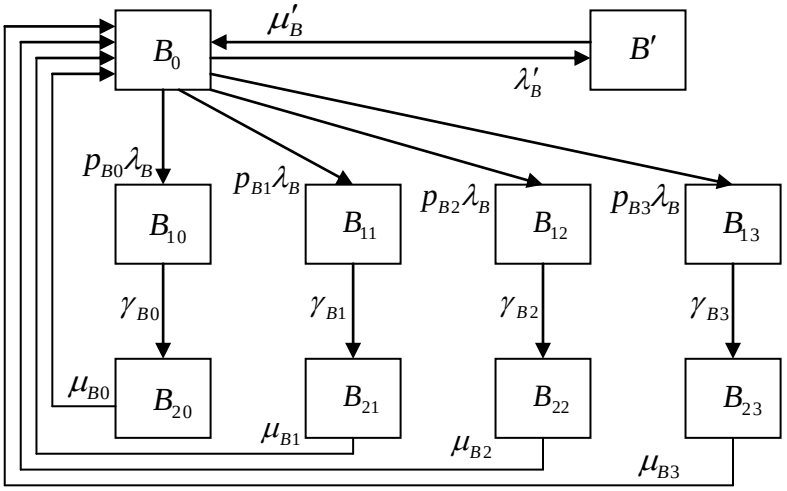

(b) Component B

Figure 5-4. Modeling a component with its protection system failures.

The models in Figure 5-4 are actually derived by adding the two-state process just mentioned above to the previous ones in Figure 5-3, respectively. Therefore, they

successfully incorporate the two significant failure modes of the protection system into the current-carrying component modeling.

5.4. Interaction Decoupling and the Complete Model

We need to point out that the Markov models in Figure 5-4 are still incomplete for the components because they have not depicted the overall reliability status of the components.

In fact, we observe that a component is possible to trip without any fault either on itself or with its protection system. It is induced by component interactions but is not reflected in the models of Figure 5-4. For example, an uncleared fault on component B could trip component A, which would be explained in the following. Thus, it is quite necessary to decouple the complex interactions between current-carrying components caused by their protection system failures.

5.4.1. Decoupling Component Interaction by Protection Failures for Modeling Component A

As in the example system of Figure 5-2, if there is a fault on component B and protection B fails to trip its breaker B_1, protection B is in the situation of unreadiness to trip. Since protection A is the backup of protection B, it will trip component A to isolate faulted component B. In such case, there is no fault on component A, nor is with

protection A, but component A is down. This is the interaction between components A and B caused by failures of protection B.

Since both components are down simultaneously due to backup protection, we can model the effect of this interaction as a special common mode failure of components A and B. However, there are two cases we need to consider.

In one case, breaker B_2 trips but breaker B_1 fails to trip. There would be three steps and the state transitions of each component in these steps are illustrated in Table 5-1. The state $\tilde{A}_{B11}$ in Table 5-1 is a new down state of component A caused by failures of protection B. The subscript of the state symbol is used to indicate the source of impact.

Table 5-1 State transitions of components in Case One

Step	Transition of component B		Transition of component A	
	Direction	Rate	Direction	Rate
1	$B_0 \rightarrow B_{11}$	$p_{B1}\lambda_B$	$A_0 \rightarrow \tilde{A}_{B11}$	$p_{B1}\lambda_B$
2	$B_{11} \rightarrow B_{21}$	γ_{B1}	$\tilde{A}_{B11} \rightarrow A_0$	γ_{B1}
3	$B_{21} \rightarrow B_0$	μ_{B1}	Independent of component B	

In step 1, component B transfers from state B_0 to state B_{11} while component A transfers from state A_0 to the new down state $\tilde{A}_{B11}$. Components A and B have the same failure rate $p_{B1}\lambda_B$ due to common mode failure of the two components. In step 2, component B transfers from before-switching state B_{11} to after-switching state B_{21}

while component A returns from state $\tilde{A}_{B11}$ (down state) to state A_0 (up state). Components A and B also have the same transition rate γ_{B1} because of the switching operation. In step 3, component B transfers from state B_{21} to state B_0 with the repair rate μ_{B1}, but this time the transition of component A is independent of component B. Thus, if we are only concerned with transitions between up and down states of component A, this case of common mode failure makes component A experience a two-state process with its transition rates derived from component B.

In the other case, both of the breakers B_1 and B_2 fail to trip. Its analysis is quite similar to the first case if we only consider its impact on component A. There would also be three steps and the state transitions of each component in these steps are shown in Table 5-2. The state $\tilde{A}_{B13}$ in Table 5-2 is another new down state of component A caused by failures of protection B.

Table 5-2 State transitions of components in Case Two

Step	Transition of component B		Transition of component A	
	Direction	Rate	Direction	Rate
1	$B_0 \to B_{13}$	$p_{B3}\lambda_B$	$A_0 \to \tilde{A}_{B13}$	$p_{B3}\lambda_B$
2	$B_{13} \to B_{23}$	γ_{B3}	$\tilde{A}_{B13} \to A_0$	γ_{B3}
3	$B_{23} \to B_0$	μ_{B3}	Independent of component B	

Therefore, the interactions between components by their protection system failures can be decoupled by modeling them as common mode failures. Given protection A is the backup of protection B as in the example power system of Figure 5-2, their interaction is caused by the unreadiness probability of protection B associated with breaker B_1. Its impact on component A can be modeled by two two-state processes associated with states $\tilde{A}_{B11}$ and $\tilde{A}_{B13}$, respectively. Figure 5-5 gives an intuitive picture of decoupling interactions caused by failures of protection B.

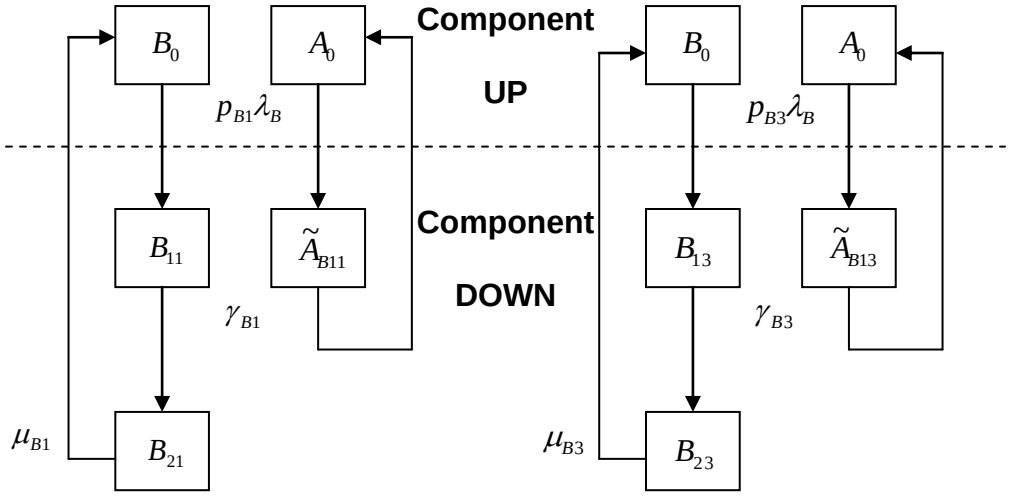

(a) Only breaker B_1 fails to trip (b) Both breakers B_1 and B_2 fail to trip

Figure 5-5. Decoupling interactions caused by failures of protection B.

It is necessary to point out that the unreadiness probability of protection B associated only with breaker B_2 should not have such influence on component A. Since breaker B_1 is tripped by protection B (primary protection) and component B is detached from component A, protection A (backup protection) will not operate. Thus, there is no

interaction between the two components. In fact, component B will also be detached from source system S_2 by its protection (backup protection) in this situation.

5.4.2. Decoupling Component Interaction by Protection Failures for Modeling Component B

Since protection B is also the backup of protection A, there exists another component interaction which is now caused by the unreadiness probability of protection A associated with breaker A_2. However, the decoupling methodology of this interaction is all the same as that of the previous one.

The interaction between components A and B caused by failures of protection A can also be decoupled by modeling them as common mode failures. There are also two cases that are necessary to consider as shown in Figure 5-6. Its impact on component B can be modeled by two independent two-state processes represented by states $\tilde{B}_{A12}$ and $\tilde{B}_{A13}$, respectively. The transition rates of these new processes of component B as shown in Figure 5-6 are actually derived from the existing model of component A as in Figure 5-4(a).

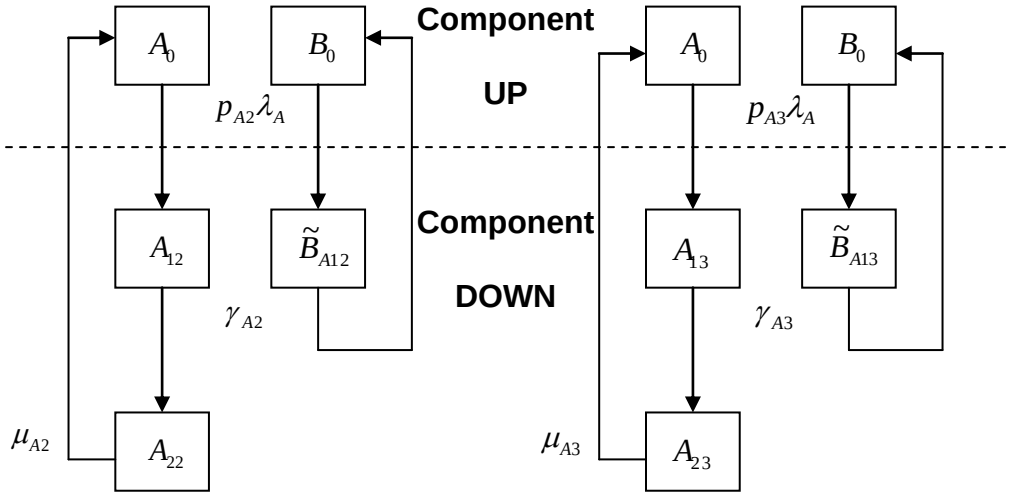

(a) Only breaker A_2 fails to trip (b) Both breakers A_1 and A_2 fail to trip

Figure 5-6. Decoupling interactions caused by failures of protection A.

For the similar reason, the unreadiness probability of protection A associated only with breaker A_1 should not have interactive impact on component B. As we have assumed before, component A will be detached from source system S_1 by its protection (backup protection) in this situation, too.

5.4.3. The Complete Markov Model for Components

After we have decoupled the interactions between current-carrying components caused by their protection system failures, we add new states to the initial component models in Figure 5-4 for completeness. Now the complete Markov model for the components can be obtained as shown in Figure 5-7, which is capable of describing their overall reliability situation.

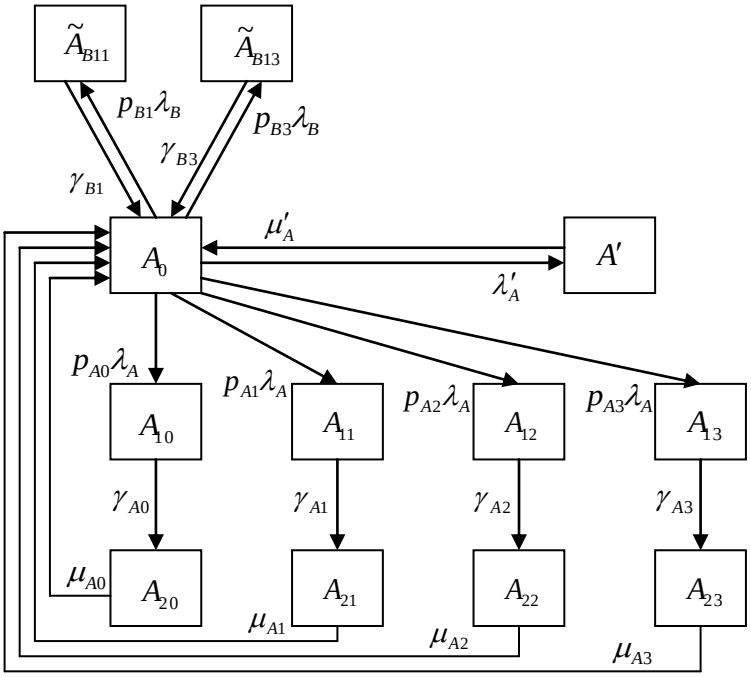

(a) Component A

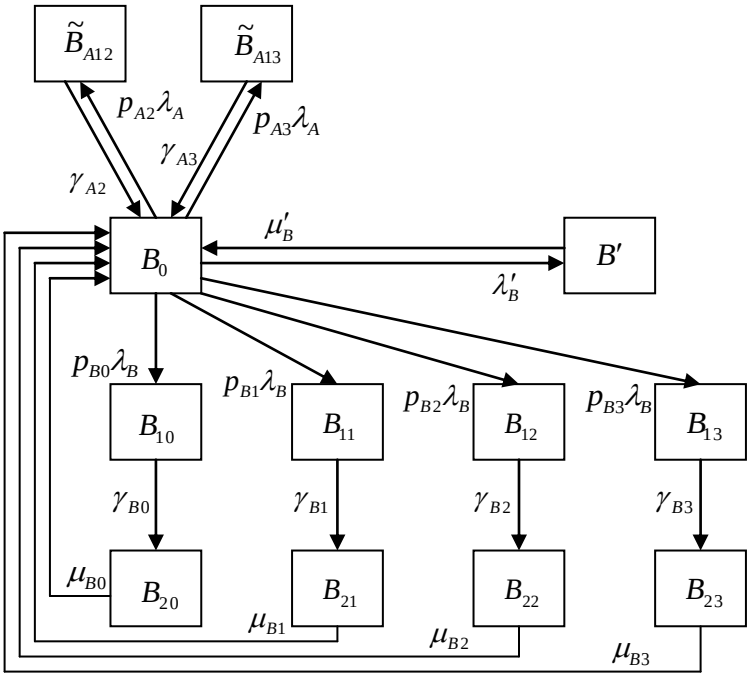

(b) Component B

Figure 5-7. Complete Markov model for current-carrying components.

In Figure 5-7, we should bear in mind that although the new states $\tilde{A}_{B11}$ and $\tilde{A}_{B13}$ of component A are individually presented in this component modeling, they are always dependent on some down states of component B as already illustrated in Figure 5-5. In addition, the transition rates of these new states are derived from those of component B. Similarly, the individually presented new states $\tilde{B}_{A12}$ and $\tilde{B}_{A13}$ of component B are always dependent on some down states of component A as illustrated in Figure 5-6. The transition rates of these new states are also derived from those of component A.

5.5. Simplification of the Complete Model

Although the reliability models in Figure 5-7 for current-carrying components are complete, they appear to be so complex that it may discourage their application in the analysis of power systems. Thus, it is necessary to simplify these Markov models. For reasons of avoiding confusion, we first use the model of component A to illustrate the simplification process in detail.

5.5.1. Simplification of Modeling Component Failure Due to Its Own Fault

We have depicted failures of component A due to its own fault by a three-stage multistate model, which is already shown in Figure 5-3(a) and is also a significant part in Figure 5-7(a). This model not only incorporates fail-to-operate faults of protection A, but

also identifies each case of unreadiness probability of protection A. It is important and indispensable to model component A in this way in order to decouple the component interactions caused by the unreadiness probability of protection A and further to identify the impact of the interactions on other related components.

However, it is unnecessary to use such a sophisticated model directly because power system reliability is determined significantly by up-and-down status of its components. We can next see that the unreadiness probability of protection A cannot influence component A regarding its up and down states.

In case there is a fault on component A, it will surely transfer from the up state to down state (either by primary protection or backup protection), despite the status of protection A. In case component A is in the up state, the undetected faults of protection A cannot turn component A into down state unless a fault happens to occur on component A. These facts just imply that the unreadiness probability of protection A cannot alter the failure rate of component A.

Although there are various states before and after switching in the previous three-stage multistate model of component A, all these states (in stages 1 and 2) belong to and exhaustively compose the down state of component A due to its own fault. If we assume that the repair of protection systems is faster than that of the corresponding protected components, which is normal in the power industry, the repair rate of component A from the down state to up state will also not be changed by the unreadiness probability of protection A.

Therefore, the unreadiness probability of protection A can only influence other components but not component A regarding up-and-down status. We no longer need to identify the down-state details of component A according to the unreadiness probability of protection A. We can simply use a two-state process represented by state $\hat{A}$ in Figure 5-8 to model the failures of component A due to its own fault. This model is actually all the same as if we had the perfect protection of component A. The transition rates are just the parameters of component A, i.e., its failure rate λ_A and its repair rate μ_A.

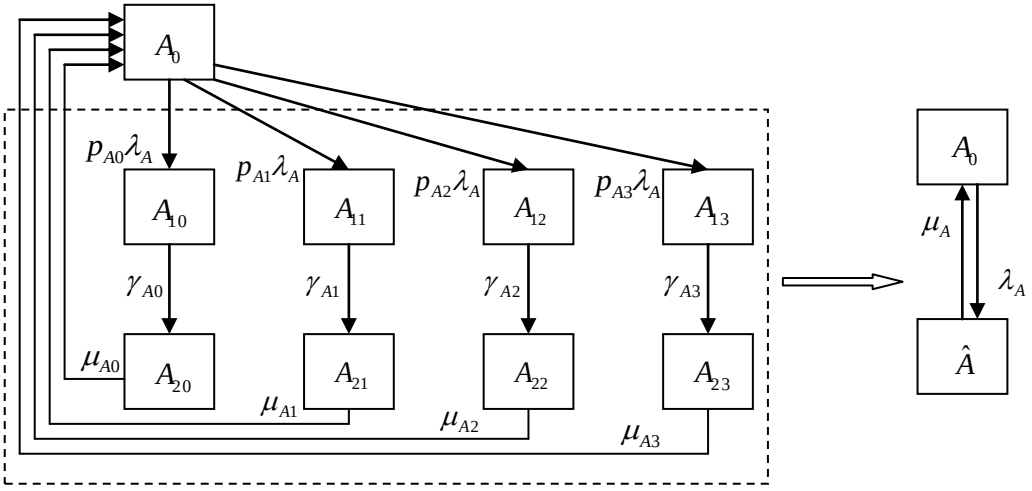

Figure 5-8. Modeling failures of component A due to its own fault.

5.5.2. The Simplified Model for Component A

Now we obtain a new concise model for component A as shown in Figure 5-9, which is simplified from Figure 5-7(a). This new model not only clearly depicts the overall reliability situation of component A in the complex environment of interactions

caused by protection system failures, but also incorporates sufficient information for applicable quantitative analysis.

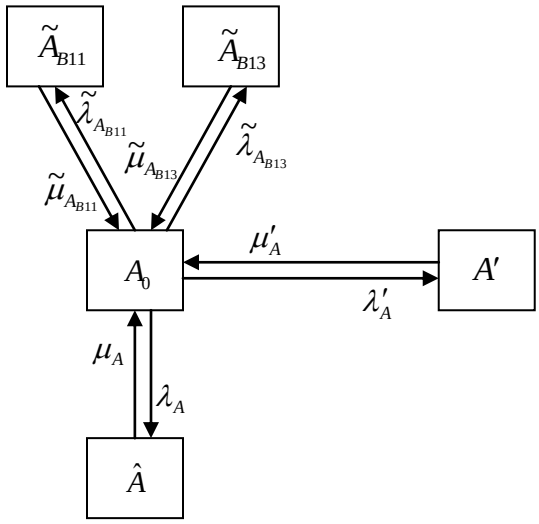

Figure 5-9. Simplified model for component A.

In Figure 5-9, all states of component A are systemized into four categories: the up state A_0, the down state $\hat{A}$ due to faults on component A, the down state A' due to undesired-tripping failure of protection A, and the down states $\tilde{A}_{B11}$ and $\tilde{A}_{B13}$ due to the unreadiness probability of protection B, respectively. Using the transition rates known previously, we can obtain the probabilities of these states by the frequency balance approach as following. Here we use P_{A_0}, $\hat{P}_A$, P'_A, $\tilde{P}_{A_{B11}}$, and $\tilde{P}_{A_{B13}}$ to represent the probabilities of states A_0, $\hat{A}$, A', $\tilde{A}_{B11}$, and $\tilde{A}_{B13}$, respectively.

For the process between states A_0 and $\hat{A}$, we have

$$P_{A_0}\lambda_A = \hat{P}_A\mu_A \Rightarrow \hat{P}_A = \frac{\lambda_A}{\mu_A}P_{A_0}. \tag{5.1}$$

For the process between states A_0 and A', we have

$$P_{A_0}\lambda'_A = P'_A\mu'_A \Rightarrow P'_A = \frac{\lambda'_A}{\mu'_A}P_{A_0}. \tag{5.2}$$

For the process between states A_0 and $\tilde{A}_{B11}$, we have

$$P_{A_0}\tilde{\lambda}_{A_{B11}} = \tilde{P}_{A_{B11}}\tilde{\mu}_{A_{B11}} \Rightarrow \tilde{P}_{A_{B11}} = \frac{\tilde{\lambda}_{A_{B11}}}{\tilde{\mu}_{A_{B11}}}P_{A_0}. \tag{5.3}$$

For the process between states A_0 and $\tilde{A}_{B13}$, we have

$$P_{A_0}\tilde{\lambda}_{A_{B13}} = \tilde{P}_{A_{B13}}\tilde{\mu}_{A_{B13}} \Rightarrow \tilde{P}_{A_{B13}} = \frac{\tilde{\lambda}_{A_{B13}}}{\tilde{\mu}_{A_{B13}}}P_{A_0}. \tag{5.4}$$

It is obvious that

$$P_{A_0} + \hat{P}_A + P'_A + \tilde{P}_{A_{B11}} + \tilde{P}_{A_{B13}} = 1. \tag{5.5}$$

Substitute (5.1), (5.2), (5.3), and (5.4) into (5.5), we can get

$$P_{A_0}\left(1 + \frac{\lambda_A}{\mu_A} + \frac{\lambda'_A}{\mu'_A} + \frac{\tilde{\lambda}_{A_{B11}}}{\tilde{\mu}_{A_{B11}}} + \frac{\tilde{\lambda}_{A_{B13}}}{\tilde{\mu}_{A_{B13}}}\right) = 1. \tag{5.6}$$

Therefore,

$$P_{A_0} = \frac{1}{K_A}, \tag{5.7}$$

wherein

$$K_A = 1 + \frac{\lambda_A}{\mu_A} + \frac{\lambda'_A}{\mu'_A} + \frac{\tilde{\lambda}_{A_{B11}}}{\tilde{\mu}_{A_{B11}}} + \frac{\tilde{\lambda}_{A_{B13}}}{\tilde{\mu}_{A_{B13}}}, \tag{5.8}$$

and

$$\tilde{\lambda}_{A_{B11}} = p_{B1}\lambda_B, \quad \tilde{\mu}_{A_{B11}} = \gamma_{B1}, \tag{5.9}$$

$$\tilde{\lambda}_{A_{B13}} = p_{B3}\lambda_B, \quad \tilde{\mu}_{A_{B13}} = \gamma_{B3}. \tag{5.10}$$

The probabilities of all the down states are

$$\hat{P}_A = \frac{\lambda_A}{K_A \mu_A}, \tag{5.11}$$

$$P'_A = \frac{\lambda'_A}{K_A \mu'_A}, \tag{5.12}$$

$$\tilde{P}_{A_{B11}} = \frac{\tilde{\lambda}_{A_{B11}}}{K_A \tilde{\mu}_{A_{B11}}}, \tag{5.13}$$

$$\tilde{P}_{A_{B13}} = \frac{\tilde{\lambda}_{A_{B13}}}{K_A \tilde{\mu}_{A_{B13}}}. \tag{5.14}$$

Let us look at the down states of the simplified complete model for component A in Figure 5-9 again. There is something interesting if we compare them from various points of view.

From the viewpoint of faults occurring on primary or secondary equipments, all the down states of component A can be classified into two groups. The first group is component A failure caused by faults on the component itself, which consists of the down state $\hat{A}$ only. All other down states A', $\tilde{A}_{B11}$, and $\tilde{A}_{B13}$ belong to the second group, which represents component A failure caused by protection system failures. If we remove the second group, the model of component A can actually fall back to the one with perfect protection systems.

From the viewpoint of tripping effect, all the down states of component A can also be generalized into two types. The down state $\hat{A}$ is the only one of the first type, which represents "desired" tripping of component A because there is a fault on component A. The second type includes all other down states A', $\tilde{A}_{B11}$, and $\tilde{A}_{B13}$, which can be regarded as "undesired" tripping of component A because they have the same tripping effect that component A is down without its own fault. It means that states $\tilde{A}_{B11}$ and $\tilde{A}_{B13}$ are like virtual undesired-tripping states, just the same tripping effect for component A as the real undesired-tripping state A'. However, the down states $\tilde{A}_{B11}$ and $\tilde{A}_{B13}$ are actually caused by the unreadiness probability of protection B. This important tripping effect just reminds us that the two apparently different failure modes of protection systems, i.e., the undesired-tripping mode and the fail-to-operate mode, have intrinsically intimate relationship with each other. The impact of the fail-to-operate mode, i.e., unreadiness probability, of protection B is showing up as an undesired-tripping mode of protection A due to backup function. It is this effect transformation of protection failure modes that causes the interactions between current-carrying components so complex and confusing. Now we know that after proper decoupling, the resulting down states A', $\tilde{A}_{B11}$, and $\tilde{A}_{B13}$ can all be regarded as undesired-tripping states of component A. The only difference among them is their transition rates because they are provided by different components.

It is worth noting that although the simplified component model shown in Figure 5-9 is better for use in computations, its equivalent parameters must be derived from data

which is only available for the corresponding complete Markov model shown in Figure 5-7(a). These parameters are derived using equations (5.9) and (5.10).

5.5.3. The Simplified Model for Component B

In the same way, we can obtain from Figure 5-7(b) the simplified model for component B as shown in Figure 5-10, in which B_0, $\hat{B}$, B', $\tilde{B}_{A12}$ and $\tilde{B}_{A13}$ represent the up state, the down state due to faults on component B, the down state due to undesired-tripping failure of protection B, and the down states due to the unreadiness probability of protection A, respectively.

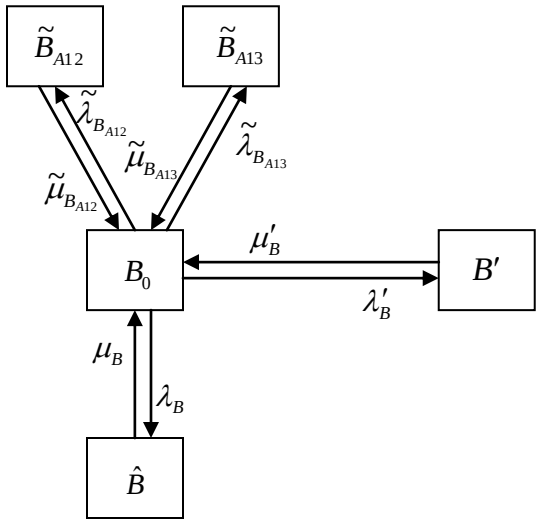

Figure 5-10. Simplified model for component B.

If we use P_{B_0}, $\hat{P}_B$, P'_B, $\tilde{P}_{B_{A12}}$, and $\tilde{P}_{B_{A13}}$ to represent the probabilities of states B_0, $\hat{B}$, B', $\tilde{B}_{A12}$ and $\tilde{B}_{A13}$, respectively, they can be determined to be given by

$$P_{B_0} = \frac{1}{K_B}, \tag{5.15}$$

$$\hat{P}_B = \frac{\lambda_B}{K_B \mu_B}, \tag{5.16}$$

$$P'_B = \frac{\lambda'_B}{K_B \mu'_B}, \tag{5.17}$$

$$\tilde{P}_{B_{A12}} = \frac{\tilde{\lambda}_{B_{A12}}}{K_B \tilde{\mu}_{B_{A12}}}, \tag{5.18}$$

$$\tilde{P}_{B_{A13}} = \frac{\tilde{\lambda}_{B_{A13}}}{K_B \tilde{\mu}_{B_{A13}}}, \tag{5.19}$$

wherein

$$K_B = 1 + \frac{\lambda_B}{\mu_B} + \frac{\lambda'_B}{\mu'_B} + \frac{\tilde{\lambda}_{B_{A12}}}{\tilde{\mu}_{B_{A12}}} + \frac{\tilde{\lambda}_{B_{A13}}}{\tilde{\mu}_{B_{A13}}}, \tag{5.20}$$

and

$$\tilde{\lambda}_{B_{A12}} = p_{A2}\lambda_A, \quad \tilde{\mu}_{B_{A12}} = \gamma_{A2}, \tag{5.21}$$

$$\tilde{\lambda}_{B_{A13}} = p_{A3}\lambda_A, \quad \tilde{\mu}_{B_{A13}} = \gamma_{A3}. \tag{5.22}$$

5.6. Numerical Case Study

In brief, the simplified models that we have built in Figure 5-9 and Figure 5-10 are actually not "simple" ones. They are derived from sophisticated modeling with numerous parameters and then reduced into the concise form. By the methodology of decoupling and the concept of equivalent transition rate, the simplified model stands out in the form of the component and successfully includes all the significant information of the complex interactions among corresponding components due to their protection system failures. Thus, it is an important Markov model which completely depicts the reliability situation including protection system failures at the current-carrying component level. For better understanding, we next give a simple case study as follows to illustrate how this simplified model effectively represents the component reliability situation including protection system failures.

The example power system we are using consists of two transmission lines and the configuration is the same as shown in Figure 5-2. Suppose the protection system of transmission line A (protection A) is designed to provide backup to the protection system of transmission line B (protection B). Here we are interested in the reliability situation of transmission line A. The necessary reliability parameters of the transmission lines and their protection systems are chosen [70], [72] and listed in Table 5-3.

Table 5-3 Data for transmission lines and their protection systems

Transmission lines	A	B
λ_j (1/year)	2	2
μ_j (1/year)	175	--
λ'_j (1/year)	0.05	--
μ'_j (1/year)	876	--
p_{j1}	--	0.02
p_{j2}	--	0.02
p_{j3}	--	0.01
γ_{j1} (1/year)	--	876
γ_{j2} (1/year)	--	876
γ_{j3} (1/year)	--	876

Note: *j* represents *A* or *B*

The state probabilities of transmission line A considering protection system failures are calculated and summarized in Table 5-4. The calculation results with perfect protection systems are also provided in the same table for comparison. We can easily see from data in Table 5-4 that the protection failures have degraded the reliability situation of transmission line A.

Table 5-4 State probabilities of transmission line A

Probabilities	Simplified complete model	Perfect protection model
P_{A_0} (up state)	0.988578	0.988701
$\hat{P}_A$ (down state)	0.011298	0.011299
P'_A (down state)	0.000056	--
$\widetilde{P}_{A_{B11}}$ (down state)	0.000045	--
$\widetilde{P}_{A_{B13}}$ (down state)	0.000023	--
Total down states	0.011422	0.011299

5.7. Summary

If protection systems were perfectly reliable, the modeling of current-carrying components would be quite simple. However, the consideration of protection system failures introduces a significant influence on the modeling. There are two types of protection system failures, the undesired-tripping mode and the fail-to-operate mode, which can cause difficulties in power system reliability evaluation.

The undesired-tripping mode protection failure of one component has no interaction with other components. We can simply use a two-state process to model the effect of this failure mode. The fail-to-operate mode protection failure is represented by unreadiness probability. The protection unreadiness probability of one component does not affect its own up-and-down status. Nevertheless, it will cause external undesired-

tripping mode failures to the adjacent component whose protection system is providing the backup function.

By the methodology of interaction decoupling and with the concept of equivalent transition rate, we have obtained the complete Markov model for components and then derived its simplified form. The simplified model not only contains important information of the component itself, but also incorporates significant information of related protection system failures for quantitative analysis. It can appropriately describe the overall reliability situation of individual components under the circumstances of complex interactions between components due to protection system failures [120], [121].

6. NEW MODELS AND CONCEPTS FOR POWER SYSTEM RELIABILITY EVALUATION INCLUDING PROTECTION SYSTEM FAILURES *

6.1. Introduction

In Section 5, we have derived the complete Markov model and its simplified form for reliability analysis including protection system failures at the current-carrying component level. Based on these applicable models, we further aim at developing new concepts and models for including protection system failures for application in overall power system reliability analysis.

---

* Part of this section is reprinted from copyrighted material with permission from IEEE.

The objective of this section is to develop concepts and techniques for modeling and analyzing the complex and interrelated effects of protection failures resulting in isolation of multiple components rather than just the faulted one. It is intuitively clear that as multiple outages happen because of protection system failures, the probability of cascading failures as a result of post-fault events will be higher than when only one component is assumed on outage. The scope of this research is limited to assess the probability of multiple component outages resulting from the protection failures. These models can also be further combined, if desired, with the models considering cascading events as can be the models that do not consider protection failures.

The remainder of this section is organized as follows. Section 6.2 introduces new concepts of down states and proposes the composite unit model as a key analysis tool. Section 6.3 illustrates how to use the composite unit model for reliability evaluation of simple power systems in detail. Section 6.4 generalizes the usage of the composite unit model for assessing the impact of protection failures on modeling system states and develops the methodology for reliability evaluation of large power systems including protection system failures. Section 6.5 is the summary of this section.

6.2. Self-down State, Induced-down State, and Composite Unit Model

We usually define the range of a current-carrying component bordered by its surrounding circuit breakers. This is also the duty zone that its protection system should

protect. From the standpoint of this component range, we recall Figure 5-2 of the example power system, Figure 5-9 of the simplified Markov model for component A, and Figure 5-10 of the model for component B to deliver new concepts and to derive new models for further application.

6.2.1. Self-down State and Induced-down State

In Figure 5-9, all down states of component A can be divided into two parts according to the range of component A. The first part is the down states resulting from internal causes, which is composed of two states $\hat{A}$ and A'. State $\hat{A}$ can be regarded as a self-fault-tripping state, while state A' can be seen as a self-undesired-tripping state. The second part is the down states from external causes, which comprises the other two states $\tilde{A}_{B11}$ and $\tilde{A}_{B13}$. These two states can be deemed as externally-induced-tripping states. If we consider the component and its protection within the range together as a virtually composite unit, we can alternatively name the first part as self-down state and the second part as induced-down state.

Similarly, all down states of component B in Figure 5-10 can also be summarized into these two parts. The self-down state includes two states $\hat{B}$ and B', and the induced-down state consists of the other two states $\tilde{B}_{A12}$ and $\tilde{B}_{A13}$.

For the self-down state, the number and form of its substates are always fixed. In addition, the transition rates between the self-down state and the up state of a component

are independent of other components. On the contrary, the induced-down state does not have fixed substates. It can be varying due to the coordination design of the backup protection systems. The transition rates between the induced-down state and the up state of a component definitely depend on other components.

6.2.2. Composite Unit Model

The number of states in component modeling plays an important role in reliability evaluation of power systems. The fewer they are, the easier it is for application. Therefore, we will merge substates of the self-down state using the concept of equivalent transition rate [91] to further reduce the number of states in the previous simplified models.

6.2.2.1. Composite unit model for component A

If we use $\overline{A}$ to represent the self-down state of component A, the simplified model in Figure 5-9 can be further reduced to the composite unit model as shown in Figure 6-1. We have also omitted the subscript "0" of the up state for simplicity, i.e. substituting A_0 with A.

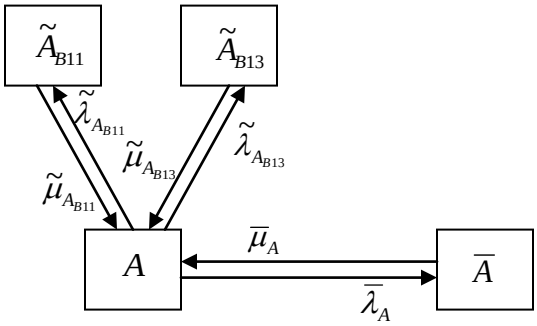

Figure 6-1. Composite unit model for component A.

We can obtain the equivalent failure and repair rates between the up state and self-down state of the composite unit model for component A, i.e., $\overline{\lambda}_A$ and $\overline{\mu}_A$, as follows. Here we use P_A, $\hat{P}_A$, P'_A, and $\overline{P}_A$ to represent the probabilities of states A, $\hat{A}$, A', and $\overline{A}$, respectively.

In Figure 5-9, for the process between states $A_{(0)}$ and $\hat{A}$, we have

$$P_A\lambda_A = \hat{P}_A\mu_A \Rightarrow \hat{P}_A = \frac{\lambda_A}{\mu_A}P_A . \tag{6.1}$$

For the process between states $A_{(0)}$ and A', we have

$$P_A\lambda'_A = P'_A\mu'_A \Rightarrow P'_A = \frac{\lambda'_A}{\mu'_A}P_A . \tag{6.2}$$

Since $\hat{A}$ and A' are mutually exclusive states, we can obtain the probability of state $\overline{A}$ from (6.1) and (6.2) as below.

$$\overline{P}_A = \hat{P}_A + P'_A = \left(\frac{\lambda_A}{\mu_A} + \frac{\lambda'_A}{\mu'_A}\right)P_A \tag{6.3}$$

Compare Figure 5-9 and Figure 6-1 using the concept of equivalent transition rate, we can easily know that

$$P_A\overline{\lambda}_A = P_A\lambda_A + P_A\lambda'_A . \tag{6.4}$$

Hence, the equivalent failure rate is

$$\overline{\lambda}_A = \lambda_A + \lambda'_A . \tag{6.5}$$

In Figure 6-1, for the process between states A and $\overline{A}$ we have

$$P_A\overline{\lambda}_A = \overline{P}_A\overline{\mu}_A \Rightarrow \overline{P}_A = \frac{\overline{\lambda}_A}{\overline{\mu}_A} P_A . \tag{6.6}$$

If we substitute (6.3) and (6.5) into (6.6), then we get the equivalent repair rate

$$\overline{\mu}_A = \frac{\mu_A\mu'_A(\lambda_A + \lambda'_A)}{\lambda_A\mu'_A + \lambda'_A\mu_A} . \tag{6.7}$$

6.2.2.2. Composite unit model for component B

Similarly, we can obtain from the simplified model in Figure 5-10 further to the composite unit model for component B as shown in Figure 6-2, in which we use $\overline{B}$ to represent the self-down state of component B and omit the subscript "0" of the up state for simplicity, i.e. substituting B_0 with *B*.

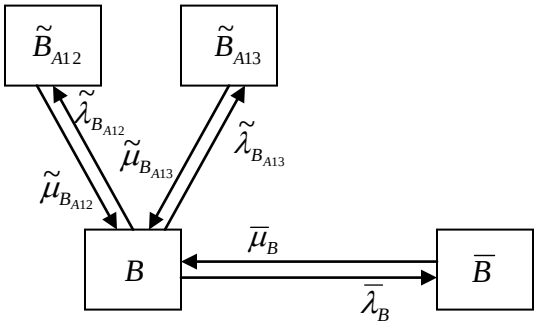

Figure 6-2. Composite unit model for component B.

In the same way, we can obtain the equivalent failure and repair rates between the up state and self-down state of the composite unit model for component B as following.

$$\overline{\lambda}_B = \lambda_B + \lambda'_B \tag{6.8}$$

$$\overline{\mu}_B = \frac{\mu_B \mu'_B (\lambda_B + \lambda'_B)}{\lambda_B \mu'_B + \lambda'_B \mu_B} \tag{6.9}$$

6.3. Illustration of Analyzing Simple Power Systems

With the concept of self-down and induced-down states and the composite unit model for current-carrying components, it becomes feasible to analyze the impact of protection failures on modeling system states. In this section, we will use the same example power system in Figure 5-2 to illustrate how to analyzing a simple power system by using the composite unit model.

6.3.1. Integration of the Induced-down State

6.3.1.1. Treatment of component A

Although substates of the induced-down state of a current-carrying component are generally not fixed, they can be determined so long as the coordination design of the backup protection systems is clear. For the example power system in Figure 5-2, the effect of induced-down state of component A has been modeled by two independent two-state processes associated with states $\tilde{A}_{B11}$ and $\tilde{A}_{B13}$ as in Figure 6-1.

We already know that the two states $\tilde{A}_{B11}$ and $\tilde{A}_{B13}$ in Figure 6-1 are both down states of component A caused by the unreadiness probability of protection B. Thus, if we use a new general state $\tilde{A}_B$ to represent the down state of component A caused by the impact of component B, the two processes regarding states $\tilde{A}_{B11}$ and $\tilde{A}_{B13}$ can be combined into a new two-state process associated with state $\tilde{A}_B$ using the concept of equivalent transition rate as shown in Figure 6-3.

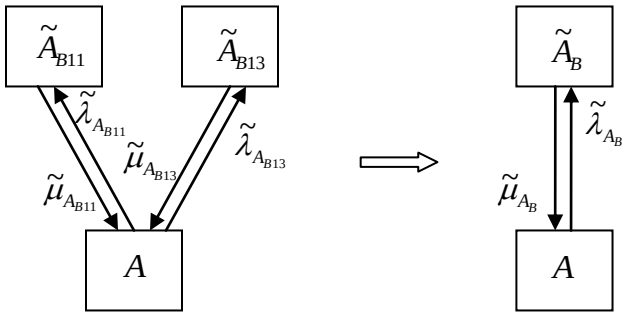

Figure 6-3. Treatment of the induced-down state of the composite unit model for component A.

Suppose the equivalent failure and repair rates of this new process are represented by $\tilde{\lambda}_{A_B}$ and $\tilde{\mu}_{A_B}$, respectively. These parameters can be easily derived by the frequency balance approach as shown in the following. Here we use P_A, $\tilde{P}_{A_{B11}}$, $\tilde{P}_{A_{B13}}$, and $\tilde{P}_{A_B}$ to represent the probabilities associated with states A, $\tilde{A}_{B11}$, $\tilde{A}_{B13}$, and $\tilde{A}_B$, respectively.

For the process between states A and $\tilde{A}_{B11}$, we have

$$P_A\tilde{\lambda}_{A_{B11}} = \tilde{P}_{A_{B11}}\tilde{\mu}_{A_{B11}} \Rightarrow \tilde{P}_{A_{B11}} = \frac{\tilde{\lambda}_{A_{B11}}}{\tilde{\mu}_{A_{B11}}} P_A . \tag{6.10}$$

For the process between states A and $\tilde{A}_{B13}$, we have

$$P_A\tilde{\lambda}_{A_{B13}} = \tilde{P}_{A_{B13}}\tilde{\mu}_{A_{B13}} \Rightarrow \tilde{P}_{A_{B13}} = \frac{\tilde{\lambda}_{A_{B13}}}{\tilde{\mu}_{A_{B13}}} P_A . \tag{6.11}$$

Since $\tilde{A}_{B11}$ and $\tilde{A}_{B13}$ are mutually exclusive states, we can obtain the probability of state $\tilde{A}_B$ from (6.10) and (6.11) as below.

$$\tilde{P}_{A_B} = \tilde{P}_{A_{B11}} + \tilde{P}_{A_{B13}} = \left(\frac{\tilde{\lambda}_{A_{B11}}}{\tilde{\mu}_{A_{B11}}} + \frac{\tilde{\lambda}_{A_{B13}}}{\tilde{\mu}_{A_{B13}}} \right) P_A \tag{6.12}$$

Using the concept of equivalent transition rate, we can know that

$$P_A\tilde{\lambda}_{A_B} = P_A\tilde{\lambda}_{A_{B11}} + P_A\tilde{\lambda}_{A_{B13}} . \tag{6.13}$$

Hence, the equivalent failure rate is

$$\tilde{\lambda}_{A_B} = \tilde{\lambda}_{A_{B11}} + \tilde{\lambda}_{A_{B13}} . \tag{6.14}$$

For the process between states A and $\tilde{A}_B$ we have

$$P_A\tilde{\lambda}_{A_B} = \tilde{P}_{A_B}\tilde{\mu}_{A_B} \Rightarrow \tilde{P}_{A_B} = \frac{\tilde{\lambda}_{A_B}}{\tilde{\mu}_{A_B}} P_A . \tag{6.15}$$

If we substitute (6.12) and (6.14) into (6.15), we get the equivalent repair rate

$$\tilde{\mu}_{A_B} = \frac{\tilde{\mu}_{A_{B11}}\tilde{\mu}_{A_{B13}}(\tilde{\lambda}_{A_{B11}} + \tilde{\lambda}_{A_{B13}})}{\tilde{\lambda}_{A_{B11}}\tilde{\mu}_{A_{B13}} + \tilde{\lambda}_{A_{B13}}\tilde{\mu}_{A_{B11}}} . \tag{6.16}$$

Note equations (5.9) and (5.10) for the details of $\tilde{\lambda}_{A_{B11}}$, $\tilde{\mu}_{A_{B11}}$, $\tilde{\lambda}_{A_{B13}}$, and $\tilde{\mu}_{A_{B13}}$. Substitute them into (6.14) and (6.16), then the equivalent transition rates $\tilde{\lambda}_{A_B}$ and $\tilde{\mu}_{A_B}$ are finally represented by

$$\tilde{\lambda}_{A_B} = (p_{B1} + p_{B3})\lambda_B , \tag{6.17}$$

$$\tilde{\mu}_{A_B} = \frac{\gamma_{B1}\gamma_{B3}(p_{B1} + p_{B3})}{p_{B1}\gamma_{B3} + p_{B3}\gamma_{B1}} . \tag{6.18}$$

After above integration treatment of the induced-down state, the composite unit model for component A in Figure 6-1 is now reduced to a concise three-state model as shown in Figure 6-4. The parameters of this model refer to equations (6.5), (6.7), (6.17), and (6.18).

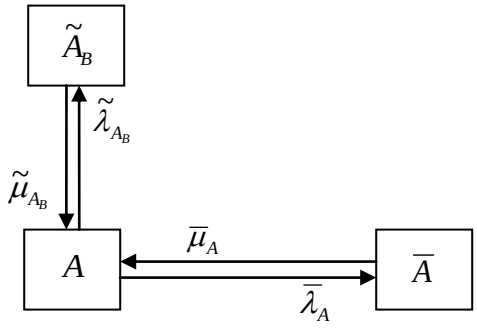

Figure 6-4. Three-state model for component A.

6.3.1.2. Treatment of component B

In the same way, we can also reduce the composite unit model for component B in Figure 6-2 to the three-state model as shown in Figure 6-5.

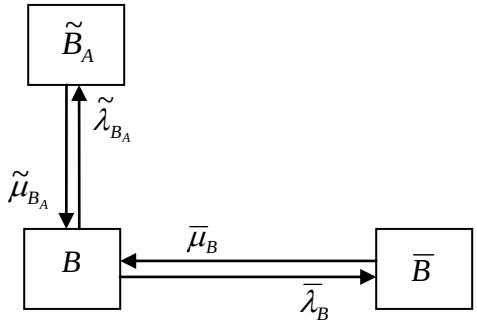

Figure 6-5. Three-state model for component B.

In Figure 6-5, the new state $\tilde{B}_A$ represents the down state of component B caused by the impact of component A, which equivalently replaces the two induced down states $\tilde{B}_{A12}$ and $\tilde{B}_{A13}$ in Figure 6-2. The equivalent failure and repair rates $\overline{\lambda}_B$ and $\overline{\mu}_B$ of this

model refer to equations (6.8) and (6.9), respectively. The equivalent failure and repair rates $\tilde{\lambda}_{B_A}$ and $\tilde{\mu}_{B_A}$ can also be easily derived by the frequency balance approach and the resulting expression is given below.

$$\tilde{\lambda}_{B_A} = (p_{A2} + p_{A3})\lambda_A \tag{6.19}$$

$$\tilde{\mu}_{B_A} = \frac{\gamma_{A2}\gamma_{A3}(p_{A2} + p_{A3})}{p_{A2}\gamma_{A3} + p_{A3}\gamma_{A2}} \tag{6.20}$$

6.3.2. Reliability Evaluation of the Example Power System

In a power system, the system state is determined by the status of its current-carrying components. Since each of components A and B has three states as shown in Figure 6-4 and Figure 6-5, the example power system in Figure 5-2 should theoretically have nine system states, which can be represented by AB, $A\overline{B}$, $A\tilde{B}_A$, $\overline{A}B$, $\overline{A}\overline{B}$, $\overline{A}\tilde{B}_A$, $\tilde{A}_B B$, $\tilde{A}_B \overline{B}$, and $\tilde{A}_B \tilde{B}_A$, respectively. However, there are actually three impossible system states which are $A\tilde{B}_A$, $\tilde{A}_B B$ and $\tilde{A}_B \tilde{B}_A$.

For the system state $\tilde{A}_B B$, we already know that $\tilde{A}_B$ is the induced-down state of component A. As we can see from the previous interaction decoupling in Figure 5-5, component B is always down simultaneously as long as component A is transferred into its induced-down state. Thus, component A cannot be in the induced-down state if component B is in the up state, which means that the system state $\tilde{A}_B B$ cannot exist. For the same reason (refer to Figure 5-6), the system state $A\tilde{B}_A$ cannot exist, too.

For the system state $\tilde{A}_B\tilde{B}_A$, we have previously assumed that all the backup functions are perfectly reliable. In addition, we can see from Figure 5-5 that the induced-down state of component A not only is always accompanied by the self-down state of component B, but also has already returned to the up state of component A before component B leaves its self-down state. Similarly, we can see from Figure 5-6 that the induced-down state of component B not only is always accompanied by the self-down state of component A, but also has already returned to the up state of component B before component A leaves its self-down state. Hence, the system state $\tilde{A}_B\tilde{B}_A$ indeed cannot exist.

The above information simply indicates that the probabilities of system states $A\tilde{B}_A$, $\tilde{A}_B B$ and $\tilde{A}_B\tilde{B}_A$ are all zero and we do not need to consider them anymore. Therefore, the example power system has only six possible system states and we can directly draw the system state transition diagram as shown in Figure 6-6. Note in the single transition from system state AB to system state $A\bar{B}$, the failure rate becomes $(\bar{\lambda}_B - \tilde{\lambda}_{A_B})$ instead of just $\bar{\lambda}_B$. This is because as component B is considered in the system state AB, the failure rate $\tilde{\lambda}_{A_B}$ is actually a portion of $\bar{\lambda}_B$ and is already distributed to another single transition from system state AB to system state $\tilde{A}_B\bar{B}$. The relationship detail between $\tilde{\lambda}_{A_B}$ and $\bar{\lambda}_B$ refers to equations (6.8) and (6.17). For the same reason, the failure rate of the single transition from system state AB to system state $\bar{A}B$

becomes $(\overline{\lambda}_A - \widetilde{\lambda}_{B_A})$ instead of just $\overline{\lambda}_A$. The relationship detail between $\widetilde{\lambda}_{B_A}$ and $\overline{\lambda}_A$ refers to equations (6.5) and (6.19).

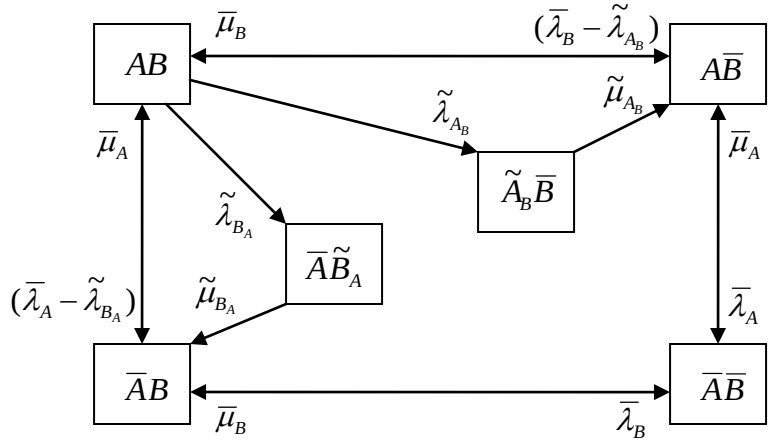

Figure 6-6. System state transition diagram of the example power system.

By using the frequency balance approach for Figure 6-6, the probability of each system state and the reliability indices such as the Loss Of Load Expectation (LOLE) and the Expected Unserved Energy (EUE) can all be easily figured out for the example power system.

Here we use P_1, P_2, P_3, P_4, P_5, and P_6 to represent the probabilities associated with system states AB, $A\overline{B}$, $\overline{A}B$, $\overline{A}\overline{B}$, $\widetilde{A}_B\overline{B}$, and $\overline{A}\widetilde{B}_A$, respectively. In order to find these probabilities, we write an equation of frequency balance for each of the six system states.

For the system state AB, we have

$$P_2\overline{\mu}_B + P_3\overline{\mu}_A = P_1(\overline{\lambda}_A + \overline{\lambda}_B). \tag{6.21}$$

For the system state $A\overline{B}$, we have

$$P_1(\overline{\lambda}_B - \widetilde{\lambda}_{A_B}) + P_4\overline{\mu}_A + P_5\widetilde{\mu}_{A_B} = P_2(\overline{\lambda}_A + \overline{\mu}_B). \tag{6.22}$$

For the system state $\overline{A}B$, we have

$$P_1(\overline{\lambda}_A - \widetilde{\lambda}_{B_A}) + P_4\overline{\mu}_B + P_6\widetilde{\mu}_{B_A} = P_3(\overline{\mu}_A + \overline{\lambda}_B). \tag{6.23}$$

For the system state $\overline{A}\overline{B}$, we have

$$P_2\overline{\lambda}_A + P_3\overline{\lambda}_B = P_4(\overline{\mu}_A + \overline{\mu}_B). \tag{6.24}$$

For the system state $\widetilde{A}_B\overline{B}$, we have

$$P_1\widetilde{\lambda}_{A_B} = P_5\widetilde{\mu}_{A_B}. \tag{6.25}$$

For the system state $\overline{A}\widetilde{B}_A$, we have

$$P_1\widetilde{\lambda}_{B_A} = P_6\widetilde{\mu}_{B_A}. \tag{6.26}$$

Since the probabilities of system states $A\widetilde{B}_A$, $\widetilde{A}_B B$ and $\widetilde{A}_B\widetilde{B}_A$ are all zero, we get

$$\sum_{i=1}^{6} P_i = 1. \tag{6.27}$$

Using any five of the six equations (6.21)-(6.26) together with equation (6.27), we can solve and obtain the state probabilities.

For the example power system in Figure 5-2, the Loss Of Load Expectation (LOLE) and the Expected Unserved Energy (EUE) are calculated as below.

$$LOLE = (P_4 + P_5 + P_6) \times 8760 \quad \text{(h/year)} \tag{6.28}$$

$$EUE = L \times LOLE \quad \text{(MWh/year)} \tag{6.29}$$

6.3.3. Numerical Case Study

Now we use some numerical data to illustrate the impact of protection system failures on reliability evaluation of the example power system. The necessary parameters of current-carrying components and their protection systems are chosen [70], [72] and listed in Table 6-1.

Table 6-1 Parameters of components and their protection systems

Components	A	B
λ_j (1/year)	2	2
μ_j (1/year)	175	175
λ'_j (1/year)	0.05	0.05
μ'_j (1/year)	876	876
p_{j1}	0.02	0.02
p_{j2}	0.02	0.02
p_{j3}	0.01	0.01
γ_{j1} (1/year)	876	876
γ_{j2} (1/year)	876	876
γ_{j3} (1/year)	876	876
L (MW)	10	

Note: *j* represents *A* or *B*

The reliability indices of the example power system are calculated and summarized in Table 6-2. The corresponding results with the perfect protection model are also provided for comparison. It is obvious that protection system failures do have influence on probabilities of all the system states. For the reliability indices LOLE and EUE, we find that they both have been doubled over those of the perfect protection model. Thus, the reliability situation of the example power system has been degraded tremendously due to the impact of protection system failures.

Table 6-2 Reliability indices of the example power system

Reliability indices	Composite unit model	Perfect protection model
P_1 (state AB)	0.977288	0.977529
P_2 (state $A\overline{B}$)	0.011225	0.011172
P_3 (state $\overline{A}B$)	0.011225	0.011172
P_4 (state $\overline{A}\overline{B}$)	0.000129	0.000128
P_5 (state $\widetilde{A}_B\overline{B}$)	0.000067	--
P_6 (state $\overline{A}\widetilde{B}_A$)	0.000067	--
LOLE (h/year)	2.302	1.118
EUE (MWh/year)	23.021	11.185

Since components A and B in a sense are symmetrical in the example power system of Figure 5-2, we change parameters of protection B only to see the trend how protection failure rates influence the system reliability. Table 6-3 gives the computation results of reliability indices for different protection failure rates of component B with all

other parameters the same as in Table 6-1. Here we need to point out that the reliability indices assuming perfect protection model will remain the same as in Table 6-2 because no change happens on the component transition rates. From Table 6-3, we can easily see that the system reliability indices become much greater as protection system failures are considered.

Table 6-3 Reliability indices for different protection failure rates

Unreadiness probability p_{B1}	Failure rate λ'_B (1/year)	Loss Of Load Expectation (LOLP)	Expected Unserved Energy (EUE) (MWh/year)
0.02	0.05	2.302	23.021
0.02	0.10	2.308	23.076
0.02	0.25	2.324	23.240
0.02	0.50	2.351	23.514
0.02	1.00	2.406	24.062
0.05	0.05	2.888	28.883
0.05	0.10	2.894	28.937
0.05	0.25	2.910	29.101
0.05	0.50	2.937	29.373
0.05	1.00	2.992	29.917
0.10	0.05	3.865	38.651
0.10	0.10	3.870	38.705
0.10	0.25	3.887	38.867
0.10	0.50	3.914	39.136
0.10	1.00	3.967	39.675
Perfect protection model		1.118	11.185

Figure 6-7 and Figure 6-8 are diagrams of the incremental percentage of EUE versus λ_B' and p_{B1}, respectively. From Figure 6-7 we find that as the undesired-tripping mode protection failure rate increases, the expected unserved energy of the example power system will increase accordingly. From Figure 6-8 we see that the expected unserved energy will also increase as the unreadiness probability of the fail-to-operate mode protection failure increases. If we look at these two diagrams together, we can intuitively see that EUE is by far more sensitive to parameter p_{B1} than to λ_B'. It simply indicates that there could be significant errors in reliability evaluation of power systems if we ignore protection system failures especially the fail-to-operate mode protection failures.

The diagrams of incremental percentage of LOLE versus λ_B' and p_{B1} are quite similar to Figure 6-7 and Figure 6-8. We can also find the same conclusion for LOLE as above for EUE. It sounds reasonable as we can see from (6.29) that EUE and LOLE are linearly correlated for our numerical case study.

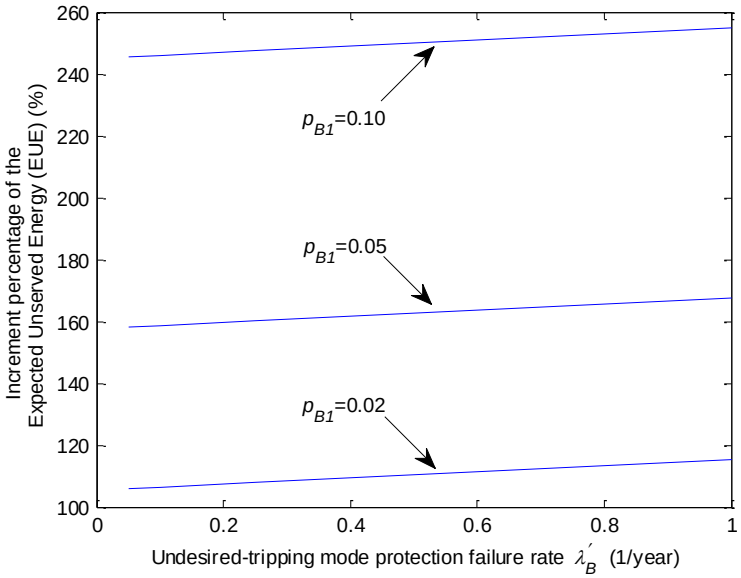

Figure 6-7. Incremental percentage of the Expected Unserved Energy (EUE) vs. undesired-tripping mode protection failure rate (λ_B').

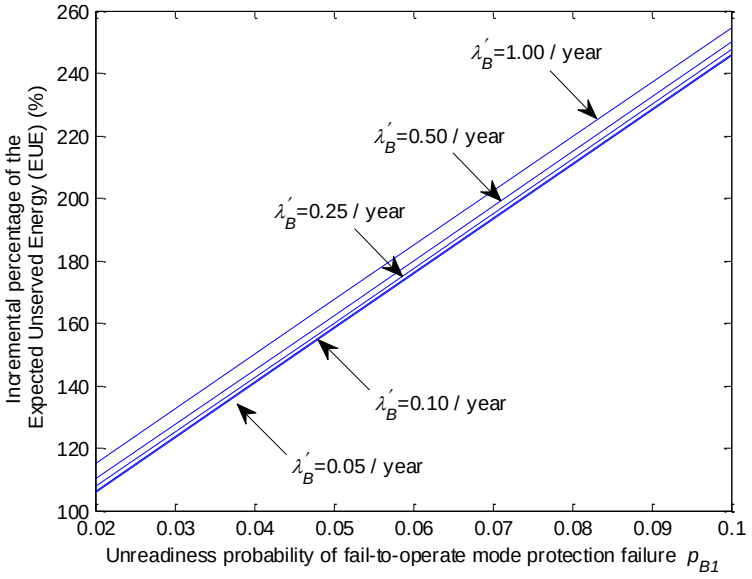

Figure 6-8. Incremental percentage of the Expected Unserved Energy (EUE) vs. unreadiness probability of fail-to-operate mode protection failure (p_{B1}).

6.4. Methodology for Analyzing Large Power Systems

For large power systems, more challenges can be expected than those of simple ones like the example power system we analyzed in Section 6.3. Since there are a lot of components in a large power system, the system states are far more in numbers and the protection coordination is much more complex. In a practical power system, every current-carrying component is primarily protected by its own protective relays. In addition, almost each component is further protected by backup protection from adjacent component protection zones. Thus, it is important to model the system states and their relationships in a general form.

6.4.1. Impact of Protection Failures on Modeling System States

We can still use the concept of self-down and induced-down states and the composite unit model for current-carrying components to analyze the impact of protection failures on modeling system states. As we have mentioned before, a component may associate with more than two breakers. But we still prefer to assume only two equivalent breakers for a component so as to deliver the concept and to illustrate the model clearer.

Suppose arbitrarily a component i is connected through its breakers i_1 and i_2 to two sets of adjacent components, say H and J, respectively. As shown in Figure 6-9, h and j are arbitrary components of these two sets, respectively.

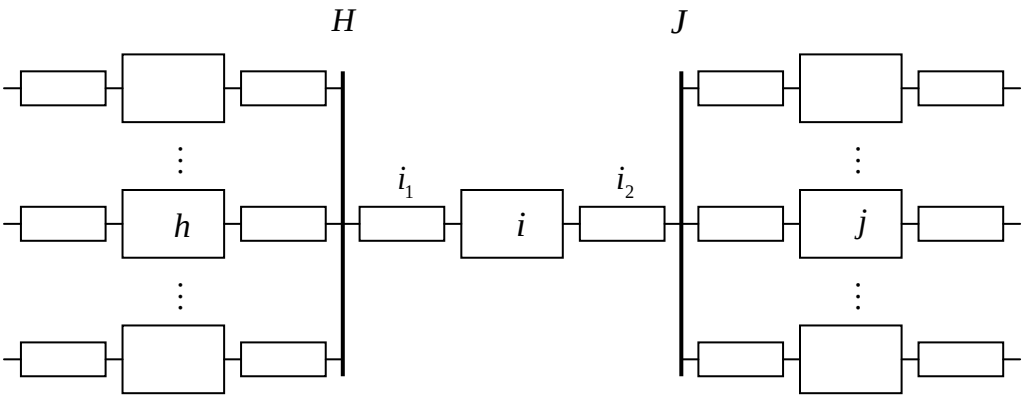

Figure 6-9. Component *i* and its adjacent components.

If there is no component induced-down state, the system state would be a simple combination of component self-down states because the self-down state of a component is independent of each other. The single-step transition rates between any two system states would be the equivalent failure and repair rates of the composite unit model for the component, say *i*, which changes its status in this transition. Similar to expressions (6.5) and (6.7), or (6.8) and (6.9), we can obtain without difficulty the formulae to calculate these transition rates of component *i* as follows.

$$\overline{\lambda}_i = \lambda_i + \lambda_i', \qquad \overline{\mu}_i = \frac{\mu_i \mu_i'(\lambda_i + \lambda_i')}{\lambda_i \mu_i' + \lambda_i' \mu_i} \tag{6.30}$$

However, the existence of component induced-down states makes the system state more complicated. Besides the system states consisting of component self-down states only, there are some new system states comprised of both component self-down and induced-down states. For each new system state, the component induced-down states are dependent on and can only be together with a specific component self-down

state which contains the inducing source, i.e. the unreadiness probability of protection failures. It will be clearer to illustrate this by Figure 6-10.

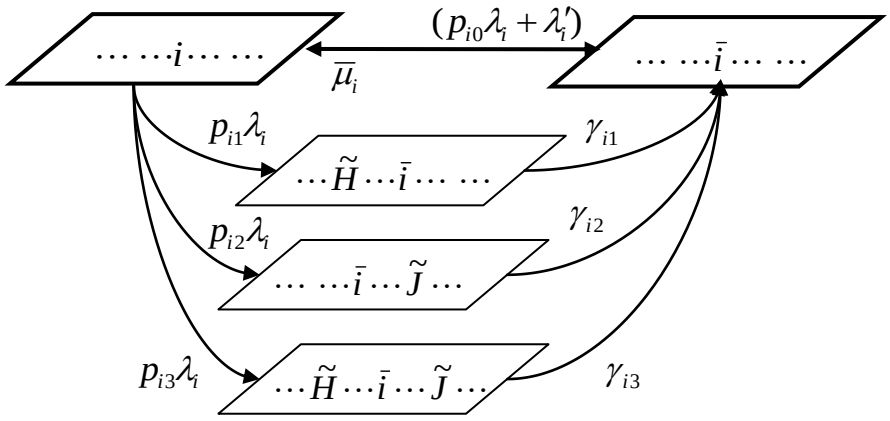

Figure 6-10. Impact of protection failures on modeling system states.

In Figure 6-10, component *i* is considered for a single-step transition. The system states $(\cdots\cdots i\cdots\cdots)$ and $(\cdots\cdots \bar{i}\cdots\cdots)$ have all components in the same status except component *i* being up and down, respectively. These two system states merely consist of self-down states.

Suppose there is at least one adjacent component $h \in H$ and $j \in J$ which is in the up state and provides backup protection to component *i*. According to different cases of protection unreadiness probability of component *i*, there will be three possible new system states $(\cdots \tilde{H}\cdots \bar{i}\cdots\cdots)$, $(\cdots\cdots \bar{i}\cdots \tilde{J}\cdots)$, and $(\cdots \tilde{H}\cdots \bar{i}\cdots \tilde{J}\cdots)$ which are comprised of component self-down and induced-down states. For example, in the system state $(\cdots \tilde{H}\cdots \bar{i}\cdots\cdots)$, all components of set *H* previously being in the up state are now in

their induced-down state together with component *i* being in its self-down state, and the status of all other components are the same as those in system states $(\cdots\cdots i\cdots\cdots)$ and $(\cdots\cdots \bar{i}\cdots\cdots)$. From previous component modeling analysis we know that the transition rates associated with this system state $(\cdots \tilde{H}\cdots \bar{i}\cdots\cdots)$ are $p_{i1}\lambda_i$ and γ_{i1} as shown in Figure 6-10. Similar explanations also apply to modeling system states $(\cdots\cdots \bar{i}\cdots \tilde{J}\cdots)$ and $(\cdots \tilde{H}\cdots \bar{i}\cdots \tilde{J}\cdots)$.

Since new system states have been added, the transition rates between system states $(\cdots\cdots i\cdots\cdots)$ and $(\cdots\cdots \bar{i}\cdots\cdots)$ may need to be modified. Specifically, the failure rate can no longer be $\overline{\lambda}_i$ because the failure rates $p_{i1}\lambda_i$, $p_{i2}\lambda_i$, and $p_{i3}\lambda_i$ associated with unreadiness probabilities allocated to the three new system states in Figure 6-10 should be subtracted from $\overline{\lambda}_i$. From expression (6-30) and previous simplification process illustrated in Figure 5-8, it is not difficult to know that the resulting failure rate after this subtraction is $(p_{i0}\lambda_i + \lambda_i')$. As for the repair rate $\overline{\mu}_i$, there is no need to change at all.

6.4.2. Markov Modeling of Power Systems with Protection Failures

6.4.2.1. Reliability modeling of power systems with perfect protections

We normally assume that the failure mode of a current-carrying component due to faults on itself is independent. If the protection systems are perfect, the reliability

modeling of power systems is a one-layer Markov processes as shown in Figure 6-11. In this figure, each block represents a system state and all transitions between any two system states are single-step transitions.

6.4.2.2. Reliability modeling of power systems with protection failures

However, the impact of protection failures on modeling system states will also influence the reliability modeling of power systems shown in Figure 6-11. From the previous analysis in Section 6.4.1, we see that for every single-step transition of component *i*, there will be a group of three new system states added reflecting interactions and dependencies of current-carrying components. This group of states is attached to and forms a closed loop along with the independent single-step transition as shown in Figure 6-10. Considering arbitrariness in the selection of component *i*, the reliability modeling of power systems including protection system failures will be a two-layer Markov processes as illustrated in Figure 6-12.

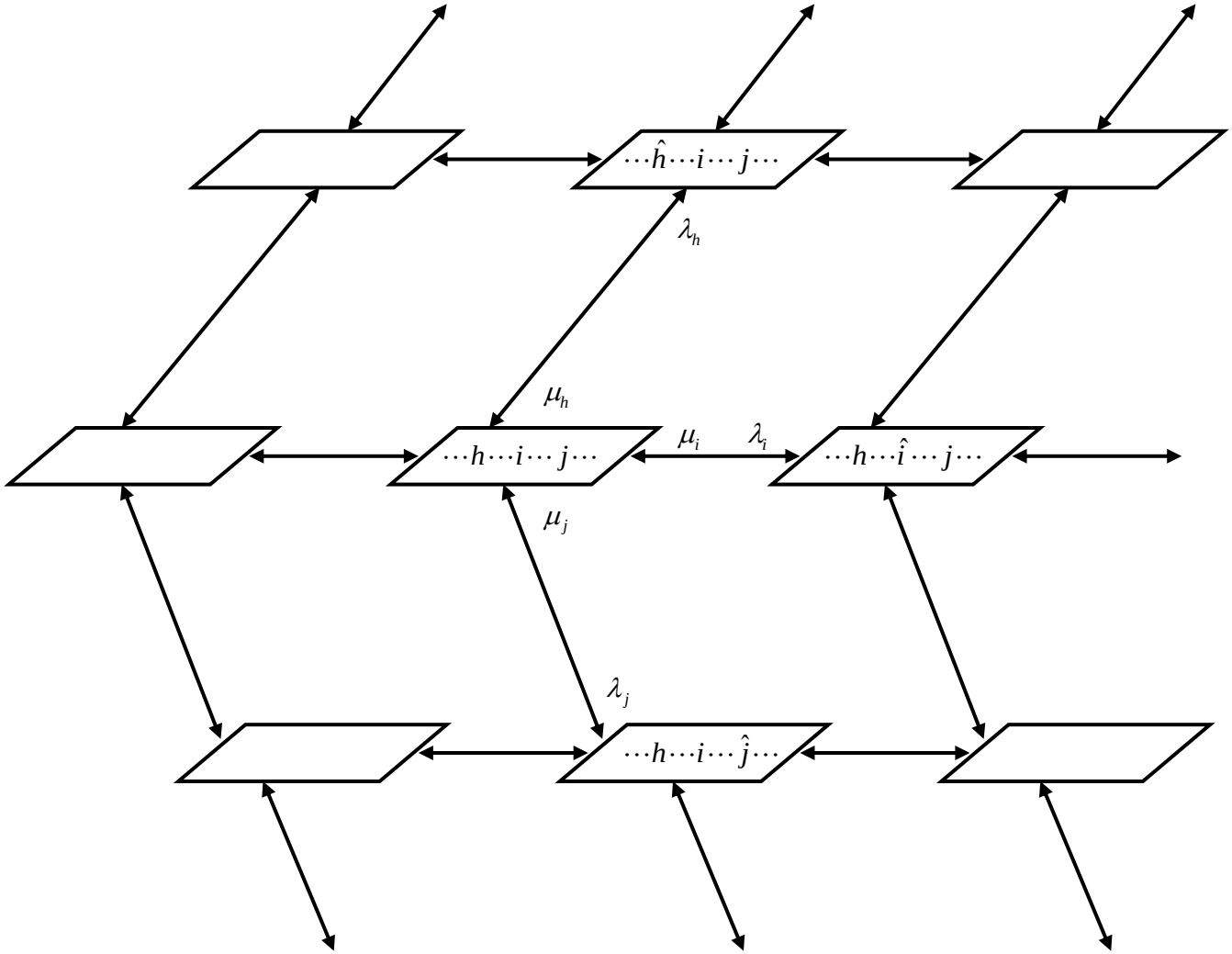

Figure 6-11. Reliability modeling of power systems with perfect protections.

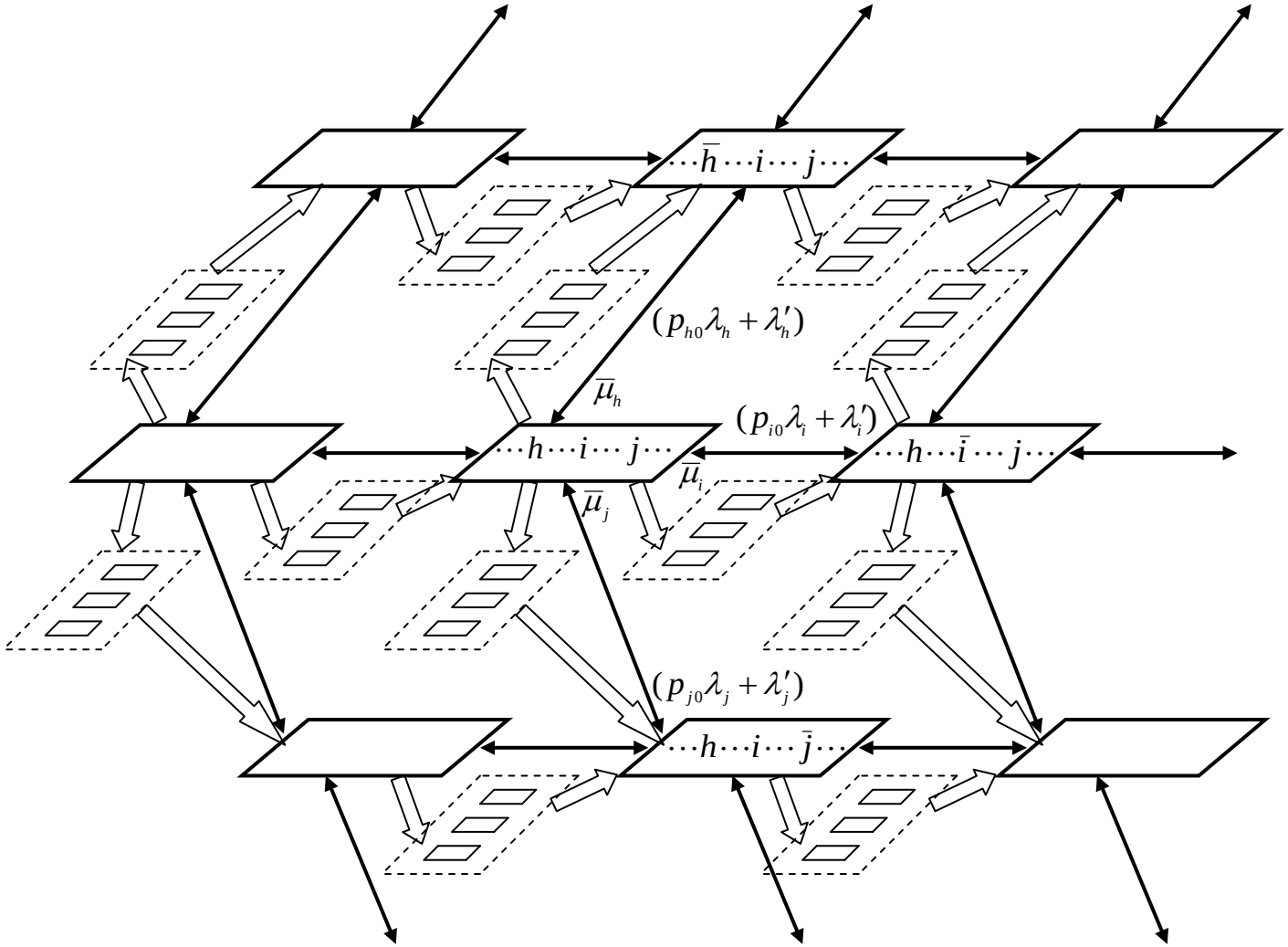

Figure 6-12. Reliability modeling of power systems with protection failures.

The first layer is shown as the bold part in Figure 6-12, which we name the primary layer. The primary layer Markov processes consist of only the independent system states with single-step transitions. Although, in structure, it looks the same as if we model power systems with perfect protections in Figure 6-11, it has totally different meanings and transition rates for its system states are different.

The second layer is shown as the dotted part in Figure 6-12. It is a dependent layer attached to the primary one, reflecting interactions and dependencies of current-carrying components by the impact of protection system failures. Each element of the second layer is actually a group of system states with common mode failures, which has been analyzed in detail just in the previous content of Section 6.4.1.

It is evident that system states in the second layer have more components down simultaneously than the corresponding system states of the primary layer, which generally indicates worse situation for system reliability. Since elements of the second layer are attached to every single-step transition in the primary layer, we can have an intuitive sense why protection failures could worsen the power system reliability.

6.4.2.3. Methodology for power system reliability evaluation

The general methodology for power system reliability evaluation including protection system failures can be stated as follows.

(1) Set up the primary layer Markov processes as if with perfect protection systems. The single-step failure and repair rates of a given component *i* are λ_i and μ_i, respectively.

(2) Replace the transition rates by component self-down failure and repair rates, i.e. $\overline{\lambda}_i$ and $\overline{\mu}_i$, as given in expression (6.30). The primary layer Markov process has been updated to include undesired-tripping mode protection failures.

(3) Set up the second layer Markov processes and attach it to the primary layer as shown in Figure 6-10 and Figure 6-12. Then modify the failure rate of the primary layer from $\overline{\lambda}_i$ to $(p_{i0}\lambda_i + \lambda_i')$. Now the fail-to-operate mode protection failures are also integrated into the system model.

(4) Evaluate the power system reliability.

6.4.3. Power System Reliability Evaluation Including Protection System Failures

There are two general approaches for reliability assessment of a system: the analytical method and the simulation method. For the system Markov model already set up in the previous Section 6.4.2, applications of these two approaches are illustrated as follows.

6.4.3.1. Analytical method

Although various analytical methods exist for assessing the system reliability, their applications to reliability evaluation of power systems with protection failures could be restricted. The main reason for this is the dependence of failures as we can see from the system Markov model in Figure 6-12.

Nevertheless, the frequency balance approach can still be used for steady state analysis in spite of dependencies in the system. For each system state of the Markov processes in Figure 6-10, we can write an equation of frequency balance as below.

For the system state $(\cdots\cdots i\cdots\cdots)$, we have

$$P_{(\cdots\bar{i}\cdots)}\overline{\mu}_i + \sum_m (P_m \rho_m) = P_{(\cdots i\cdots)}(\lambda_i + \lambda_i' + \sum_n \rho_n)\,. \tag{6.31}$$

For the system state $(\cdots\tilde{H}\cdots\bar{i}\cdots\cdots)$, we have

$$P_{(\cdots i\cdots)} \cdot p_{i1}\lambda_i = P_{(\cdots\tilde{H}\cdots\bar{i}\cdots)}\gamma_{i1}\,. \tag{6.32}$$

For the system state $(\cdots\cdots\bar{i}\cdots\tilde{J}\cdots)$, we have

$$P_{(\cdots i\cdots)} \cdot p_{i2}\lambda_i = P_{(\cdots\bar{i}\cdots\tilde{J}\cdots)}\gamma_{i2}\,. \tag{6.33}$$

For the system state $(\cdots\tilde{H}\cdots\bar{i}\cdots\tilde{J}\cdots)$, we have

$$P_{(\cdots i\cdots)} \cdot p_{i3}\lambda_i = P_{(\cdots\tilde{H}\cdots\bar{i}\cdots\tilde{J}\cdots)}\gamma_{i3}\,. \tag{6.34}$$

For the system state $(\cdots\cdots\bar{i}\cdots\cdots)$, we have

$$\begin{aligned} &P_{(\cdots i\cdots)}(p_{i0}\lambda_i + \lambda_i') + P_{(\cdots\tilde{H}\cdots\bar{i}\cdots)}\gamma_{i1} + P_{(\cdots\bar{i}\cdots\tilde{J}\cdots)}\gamma_{i2} + P_{(\cdots\tilde{H}\cdots\bar{i}\cdots\tilde{J}\cdots)}\gamma_{i3} + \sum_r (P_r\rho_r) \\ &= P_{(\cdots\bar{i}\cdots)}(\overline{\mu}_i + \sum_s \rho_s) \end{aligned}\,. \tag{6.35}$$

Here $P_{(\cdot)}$ represents the probability of system state $(\cdot)$. The subscripts *m* and *n* are used for other system states not seen from Figure 6-10 but existing in Figure 6-12 with direct transitions to and from system state $(\cdots\cdots i\cdots\cdots)$, respectively. Similar explanation applies to subscripts *r* and *s* with respect to system state $(\cdots\cdots \bar{i}\cdots\cdots)$. We also use the symbol ρ to represent the corresponding transition rates.

If there are finite number, say ℓ, of system states, we can theoretically obtain a set of ℓ such equations. Then we solve for system state probabilities combining any $\ell-1$ equations with the following total probability equation.

$$\sum_{k=1}^{\ell} P_k = 1 \tag{6.36}$$

It is obvious that this approach is only suitable for systems with a small number of system states. For a large power system, the state space could be so huge that it becomes impractical to solve simultaneous equations for all the system states. Thus, a feasible simulation method is proposed as following for handling large power systems.

6.4.3.2. Monte Carlo simulation method

The Monte Carlo simulation methods can be classified into two categories: random sampling and sequential simulation. The random sampling approach is non-sequential and thus difficult to deal with cases of dependent transition modes such as our system Markov model. So, the sequential simulation approach is selected and the system

states are generated sequentially by transition from one state to the next using probability distributions of component state durations and the random numbers [122], [123].

Suppose a component *i* with its state duration represented by a random variable D_i. If Z_i is a random number, then the observation of D_i can be obtained by

$$d_i = F_i^{-1}(z_i) \tag{6.37}$$

wherein F_i is the duration distribution function of component *i*. For exponential distribution, (6.37) would be

$$d_i = -\frac{\ln(z_i)}{\rho_i} \tag{6.38}$$

wherein ρ_i is the transition rate of component *i*.

Although the component with minimal time makes a transition and causes system transition as in the standard simulation procedure, two special treatments are necessary during the simulation to accommodate our system modeling.

The special treatment type I is for component transitions from its up state to self-down states. As we can see in Figure 6-10, there are four such possible transitions for component *i* with transition rates $(p_{i0}\lambda_i + \lambda_i')$, $p_{i1}\lambda_i$, $p_{i2}\lambda_i$, and $p_{i3}\lambda_i$, respectively. Since all these transitions are independent of other components, this is actually a multistate problem in sequential simulation. It can be handled by using four random numbers to generate four transition time values with respect to these possible transitions. Then the transition with the minimal value is chosen as the effective for simulation process [124].

The special treatment type II is for component transitions into and out from induced-down states. Since a certain component induced-down state is dependent on some other component, such a transition is passive and we cannot assign it an extra random number to avoid transition time conflict with the self-down and/or switching transitions inducing it. Instead we handle the case in the way described as follows.

If component *i* is sampled in the up state and chosen for the next system event with the transition time T_i obtained from its transition rate $p_{i1}\lambda_i$ using (6.38), it means that the system will change after time T_i from system state $(\cdots\cdots i\cdots\cdots)$ to system state $(\cdots\tilde{H}\cdots\bar{i}\cdots\cdots)$ as shown in Figure 6-10. Then at the moment of this transition, besides handling component *i*, we also need to check the status of all components belonging to set *H*. For those components already in down states (their protection systems thus cannot provide backup function), nothing needs to be done. But for each component in the up state, we need to change it to the down state so as to reflect the dependent induced-down transition. In addition, we override the transition time of this component with a new value the same as the switching time of component *i* with respect to the switching rate γ_{i1}. Thus, the switching process is also simulated.

Now we give the steps of the whole simulation algorithm:

Suppose the nth transition has just taken place at time t_n.

Step 1) Determine the value of T_i, the effective time to the next transition of component *i*.

Case a) If component *i* is in the up state, T_i is obtained using the special treatment type I described previously.

Case b) If component *i* is in one of its self-down state with unreadiness probabilities, check all its adjacent components on the corresponding side and make necessary changes using the special treatment type II described previously.

Case c) For all other cases, T_i is obtained in the normal way using (6.38), no special action needs to be taken.

Step 2) The time to the next system transition is given by

$$T = \min\{T_i\}. \tag{6.39}$$

If this T corresponds to T_p, the next transition is determined by the pth component. Note that there could be several such components to change their states simultaneously due to Case b) of Step 1).

Step 3) The simulation time is now advanced.

$$t_{n+1} = t_n + T \tag{6.40}$$

Step 4) The residual time to transition of component *i* is

$$T_i^r = T_i - T. \tag{6.41}$$

Step 5) The residual time for component *p* causing the transition becomes zero and the time to its next transition T_p is determined the same as in Step 1).

Step 6) The time T_i is then set as

$$T_i = \begin{cases} T_i^r, & i \neq p \\ T_p, & i = p \end{cases}. \tag{6.42}$$

Step 7) From t_n to t_{n+1}, the status of equipment stays fixed and the following steps are performed.

(a) The load for each node is updated to current hour.

(b) If no node has load loss, the simulation proceeds to the next hour, otherwise remedial actions are called.

(c) If after remedial actions all loads are satisfied, then simulation proceeds to next hour. Otherwise, this is counted as loss of load hour for those nodes and the system. If in the previous hour there was no load loss, it is counted as one event of loss of load.

(d) Repeat steps (a)-(c) until simulation time t_{n+1}.

Step 8) Go back to Step 2) and continue the simulation until convergence criterion is satisfied or the preset maximal number of simulation is reached.

Step 9) Terminate the simulation and calculate reliability indices as needed.

6.4.4. Numerical Case Study

The 24-bus IEEE Reliability Test System (RTS) is used for our numerical case study and the one-line diagram of this power system is shown in Figure 6-13 [125],

[126]. The original parameters of current-carrying components are used with a flat load curve of the annual peak load for 8760 hourly values. However, important parameters associated with protection system failures are not a part of the RTS database.

It is necessary to point out here that data are of great significance for model application and system evaluation. As to the protective relays, the reliability characteristics are quite different for various types such as electromechanical relays, analog electronic relays, and microprocessor-based relays. Even for the same type of equipments, their reliability behavior could be influenced by many factors such as installation environment, test interval, and maintenance quality. Thus, the reliability parameters of each practical protection system can be regarded as "unique". For important parameters such as undesired-tripping failure rate λ_i' and the unreadiness probability p_{ik}, they can be computed by appropriately developed reliability models if the failure and repair rates of elements of protection systems are known [69], [80]. As an alternative approach, these parameters could also be estimated from field data using the following equations.

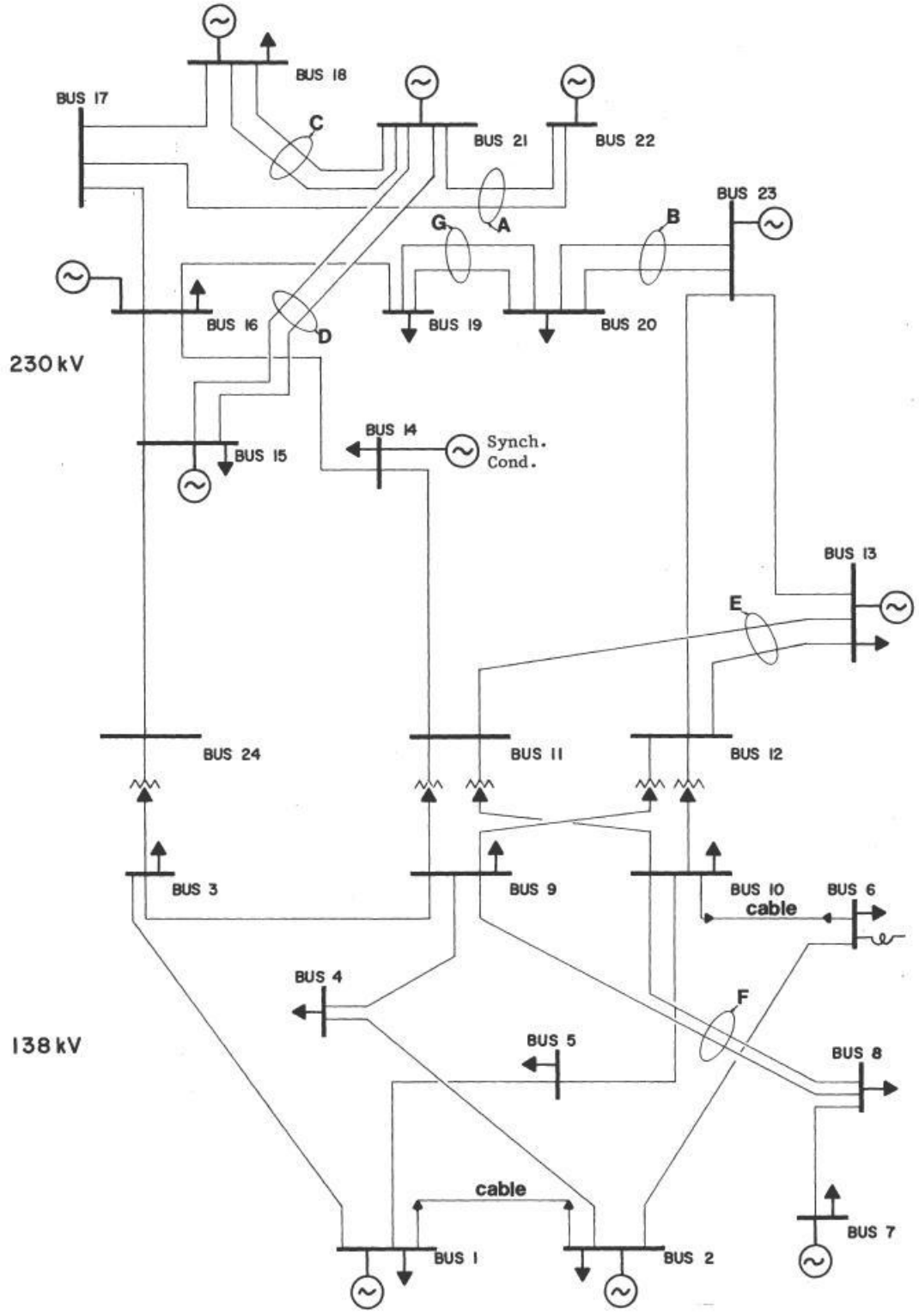

Figure 6-13. 24-bus IEEE Reliability Test System (RTS).

$$\lambda_i' = \frac{\text{number of undesired trips}}{\text{in - service time}} \tag{6.43}$$

$$p_{ik} = \frac{N_{ik}}{N_{tc}} \tag{6.44}$$

Here N_{ik} is the number of times all breakers in subset I_k fail to trip, and N_{tc} is the number of trip commands [80]. In practice, these estimated parameters should be accumulating data, which means that not only the historical information representing the past transition behavior needs to be collected, but also new information about recent failures when available should be included to keep the parameters updated.

Since protection data for components of RTS are currently unavailable, we assume for simplicity that all protections have the same behavior. A set of protection reliability parameters is adopted based on reasonable estimation from various sources such as research, testing, and experience data [70]-[72], [76]-[78], [125], [126].

(1) Protection failure rate

The protection failure rate is often shown in the range of 0.01-0.5/year without indicating distinct types. Sometimes failure rate data are given for undesired-tripping mode between 0.01-0.08/year and for fail-to-operate mode 0.1-0.4/year. By comparison, we see that the fail-to-operate mode dominates the two types of protection failures. Conservatively, we take the value of 0.05/year for the undesired-tripping mode protection failures.

We observe from RTS data that the transmission line outage rate mainly resides in the range of 1-3/year, given both permanent and transient outages are considered.

Thus we take about 5% of the component outages accounting for hidden protection failures. It yields the fail-to-operate mode protection failure rate to be 0.05-0.15/year, which we think is reasonable based on previous discussion of data.

For the current-carrying component model used in our research, the two breakers are considered identical in behavior and have the same chance of consequences due to fail-to-operate protection failures. However, the probability of both breakers failing to operate should be much less than only one of them failing to operate. Therefore, the 5% of the component outages is further decomposed into 2%, 2%, and 1% for three types of unreadiness probabilities. Of course the remaining 95% are for component outages without protection failures.

(2) Protection repair rate

The majority of data show that the protection repair process in power industry can be done within 2-10 hours, though some extreme data indicate that the length could be as long as 40 hours. Conservatively, we consider that 10 hours would be an appropriate estimate, yielding the repair rate to be 876/year.

(3) Switching rate

Given a faulted component fails to trip, its adjacent healthy components will be tripped quickly by backup protections. However, switching these tripped healthy components back to service could take quite a few hours. It can only be carried out after some checking processes including but not limited to investigating tripping causes, locating the actual fault, and manually isolating the faulted components, etc. So, we consider 10 hours as appropriate for all model applications.\

The protection reliability parameters we adopted are summarized in Table 6-4.

Table 6-4 Parameters associated with protection system failures

Parameters	Values	Parameters	Values
λ_i' (1/year)	0.05	μ_i' (1/year)	876
p_{i1}	0.02	γ_{i1} (1/year)	876
p_{i2}	0.02	γ_{i2} (1/year)	876
p_{i3}	0.01	γ_{i3} (1/year)	876
p_{i0}	0.95	--	--

The Monte Carlo simulation is used for evaluating the system reliability. The reliability indices are estimated by the sequential simulation method programmed in MATPOWER software [127]. Figure 6-14 is a sampling of the system Loss Of Load Probability (LOLP) with 100,000 samples.

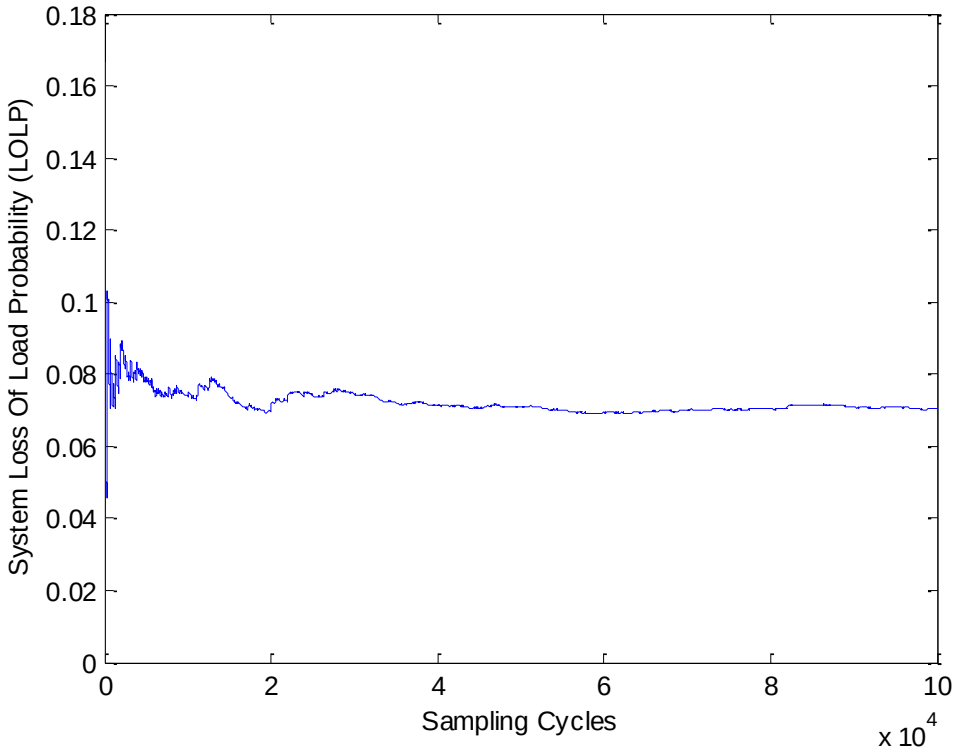

Figure 6-14. Sampling of the system Loss Of Load Probability (LOLP).

Figure 6-15 gives the system reliability indices of LOLP and frequency of system loss of load, compared with the corresponding results of the model assuming perfectly reliable protections. The results in Figure 6-15 have quantified the expectation that protection system failures do have an influence on system reliability. We can see that these indices show an increase over those of the perfect protection model. Thus, the system reliability situation has been degraded due to the impact of protection failures.

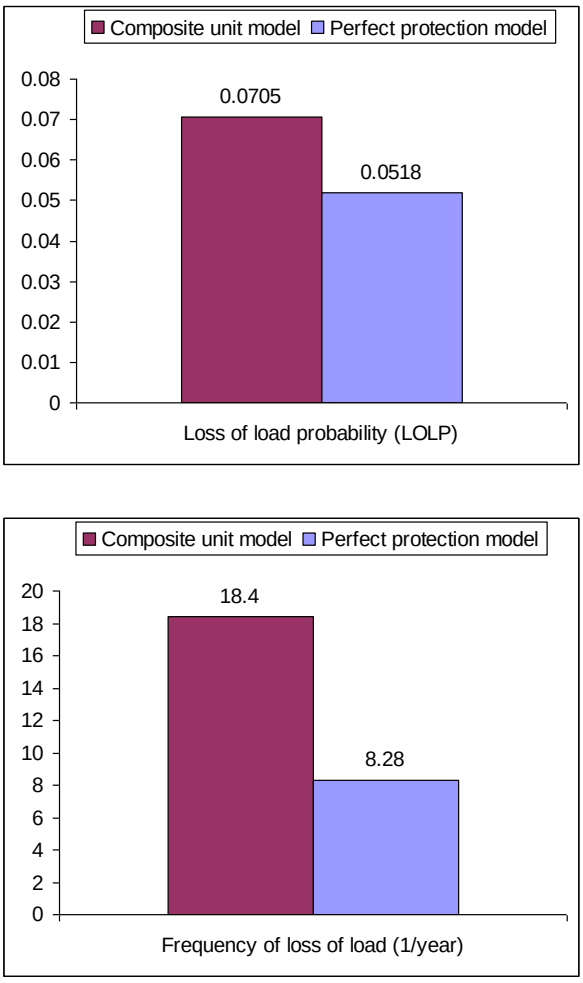

Figure 6-15. System reliability indices.

6.5. Summary

For the purpose of application in the overall power system reliability analysis including protection failures, concepts of self-down state and induced-down state are introduced. Then the composite unit model is built for quantitatively assessing the

impact of protection failures on modeling system states. Finally, the reliability Markov model of power systems with protection failures has been proposed. The methodology for reliability evaluation of power systems including protection system failures is also illustrated in detail. From the numerical case studies, we can see that assumption of perfectly reliable protection can introduce errors in power system reliability evaluation [120], [121].

7. CONCLUSIONS

The reliability of protection systems has critical influence on the reliability of power systems. The existence of protection failures can significantly impact reliability evaluation of power systems. According to the nature of the problem, the hierarchical layers of three levels have been proposed. These layers provide a broad view of how the problems concerning protection system failures relate to each other. However, this research does not intend to cover everything but focuses on the following issues within the proposed three layers.

(1) Research scope of Layer 1: Reliability modeling of all-digital protection systems including special protection systems with consideration of repair;

(2) Research scope of Layer 2: Modeling the overall reliability situation of current-carrying components including protection system failures;

(3) Research scope of Layer 3: Developing applicable methodology for power system reliability evaluation including protection system failures.

7.1. Summary of Contributions

The contributions of this research are summarized as follows.

(1) Section 2 explores the impact of including component repair on the reliability modeling of all-digital protection systems. It is shown that repairable and non-repairable assumptions make a remarkable difference in the computed reliability indices of the

MTTF and MTTFF. A typical all-digital protection system architecture is modeled and numerically analyzed. Some interesting results are found by comparing reliability indices of MTTF and MTTFF and explanations of these results are provided.

(2) Section 3 proposes a conceptual all-digital SPS architecture for the future smart grid. The smart grid is emerging with the penetration of information-age technologies and the development of the SPS will be greatly influenced. The focus of this section is how to apply reliability analysis approaches to the new all-digital SPS schemes. Calculation of important reliability indices by the network reduction method and the Markov modeling method is illustrated in detail.

(3) Section 4 focuses on reliability modeling of the 2-out-of-3 voting gates structure in a generation rejection scheme. Due to different assumptions, two corresponding Markov models are proposed for reliability evaluation. The major difference between these two models is whether the failures of a logic gate are distinguished as detectable or undetectable. The numerical case study shows that the reliability indices obtained from these two models could be very different.

(4) Section 5 reconsiders reliability modeling of current-carrying components including protection system failures from a new perspective. The two types of protection failures, i.e. undesired-tripping mode and fail-to-operate mode, and their impact on reliability modeling are discussed. A complete Markov model is established and its simplified form is then derived. The simplified model not only contains important information of the component itself, but also incorporates significant information of related protection system failures for quantitative analysis.

(5) Section 6 develops new models and concepts for incorporating the effect of protection system failures into power system reliability evaluation. New concepts of the self-down state and the induced-down state are introduced and then utilized to build up the composite unit model. This new model is the key for quantitatively assessing the influence of protection failures on modeling system states. Finally, a two-layer Markov model for power systems with protection failures is proposed for system reliability evaluation. The proposed methodology is also illustrated in detail.

7.2. Research Conclusions

The conclusions of this research are summarized as following.

(1) Repair plays an important role in reliability modeling of all-digital protection systems concerning MTTF and MTTFF. If an all-digital protection system is indeed repairable but is modeled in a non-repairable manner for analysis, the calculated values for the MTTF and MTTFF could be grossly pessimistic.

(2) If components tend to be less reliable, the SPS reliability will be degraded. However, increasing component repair rates will be helpful to enhance the reliability of SPS. The approaches applied in this research can quantify these effects and help in cost-benefit trade-off and selection of components as well as configurations.

(3) If the Markov model with consideration of both detectable and undetectable logic gate failures is used as a benchmark, the simple Markov model which only

considers detectable failures will significantly overestimate the reliability of the 2-out-of-3 voting gates structure in a generation rejection scheme.

(4) The simplified complete Markov model for current-carrying components is applicable for quantitative analysis. It can appropriately describe the overall reliability situation of individual components under the circumstances of complex interactions between components due to protection system failures.

(5) The proposed composite unit model and the two-layer system Markov model can quantify the impact of protection failures on power system reliability evaluation. Using the developed methodology, we can see that assumption of perfectly reliable protection can introduce errors in reliability evaluation of power systems.

7.3. Suggestions for Future Work

It is worth noting that although the scope of this research is limited to assessment of the probability of multiple component outages resulting from the protection failures, these models can be further combined with the models considering cascading events as can be the models that do not consider protection failures.

REFERENCES

[1] R. Billinton, *Power System Reliability Evaluation*. New York: Gordon and Breach Science Publishers, 1970.

[2] C. Singh and R. Billinton, *System Reliability Modeling and Evaluation*. London, UK: Hutchinson Educational Publishers, 1977. [Online]. Available: http://www.ece.tamu.edu/People/bios/singh/sysreliability

[3] J. Endrenyi, *Reliability Modeling in Electric Power Systems*. New York: Wiley, 1979.

[4] B. S. Dhillon and C. Singh, *Engineering Reliability - New Techniques and Applications*. Hoboken, New Jersey, USA: Wiley, 1981.

[5] R. Billinton and W. Li, *Reliability Assessment of Electric Power Systems Using Monte Carlo Methods*. New York: Plenum, 1994.

[6] R. Billinton and R. N. Allan, *Reliability Evaluation of Power Systems*, 2nd ed. New York: Plenum, 1996.

[7] M. P. Bhavaraju, R. Billinton, R. E. Brown, J. Endrenyi, W. Li, A. P. Meliopoulos, and C. Singh, "IEEE tutorial on electric delivery system reliability evaluation," *tutorial presentation at the 2005 IEEE Power Engineering Society General Meeting*, Jun. 2005.

[8] J. Endrenyi, M. P. Bhavaraju, K. A. Clements, K. J. Dhir, M. F. McCoy, K. Medicherla, N. D. Reppen, L. A. Salvaderi, S. M. Shahidehpour, C. Singh, and J. A.

Stratton, "Bulk power system reliability concepts and applications," *IEEE Trans. Power Systems*, vol. 3, no. 1, pp. 109-117, Feb. 1988.

[9] B. Porretta and E. G. Neudorf, "Conceptual framework for evaluation and interpretation of the reliability of the composite power system," *IEEE Trans. Power Systems*, vol. 10, no. 2, pp. 1094-1103, May 1995.

[10] R. Billinton, L. Salvaderi, J. D. McCalley, H. Chao, T. Seitz, R. N. Allan, J. Odom, and C. Fallon, "Reliability issues in today's electric power utility environment," *IEEE Trans. Power Systems*, vol. 12, no. 4, pp. 1708-1714, Nov. 1997.

[11] R. Allan and R. Billinton, "Power system reliability and its assessment - Part 1: Background and generating capacity," *Power Engineering Journal*, vol. 6, no. 4, pp. 191-196, Jul. 1992.

[12] R. Allan and R. Billinton, "*Power system* reliability and its assessment - Part 2: Composite generation and transmission systems," *Power Engineering Journal*, vol. 6, no. 6, pp. 291-297, Nov. 1992.

[13] R. Allan and R. Billinton, "*Power system* reliability and its assessment - Part 3: Distribution systems and economic considerations," *Power Engineering Journal*, vol. 7, no. 4, pp. 185-192, Nov. 1993.

[14] B. L. Silverstein and D. M. Porter, "Contingency ranking for bulk system reliability criteria," *IEEE Trans. Power Systems*, vol. 7, no. 3, pp. 956-964, Aug. 1992.

[15] B. Eua-Arporn and A. Karunanoon, "Reliability evaluation in electrical power generation with uncertainty modeling by fuzzy number," in *Proc. 2000 IEEE Power Engineering Society Summer Meeting*, vol. 4, pp. 2051-2056, Jul. 2000.

[16] J. T. Saraiva, "Reliability evaluation of generation/transmission power systems including fuzzy data," in *Proc. 1996 IEEE International Symposium on Circuits and Systems (ISCAS 96)*, vol. 1, pp. 609-612, May 1996.

[17] J. T. Saraiva, V. Miranda, and L. M. V. G. Pinto, "Generation/transmission power system reliability evaluation by Monte-Carlo simulation assuming a fuzzy load description," *IEEE Trans. Power Systems*, vol. 11, no. 2, pp. 690-695, May 1996.

[18] J. T. Saraiva and A. V. Sousa, "New advances in integrating fuzzy data in Monte Carlo simulation to evaluate reliability indices of composite power systems," in *Proc. the 9th Mediterranean Electrotechnical Conference (MELECON 98)*, vol. 2, pp. 1084-1088, May 1998.

[19] M. T. Schilling, R. Billinton, A. M. Leite da Silva, and M. A. El-Kady, "Bibliography on composite system reliability (1964-1988)," *IEEE Trans. Power Systems*, vol. 4, no. 3, pp. 1122-1132, Aug. 1989.

[20] R. N. Allan, R. Billinton, S. M. Shahidehpour, and C. Singh, "Bibliography on the application of probability methods in power system reliability evaluation: 1982-1987," *IEEE Trans. Power Systems*, vol. 3, no. 4, pp. 1555-1564, Nov. 1988.

[21] R. N. Allan, R. Billinton, A. M. Breipohl, and C. H. Grigg, "Bibliography on the application of probability methods in power system reliability evaluation: 1987-1991," *IEEE Trans. Power Systems*, vol. 9, no. 1, pp. 41-49, Feb. 1994.

[22] R. N. Allan, R. Billinton, A. M. Breipohl, and C. H. Grigg, "Bibliography on the application of probability methods in power system reliability evaluation: 1992-1996," *IEEE Trans. Power Systems*, vol. 14, no. 1, pp. 51-57, Feb. 1999.

[23] R. Billinton, M. Fotuhi-Firuzabad, and L. Bertling, "Bibliography on the application of probability methods in power system reliability evaluation: 1996-1999," *IEEE Trans. Power Systems*, vol. 16, no. 4, pp. 595-602, Nov. 2001.

[24] K. A. Clements, B. P. Lam, D. J. Lawrence, T. A. Mikolinnas, N. D. Reppen, R. J. Ringlee, and B. F. Wollenberg, "Transmission system reliability methods," Electric Power Research Institute (EPRI), Palo Alto, CA, Tech. Rep. EL-2526, Jul. 1982.

[25] B. P. Lam, D. J. Lawrence, N. D. Reppen, R. J. Ringlee, A. P. Meliopoulos, M. P. Bhavaraju, R. R. Kovacs, and R. Billinton, "Reliability evaluation for large-scale bulk transmission systems," Electric Power Research Institute (EPRI), Palo Alto, CA, Tech. Rep. EL-5291, Jan. 1988.

[26] R. Billinton and A. Sankarakrishnan, "A comparison of Monte Carlo simulation techniques for composite power system reliability assessment," in *Proc. 1995 IEEE Conference on Communications, Power, and Computing (WESCANEX 95)*, vol. 1, pp. 145-150, May 1995.

[27] M. E. Khan and R. Billinton, "A hybrid model for quantifying different operating states of composite power systems," *IEEE Trans. Power Systems*, vol. 7, no. 1, pp. 187-193, Feb. 1992.

[28] Y. Guo, Y. Xi, K. Xiao, and H. Yang, "Composite system reliability evaluation based on Monte-Carlo simulation combined with outages screening," *IEEE Trans. Power Systems*, vol. 14, no. 2, pp. 785-790, May 1999.

[29] R. Billinton and W. Zhang, "State extension in adequacy evaluation of composite power systems – concept and algorithm," *Electric Power Systems Research*, vol. 47, no. 3, pp. 189-195, Nov. 1998.

[30] R. Billinton and W. Zhang, "State extension in adequacy evaluation of composite power systems – applications," *IEEE Trans. Power Systems*, vol. 15, no. 1, pp. 427-432, Feb. 2000.

[31] R. Billinton and S. K. Agarwal, "Examination of severe contingencies in a small area of a large composite power system using adequacy equivalents," *IEE Proc. C - Generation, Transmission and Distribution*, vol. 137, no. 2, pp. 107-114, Mar. 1990.

[32] S. Kumar and R. Billinton, "Adequacy equivalents in composite power system evaluation," *IEEE Trans. Power Systems*, vol. 3, no. 3, pp. 1167-1173, Aug. 1988.

[33] R. Billinton and W. Zhang, "Enhanced adequacy equivalent for composite power system reliability evaluation," *IEE Proc. - Generation, Transmission and Distribution*, vol. 143, no. 5, pp. 420-426, Sep. 1996.

[34] W. Zhang and R. Billinton, "Application of an adequacy equivalent method in bulk power system reliability evaluation," *IEEE Trans. Power Systems*, vol. 13, no. 2, pp. 661-666, May 1998.

[35] H. A. M. Maghraby and R. N. Allan, "Application of DC equivalents to the reliability evaluation of composite power systems," *IEEE Trans. Power Systems*, vol. 14, no. 1, pp. 355-361, Feb. 1999.

[36] C. L. T. Borges, D. M. Falcao, J. C. O. Mello, and A. C. G. Melo, "Composite reliability evaluation by sequential Monte Carlo simulation on parallel and distributed processing environments," *IEEE Trans. Power Systems*, vol. 16, no. 2, pp. 203-209, May 2001.

[37] N. Gubbala, and C. Singh, "Models and considerations for parallel implementation of Monte Carlo simulation methods for power system reliability evaluation," *IEEE Trans. Power Systems*, vol. 10, no. 2, pp. 779-787, May 1995.

[38] C. Singh and J. Mitra, "Composite system reliability evaluation using state space pruning," *IEEE Trans. Power Systems*, vol. 12, no. 1, pp. 471-479, Feb. 1997.

[39] D. P. Clancy, G. Gross, and F. F. Wu, "Probabilistic flows for reliability evaluation of multiarea power system interconnections," *International Journal of Electrical Power & Energy Systems*, vol. 5, no. 2, pp. 101-114, Apr. 1983.

[40] C. Singh and Z. Deng, "A new algorithm for multi-area reliability evaluation - simultaneous decomposition-simulation approach," *Electric Power Systems Research*, vol. 21, no. 2, pp. 129-136, Jun. 1991.

[41] Z. Deng and C. Singh, "A new approach to reliability evaluation of interconnected power systems including planned outages and frequency calculations," *IEEE Trans. Power Systems*, vol. 7, no. 2, pp. 734-743, May 1992.

[42] J. Mitra and C. Singh, " " Incorporating the DC load flow model in the decomposition-simulation method of multi-area reliability evaluation," *IEEE Trans. Power Systems*, vol. 11, no. 3, pp. 1245-1254, Aug. 1996.

[43] J. Mitra, "Models for reliability evaluation of multi-area and composite systems," Ph.D. dissertation, Department of Electrical Engineering, Texas A&M University, College Station, 1997.

[44] J. Mitra and C. Singh, "Pruning and simulation for determination of frequency and duration indices of composite power systems," *IEEE Trans. Power Systems*, vol. 14, no. 3, pp. 899-905, Aug. 1999.

[45] M. V. F. Pereira, M. E. P. Maceira, G. C. Oliveira, and L. M. V. G. Pinto, "Combining analytical models and Monte-Carlo techniques in probabilistic power system analysis," *IEEE Trans. Power Systems*, vol. 7, no. 1, pp. 265-272, Feb. 1992.

[46] A. C. G. Melo, G. C. Oliveira, M. Morozowski Fo, and M. V. F. Pereira, "A hybrid algorithm for Monte Carlo/enumeration based composite reliability evaluation," in *Proc. the 3rd International Conference on Probabilistic Methods Applied to Electric Power Systems*, pp. 70-74, Jul. 1991.

[47] R. Billinton and A. Jonnavithula, "Variance reduction techniques for use with sequential Monte Carlo simulation in bulk power system reliability evaluation," in

Proc. 1996 Canadian Conference on Electrical and Computer Engineering, vol. 1, pp. 416-419, May 1996.

[48] R. Billinton and A. Jonnavithula, "Composite system adequacy assessment using sequential Monte Carlo simulation with variance reduction techniques," *IEE Proc. - Generation, Transmission and Distribution*, vol. 144, no. 1, pp. 1-6, Jan. 1997.

[49] A. Sankarakrishnan and R. Billinton, "Sequential Monte Carlo simulation for composite power system reliability analysis with time varying loads," *IEEE Trans. Power Systems*, vol. 10, no. 3, pp. 1540-1545, Aug. 1995.

[50] C. Dornellas, M. Schilling, A. Melo, J. C. S. Souza, and M. B. Do Coutto Filho, "Combining local and optimised power flow remedial measures in bulk reliability assessment," *IEE Proc. - Generation, Transmission and Distribution*, vol. 150, no. 5, pp. 629-634, Sep. 2003.

[51] R. Billinton and E. Khan, "A security based approach to composite power system reliability evaluation," *IEEE Trans. Power Systems*, vol. 7, no. 1, pp. 65-72, Feb. 1992.

[52] R. Billinton and S. Aboreshaid, "Security evaluation of composite power systems," *IEE Proc. - Generation, Transmission and Distribution*, vol. 142, no. 5, pp. 511-516, Sep. 1995.

[53] M. E. Khan, "Bulk load points reliability evaluation using a security based model," *IEEE Trans. Power Systems*, vol. 13, no. 2, pp. 456-463, May 1998.

[54] R. Billinton and M. E. Khan, "Security considerations in composite power system reliability evaluation," in *Proc. the 3rd International Conference on Probabilistic Methods Applied to Electric Power Systems*, pp. 58-63, Jul. 1991.

[55] D. Romero-Romero, J. A. Gomez-Hernandez, and J. Robles-Garcia, "Reliability optimisation of bulk power systems including voltage stability," *IEE Proc. - Generation, Transmission and Distribution*, vol. 150, no. 5, pp. 561-566, Sep. 2003.

[56] A. M. Leite da Silva, J. Endrenyi, and L. Wang, "Integrated treatment of adequacy and security in bulk power system reliability evaluations," *IEEE Trans. Power Systems*, vol. 8, no. 1, pp. 275-285, Feb. 1993.

[57] A. M. Rei, A. M. Leite da Silva, J. L. Jardim, and J. C. O. Mello, "Static and dynamic aspects in bulk power system reliability evaluations," *IEEE Trans. Power Systems*, vol. 15, no. 1, pp. 189-195, Feb. 2000.

[58] V. A. Levi, J. M. Nahman, and D. P. Nedic, "Security modeling for power system reliability evaluation," *IEEE Trans. Power Systems*, vol. 16, no. 1, pp. 29-37, Feb. 2001.

[59] B. Porretta, D. L. Kiguel, G. A. Hamoud, and E. G. Neudorf, "A comprehensive approach for adequacy and security evaluation of bulk power systems," *IEEE Trans. Power Systems*, vol. 6, no. 2, pp. 433-441, May 1991.

[60] R. Billinton and S. Aboreshaid, "Voltage stability considerations in composite power system reliability evaluation," *IEEE Trans. Power Systems*, vol. 13, no. 2, pp. 655-660, May 1998.

[61] L. Cheng, Y. Guo, and K. Xiao, "Reliability evaluation of composite systems considering voltage stability problems," in *Proc. 1998 International Conference on Power System Technology (POWERCON '98)*, vol. 2, pp. 1489-1493, Aug. 1998.

[62] J. A. Momoh, Y. V. Makarov, and W. Mittelstadt, "A framework of voltage stability assessment in power system reliability analysis," *IEEE Trans. Power Systems*, vol. 14, no. 2, pp. 484-491, May 1999.

[63] N. Amjady, "A framework of reliability assessment with consideration effect of transient and voltage stability," *IEEE Trans. Power Systems*, vol. 19, no. 2, pp. 1005-1014, May 2004.

[64] F. Yang, A. P. S. Meliopoulos, G. J. Cokkinides, and G. Stefopoulos, "A bulk power system reliability assessment methodology," in *Proc. the 8th International Conference on Probabilistic Methods Applied to Power Systems*, pp. 44-49, Sep. 2004.

[65] F. Yang, A. P. S. Meliopoulos, G. J. Cokkinides, and G. K. Stefopoulos, "Security-constrained adequacy evaluation of bulk power system reliability," in *Proc. the 9th International Conference on Probabilistic Methods Applied to Power Systems (PMAPS 2006)*, pp. 1-8, Jun. 2006.

[66] F. Yang, A. P. S. Meliopoulos, G. J. Cokkinides, and G. K. Stefopoulos, "A comprehensive approach for bulk power system reliability assessment," in *Proc. 2007 IEEE Lausanne Power Tech Conference*, pp. 1587-1592, Jul. 2007.

[67] J. W. M. Cheng, D. T. McGillis, and F. D. Galiana, "Power system reliability in a deregulated environment," in *Proc. 2000 Canadian Conference on Electrical and Computer Engineering*, vol. 2, pp. 765-768, May 2000.

[68] P. M. Anderson, *Power System Protection – Part IV: Reliability of Protection Systems*. New York: McGraw-Hill: IEEE Press, 1999.

[69] C. Singh and A. D. Patton, "Protection system reliability modeling: Unreadiness probability and mean duration of undetected faults," *IEEE Trans. Reliability*, vol. R-29, no. 4, pp. 339-340, Oct. 1980.

[70] P. M. Anderson and S. K. Agarwal, "An improved model for protective-system reliability," *IEEE Trans. Reliability*, vol. 41, no. 3, pp. 422-426, Sep. 1992.

[71] J. J. Kumm, D. Hou, and E. O. Schweitzer, "Predicting the optimum routine test interval for protective relays," *IEEE Trans. Power Delivery*, vol. 10, no. 2, pp. 659-665, Apr. 1995.

[72] P. M. Anderson, G. M. Chintaluri, S. M. Magbuhat, and R. F. Ghajar, "An improved reliability model for redundant protective systems – Markov models," *IEEE Trans. Power Systems*, vol. 12, no. 2, pp. 573-578, May 1997.

[73] *Communication networks and systems in substations – Part 8-1: Specific communication service mapping (SCSM) – Mappings to MMS (ISO 9506-1 and ISO 9506-2) and to ISO/IEC 8802-3*, IEC International Standard 61850-8-1, 1st ed., May 2004.

[74] *Communication networks and systems in substations – Part 9-2: Specific communication service mapping (SCSM) – Sampled values over ISO/IEC 8802-3*, IEC International Standard 61850-9-2, 1st ed., Apr. 2004.

[75] P. Zhang, L. Portillo, and M. Kezunovic, "Reliability and component importance analysis of all-digital protection systems," in *Proc. 2006 IEEE Power Engineering Society Power Systems Conf. and Exposition*, pp. 1380-1387, Oct. 2006.

[76] X. Yu and C. Singh, "A practical approach for integrated power system vulnerability analysis with protection failures," *IEEE Trans. Power Systems*, vol. 19, no. 4, pp. 1811-1820, Nov. 2004.

[77] X. Yu and C. Singh, "Power system reliability analysis considering protection failures," in *Proc. 2002 IEEE Power Engineering Society Summer Meeting*, vol. 2, pp. 963-968, Jul. 2002.

[78] M. C. Bozchalui, M. Sanaye-Pasand, and M. Fotuhi-Firuzabad, "Composite system reliability evaluation incorporating protection system failures," in *Proc. 2005 IEEE Canadian Conference on Electrical and Computer Engineering*, pp. 486-489, May 2005.

[79] H. Wang and J. S. Thorp, "Enhancing reliability of power protection systems economically in the post-restructuring era," in *Proc. 2000 IEEE 32nd North American Power Symposium*, 2000.

[80] C. Singh and A. D. Patton, "Models and concepts for power system reliability evaluation including protection-system failures," *International Journal of Electrical Power & Energy Systems*, vol. 2, no. 4, pp. 161-168, Oct. 1980.

[81] J. De La Ree, Y. Liu, L. Mili, A. G. Phadke, and L. DaSilva, "Catastrophic failures in power systems: Cause, analysis, and countermeasures," *Proceedings of the IEEE*, Vol. 93, No. 5, pp. 956-964, May 2005.

[82] D. C. Elizondo and J. De La Ree, "Analysis of hidden failures of protection schemes in large interconnected power systems," in *Proc. 2004 IEEE Power Engineering Society General Meeting*, Vol. 1, pp. 107-114, Jun. 2004.

[83] A. G. Phadke and J. S. Thorp, "Expose hidden failures to prevent cascading outages," *IEEE Computer Applications in Power*, Vol. 9, No. 3, pp. 20-23, 1996.

[84] K. Bae and J. S. Thorp, "An importance sampling application: 179 bus WSCC system under voltage based hidden failures and relay misoperations," in *Proc. the 31st Hawaii International Conference on System Sciences*, Vol. 3, pp. 39-46, Jan. 1998.

[85] D. C. Elizondo, J. De La Ree, A. G. Phadke, and S. Horowitz, "Hidden failures in protection systems and their impact on wide-area disturbances," in *Proc. 2001 IEEE Power Engineering Society Winter Meeting*, Vol. 2, pp. 710-714, Jan. 2001.

[86] D. C. Elizondo, "Hidden failures in protection systems and its impact on power system wide-area disturbances," M.S. thesis, Dept. Electrical Engineering, Virginia Polytechnic Institute and State University, Blacksburg, 2000.

[87] S. Tamronglak, "Analysis of power system disturbance due to relay hidden failures," Ph.D. dissertation, Dept. Electrical Engineering, Virginia Polytechnic Institute and State University, Blacksburg, 1994.

[88] F. Yang, "A comprehensive approach for bulk power system reliability assessment," Ph.D. dissertation, School of Electrical and Computer Engineering, Georgia Institute of Technology, Atlanta, 2007.

[89] F. Yang, A. P. S. Meliopoulos, G. J. Cokkinides, and Q. B. Dam, "Effects of protection system hidden failures on bulk power system reliability," in *Proc. 2006 IEEE 38th North American Power Symposium*, pp. 517-523, Sep. 2006.

[90] R. Billinton and J. Tatla, "Composite generation and transmission system adequacy evaluation including protection system failure modes," *IEEE Trans. Power Apparatus and Systems*, vol. PAS-102, no. 6, pp. 1823-1830, Jun. 1983.

[91] C. Singh and R. Billinton, "Frequency and duration concepts in system reliability evaluation," *IEEE Trans. Reliability*, vol. R-24, no. 1, pp. 31-36, Apr. 1975.

[92] W. Kuo and M. J. Zuo, *Optimal Reliability Modeling: Principles and Applications*. Hoboken, New Jersey, USA: John Wiley & Sons, 2003.

[93] M. Rausand and A. Høyland, *System Reliability Theory: Models, Statistical Methods, and Applications*, 2nd ed. Hoboken, New Jersey, USA: John Wiley & Sons, 2004.

[94] C. Singh, "A matrix approach to calculate the failure frequency and related indices," *Microelectronics and Reliability*, vol. 19, pp. 395-398, 1979.

[95] K. Jiang and C. Singh, "Reliability modeling of all-digital protection systems including impact of repair," *IEEE Trans. Power Delivery*, vol. 25, no. 2, pp. 579-587, Apr. 2010.

[96] Glossary of terms used in NERC reliability standards. North American Electric Reliability Corporation (NERC), Apr. 2010 [Online]. Available: http://www.nerc.com/docs/standards/rs/Glossary_of_Terms_2010April20.pdf

[97] CIGRE WG 39.05, P. M. Anderson and B. K. LeReverend, et al. "Industry experience with special protection schemes," Electra, no. 155, pp. 103-127, Aug. 1994.

[98] P. M. Anderson and B. K. LeReverend, "Industry experience with special protection schemes," *IEEE Trans. Power Systems*, vol. 11, no. 3, pp. 1166-1179, Aug. 1996.

[99] P. C. K. Lau, M. Grover, and W. Tanaka, "Reliability assessment of special protection systems," CIGRE paper AA-11, presented at the CIGRE Symposium on Electric Power System Reliability, Montreal, Sep. 1991.

[100] J. McCalley and W. Fu, "Reliability of special protection systems," *IEEE Trans. Power Systems*, vol. 14, no. 4, pp. 1400-1406, Nov. 1999.

[101] W. Fu, S. Zhao, J. McCalley, V. Vittal, and N. Abi-Samra, "Risk assessment for special protection systems," *IEEE Trans. Power Systems*, vol. 17, no. 1, pp. 63-72, Feb. 2002.

[102] S. C. Pai and J. Sun, "BCTC's experience towards a smarter grid - Increasing limits and reliability with centralized intelligence remedial action schemes," in *Proc. 2008 IEEE Electrical Power and Energy Conf.*, pp. 1-7, Oct. 2008.

[103] D. Chatrefou, J. P. Dupraz, and G.F. Montillet, "Interoperability between non-conventional instrument transformers (NCIT) and intelligent electronic devices

(IED)," in *Proc. 2005/2006 IEEE Power Engineering Society (PES) Transmission and Distribution Conf. and Exhibition*, pp. 1274-1279, May 2006.

[104] M. Adamiak, D. Baigent, and R. Mackiewicz, "IEC 61850 communication networks and systems in substations: An overview for users," *The Protection & Control Journal*, 8th ed., pp. 61-68, 2009.

[105] D. McGinn, V. Muthukrishnan, and W. Wang, "Enhanced security and dependability in process bus protection systems," *The Protection & Control Journal*, 8th ed., pp. 69-83, 2009.

[106] J. F. Burger, D. A. Krummen, and J. R. Abele, "AEP process bus replaces copper: Innovations in stations translate to more savings in material, time and manpower," *The Protection & Control Journal*, 8th ed., pp. 85-88, 2009.

[107] Non-conventional instrument transformer solutions. AREVA T&D [Online]. Available: http://www.areva-td.com/solutions/liblocal/docs/ NCIT /NCIT_BRen_1720.pdf

[108] P. Zhang, J. Chen, and M. Shao, "Phasor measurement unit (PMU) implementation and applications," Electric Power Research Institute (EPRI), Palo Alto, CA, Tech. Rep. 2007.1015511. [Online]. Available: http://my.epri.com/portal/server.pt?Abstract_id=000000000001015511

[109] Y. Wang, W. Li, and J. Lu, "Reliability analysis of phasor measurement unit using hierarchical Markov modeling," *Electric Power Components and Systems*, vol. 37, no. 5, pp. 517-532, May 2009.

[110] Y. Wang, W. Li, J. Lu, and H. Liu, "Evaluating multiple reliability indices of regional networks in wide area measurement systems," *Electric Power Systems Research*, vol. 79, no. 10, pp. 1353-1359, 2009.

[111] Y. Wang, W. Li, and J. Lu, "Reliability analysis of wide-area measurement system," *IEEE Trans. Power Delivery*, vol. 25, no. 3, pp. 1483-1491, Jul. 2010.

[112] Y. J. Wang, C. W. Liu, and Y. H. Liu, "A PMU based special protection scheme: a case study of Taiwan power system," *International Journal of Electrical Power & Energy Systems*, vol. 27, no. 3, pp. 215-223, Mar. 2005.

[113] B. Kasztenny, J. Whatley, E. A. Udren, J. Burger, D. Finney, M. Adamiak, "Unanswered questions about IEC 61850: What needs to happen to realize the vision?" presented at 32nd Annual Western Protective Relay Conference, USA, Oct. 2005.

[114] K. Jiang and C. Singh, "Reliability analysis of future special protection schemes," in *Proc. 48th Annual Allerton Conference on Communication, Control, and Computing*, pp. 1614-1621, Sep. 2010.

[115] K. Jiang and C. Singh, "Reliability evaluation of a conceptual all-digital special protection system architecture for the future smart grid," in *Proc. 2011 IEEE Power & Energy Society General Meeting*, pp. 1-8, Jul. 2011.

[116] J. McCalley, O. Oluwaseyi, V. Krishnan, R. Dai, C. Singh, and K. Jiang, "System protection schemes: Limitations, risks, and management," Power Systems Engineering Research Center (PSERC), Tempe, AZ, PSERC Publication 10-S35, Aug. 2010.

[117] V. Vittal, J. McCalley, V. Van Acker, W. Fu, and N. Abi-Samra, "Transient instability risk assessment," in *Proc. 1999 IEEE Power Engineering Society (PES) Summer Meeting*, pp. 206-211, Jul. 1999.

[118] K. Jiang and C. Singh, "Reliability evaluation of the 2-out-of-3 voting gates structure in a generation rejection scheme using Markov models," presented at *the 12th International Conference on Probabilistic Methods Applied to Power Systems (PMAPS 2012)*, Istanbul, Turkey, Jun. 2012.

[119] B. Kalinowski and G. Anders, "A new look at component maintenance practices and their effect on customer, station and system reliability," *International Journal of Electrical Power & Energy Systems*, vol. 28, no. 10, pp. 679-695, Dec. 2006.

[120] K. Jiang and C. Singh, "The concept of power unit zone in power system reliability evaluation including protection system failures," in *Proc. 2009 IEEE Power & Energy Society Power Systems Conference and Exposition (PSCE 2009)*, pp. 1-10, Mar. 2009.

[121] K. Jiang and C. Singh, "New models and concepts for power system reliability evaluation including protection system failures," *IEEE Trans. Power Systems*, vol. 26, no. 4, pp. 1845-1855, Nov. 2011.

[122] C. Singh and P. Jirutitijaroen, "Monte Carlo simulation techniques for transmission systems reliability analysis," *tutorial presentation at the 2007 IEEE Power Engineering Society General Meeting*, Jun. 2007.

[123] R. Billinton and W. Li, *Reliability Assessment of Electric Power Systems Using Monte Carlo Methods*, New York: Plenum Press, 1994.

[124] M. R. Bhuiyan and R. N. Allan, "Modelling multistate problems in sequential simulation of power system reliability studies," *IEE Proc. Generation, Transmission and Distribution*, vol. 142, no. 4, pp. 343-349, 1995.

[125] IEEE RTS Task Force of the APM Subcommittee, "IEEE reliability test system," *IEEE Trans. Power Apparatus and Systems*, vol. PAS-98, no. 6, pp. 2047-2054, Nov./Dec. 1979.

[126] IEEE RTS Task Force of the APM Subcommittee, "The IEEE reliability test system - 1996," *IEEE Trans. Power Systems,* vol. 14, no. 3, pp. 1010-1020, Aug. 1999.

[127] R. D. Zimmerman, C. E. Murillo-Sánchez, and R. J. Thomas, "MATPOWER steady-state operations, planning and analysis tools for power systems research and education," *IEEE Trans. Power Systems*, vol. 26, no. 1, pp. 12-19, Feb. 2011.

[128] C. Singh and R. Billinton, Closure to discussion of "Reliability modeling in systems with non-exponential down time distributions," *IEEE Trans. Power Apparatus and Systems*, vol. PAS-92, no. 2, pp. 790-800, Mar./Apr. 1973.

APPENDIX: DISTRIBUTIONS OF SWITCHING AND REPAIR TIMES

It has been shown in [128] that for calculation of steady state probabilities and frequencies, irrespective of the form of distribution, an equivalent constant transition rate from state *i* to state *j* can be given by

$$\lambda_{ij} = \frac{\alpha_{ij}}{\sum_{k} \tau_{ik} \alpha_{ik}},$$

wherein

α_{ij} = transition probability from state *i* to state *j*,

τ_{ik} = mean duration of state *i* given that the next transition is to state *k*.

Now if there is only one possible transition from state *i* to state *j*, then $\alpha_{ij} = 1$ and thus

$$\lambda_{ij} = \frac{1}{\tau_{ij}}.$$

For this situation, for steady state calculations, one can always use the reciprocal of the mean time of residence in the state as a constant transition rate which implies an exponential distribution. In other words, in this case, irrespective of the actual form of the distribution one can always assume exponential distribution without introducing any error.